Real-time Three-dimensional Ultrasound in Obstetric Application

XIONG, Yi

A Thesis Submitted in Partial Fulfillment for the Requirement for the Degree of
Doctor of Philosophy
in
Obstetrics and Gynaecology

The Chinese University of Hong Kong
August 2010

Acknowledgements

I would like to express my sincere thanks to my supervisor, Professor TzeKin Lau, for his excellent supervision and encouragement on my PhD study. His spirits of hard working impressed me greatly and encouraged me to improve myself in all aspects. He gave me adequate freedom to perform my research independently and gave me a lot of supports when I need help. My knowledge about fetal medicine had been enriched greatly in the past three years. I would like to thanks Professor Lau for giving a lot of chances to attend the high level academic congress and communicate with the top scholars in fetal medicine areas.

I would like to thank Professor T.Y. Leung, Professor T.Y. Fung, Professor L.W. Chan, Dr. Y.H. Ting, Dr. L.W. Law, Dr. S.H. Sun, Professor Min Chen, Professor Terrence Lau, Professor Ronald Wang and Professor Richard Choy for their great supports and encouragement concerning my study and research.

I would like to give deepest thanks to all the PDC members in Department of O&G, PWH. Without their help, I cannot finish my research.

I would like to thank Professor Wu Ying, Wang Huifang, Xu Jingfeng, Liang Hainan, She zhihong, Zhang shaowen and all the staff of Department of Ultrasound of Shenzhen People担Hospital for their continuous supports to me.

Finally, I gratefully dedicate this thesis to my family, especially my wife and her parents. Without their supports, I cannot finish my study and research. I would like to say sorry to my little daughter for little care being put on her since she came to the world.

Publications

1. **Xiong Y,** Wah YMI, Chen M, Fung TY, Leung TY, Lau TK. Real-time three-dimensional echocardiography using a matrix probe with live xPlane imaging of the interventricular septum. Ultrasound Obstet Gynaecol 2009; 34: 534-537.

2. **Xiong Y,** Wah YMI, Chen M, Fung TY, Leung TY, Lau TK. Assessment of the Fetal Interventricular Septum by Real-time Three-dimensional Echocardiography with Live 3D Imaging. Ultrasound Obstet Gynaecol 2010; 35: 754-755.

3. **Xiong Y**, Wah YMI, Chen M, Chan LW, Fung TY, Leung TY, Lau TK. Assisting the Acquisition of a True Midsagittal Section in the First Trimester Using a Matrix Probe with Real-Time Live xPlane Imaging. Ultrasound Obstet Gynaecol 2010; 36: 136-140.

4. Yu YM, Chen M, **Xiong Y,** Chau MC, Li SH, Lau TK. Comparison of Conventional and Purewave crystal transducer in Obstetric sonography. The Journal of Maternal-fetal and Neonatal Medicine 2009; 22: 616-621.

Academic Awards

2009 CUHK Postgraduate Student Grants For Overseas Academic Activities. The 19th World Congress of Ultrasound in Obstetrics and Gynecology, Hamburg, Germany, 13 Sep 2009---17 Sep 2009.

Table of Contents

List of Tables

List of Figures

List of abbreviations

2D	Two-dimensional
3D	Three-dimensional
3DE	Three-dimensional echocardiography
3VT	Three-vessel and trachea view
3VV	Three-vessel view
AAO	Ascending aorta
AIUM	American institute of ultrasound in Medicine
ASD	Atrial septal defect
AVSD	Atrioventricular septal defect
BMI	Body Mass Index
CHD	Congenital heart disease
DORV	Double-outlet right ventricle
ECG	Electrocardiogram
FMF	The Fetal Medicine Foundation, UK
HLHS	Hypoplastic left heart syndrome
IM	Inversion mode
IQR	Inter-quartile range
ISUOG	International Society of Ultrasound in Obstetrics and Gynecology
IVS	Interventricular septum

LSVC	Persistent left superior vena cava
LVOT	Left outflow tract view
MPV	Multiplanar view
NT	Nuchal translucency
PA	Pulmonary artery
PS	Pulmonary stenosis
RVOT	Right outflow tract view
SD	Standard deviation
SonoAVC	Sonographic automatic volume calculation
STIC	Spatiotemporal image correlation
SVC	Superior vena cava
TGA	Transposition of the great arteries
TUI	Tomographic ultrasound image
VOCAL	Virtual organ computer-aided analysis
VSD	Ventricular septal defects

Abstract

This thesis summarized real-time 3D ultrasound in obstetric application. With the introduction of matrix transducer, 3DE scanning the fetus in real time became available.

We explored the feasibility to perform the fetal heart screening using real-time 3DE with live xPlane imaging. We developed and reported the methodology of acquiring and examining the screening planes of the fetal heart with live xPlane imaging. The procedure was simple and straight. When performing the fetal heart screening with live xPlane imaging, we just need display the apical four-chamber view and mid-sagittal view of fetal upper thorax and other thing could be done by moving the reference line. The overall detection of four cardiac screen planes can reach 100%.

We demonstrated a novel method to visualize the aortic and ductal arch with live xPlane imaging. The visualization rate is 100%. Ductal arch view can be visualized by placing the reference line through pulmonary artery and descending aorta and aortic arch view can be acquired by putting the reference line along the transverse view of aortic arch and descending aorta on the 3VT view with live xPlane imaging. Therefore, live xPlane imaging is an easy and feasible method for real-time imaging of the ductal and aortic arch.

We explored to evaluate the entire fetal IVS with both live xPlane imaging and live 3D imaging. We can successfully assess the entire IVS in most fetuses (153/154). We also compared the images acquired by real-time 3DE and STIC in this thesis. It showed that less motion artifact encounters with real-time 3DE and the image quality of real-time 3DE is similar to STIC volume acquired from the sagittal view ($P>0.05$) and superior to STIC volume from the four-chamber view ($P<0.05$). Therefore, real-time 3DE can be used to display the lateral view of the fetal IVS, and potentially may be a useful tool for the assessment and diagnosis of fetal VSDs.

Conotruncal anomalies are the leading causes of cyanotic congenital heart disease. We attempted to use live xPlane imaging of ductal arch view and in-plane view of IVS to screen the fetal conotruncal anomalies in 200 fetuses. There were 152 normal cases, 25 conotruncal anomalies and 23 other types of fetal CHDs were involved in this study. The visualization rate of the normal ductal arch view and in-plane view of IVS with live xPlane imaging was 100% (152/152), 100% (152/152) in normal cases, 8% (2/25), 12% (3/25) in conotruncal anomalies and 69.7% (16/23), 73.9% (17/23) in non-conotruncal CHDs, respectively. The visualization rate of abnormal ductal arch and in-plane view in conotruncal anomalies was much higher than that in non-conotruncal anomalies ($P<0.001$). Therefore, it may be a useful tool for the assessment and diagnosis of fetal conotruncal anomalies.

We attempted to use real-time 3D ultrasound in obstetrics outside the fetal heart. We

evaluated the feasibility of using real-time 3D ultrasound to assist in obtaining a true midsagittal view in first trimester. Eight sonographers, including four FMF-certified and four non FMF-certified operators, were asked to perform ultrasound examinations on five patients and forty patients were examined in total. It showed that the deviation from true midsagittal view was reduced greatly with the guidance of live xPlane imaging. Real-time 3D ultrasound can improve the accuracy of acquisition of a defined sonographic plane, and reduce the difference in performance between operators who are formally certified or not.

In conclusion, real-time 3DE is a novel and promising technique to perform the prenatal examination, both the fetal heart and other system. It represents the future of 3D ultrasound and will become a useful tool for prenatal screening and diagnosis.

摘 要

矩阵超声探头的问世使得实时三维超声应用于产科成为可能，本论文概述了一系列实时三维超声在产科的应用，尤其是在胎儿心脏领域的应用。

首先，本研究探讨了实时三维超声进行胎儿心脏筛查的可行性。本研究详细描述了实时三维超声 live xPlane 模式显示胎儿心脏筛查切面的方法学，并进行了 50 例正常胎儿心脏筛查。该方法简单、直接，只需显示胎儿心尖四腔心切面和胎儿胸廓正中矢状切面，然后按照本研究介绍的方法移动取样线，即可显示所需胎儿心脏筛查切面，其显示率为 100%。

其次，本研究探讨了实时三维超声显示胎儿动脉导管弓和主动脉弓切面的可行性。显示动脉导管弓切面，只需先显示三血管气管切面，再将取样线通过肺动脉、动脉导管和降主动脉即可获得；显示主动脉弓切面，则只需将取样线通过三血管气管切面上主动脉弓的横切面和降主动脉即可。本研究对象包括 100 例正常胎儿和 7 例胎儿心脏畸形，100 例正常胎儿的显示率为 100%，在 7 例胎儿心脏畸形中则有助于显示异常排列的动脉弓。实时三维超声是实时显示动脉导管弓和主动脉弓长轴切面简单而易行的方法。

再次，本研究还探讨了实时三维超声观察胎儿室间隔全貌的可行性，在 154 例胎儿中仅 1 例未能成功。实时三维超声观察室间隔全貌时，只需显示心尖四腔心切面，再通过将取样线放在室间隔的右侧面上或切割三维容积至室间隔的右室面上即可。随后，本研究进行了 50 例实时三维超声和时间空间相关成像技术（STIC）显示室间隔全貌的对比研究。结果显示实时三维超声能清晰勾勒胎儿室间隔的全貌，其效果与以胎儿胸廓正中矢状切面为起始切面采集容积数据

的 STIC 技术相当（P>0.05），但明显优于以胎儿四腔心切面为起始切面采集容积数据的 STIC 技术（P<0.05）。实时三维超声能应用于观察胎儿室间隔的全貌，它具有潜力成为胎儿室间隔缺损的有效检测手段。

胎儿圆锥动脉干畸形一直是产前超声筛查和诊断的难点，容易漏误诊。本研究探讨了应用实时三维超声 live xPlane 模式显示胎儿动脉导管弓和室间隔全貌（in-plane 切面）来筛查胎儿圆锥动脉干畸形的可行性。结果显示，胎儿圆锥动脉干畸形动脉导管弓异常（92%）和室间隔 in-plane 切面异常（88%）的比例明显高于其他胎儿心脏畸形（69.7%和 73.9%，P<0.05）和正常胎儿（0%和 0%）。而实时三维超声显示胎儿动脉导管弓切面和室间隔 in-plane 切面的方法直接、简单，因而实时三维超声有潜力成为胎儿圆锥动脉干畸形的有效工具。

最后，本研究还尝试将实时三维超声应用于胎儿心脏以外的领域。本研究应用实时三维超声帮助获得胎儿头颈部正中矢状面。众所周知，早中孕期测量胎儿颈项透明层（NT）有一系列的测量标准，其中之一就是要在正中矢状面上测量。然而众多研究表明，二维超声获得的正中矢状面往往并不是正中矢状面，本研究也证实了这一点，并往往与真正的正中矢状面有一定的偏差。应用实时三维超声可以帮助缩小这一偏差，甚至获得真正的胎儿头颈部正中矢状面，从而使 NT 测量更加标准化、准确化。

因此，本研究结果表明实时三维超声是一种具有发展潜力的新型胎儿三维超声技术，它可以应用于胎儿心脏领域，也可以应用于胎儿心脏以外的领域。实时三维超声代表了胎儿三维超声技术的未来，随着成像技术的不断丰富和图像质量的不断提高，它必将成为产前诊断和筛查胎儿畸形的有效方法。

Chapter 1 Prenatal screening and diagnosis of fetal congenital heart disease by two-dimensional ultrasonography (Literature review)

Congenital heart disease (CHD) represents the most common form of congenital anatomical anomalies and is a main cause of newborn mortality (Grandjean et al., 1999; Rosano et al., 2000). The prevalence of congenital heart disease is approximate 4-13 per 1000 live births (Ferencz et al., 1985; Meberg et al., 2000; Cuneo et al., 2004). Congenital heart disease has a multifactorial etiology, such as family history, maternal infections, cardiac teratogen exposure and maternal antibody, et al., and it often occurs in patients without any risk factors or extra-cardiac abnormalities (Stumpflen et al., 1996). Therefore, fetal heart screening program is of great importance to detect the fetal congenital cardiac anomalies.

1.1 Prenatal screening of fetal congenital heart diseases by two-dimensional ultrasonography

1.1.1 Screening strategies

Prenatal screening of fetal heart anomalies was firstly introduced in the 1980s when the four-chamber view was used as part of routine obstetrical ultrasound scan between 18 and 22 weeks of gestation (Allan et al., 1985). However, the detection

rate varied greatly in different studies either in low-risk populations or in high-risk populations, ranging from 5% to 92% (Copel et al., 1987; Rustico et al., 1995; Tegnander et al., 1995; Stumpflen et al., 1996; Buskens et al., 1996; Yagel et al., 1997; Todros et al., 1997). The limited sensitivity of the four-chamber view may be partly due to the fact that four-chamber can only examine some structures of the fetal heart, such as the ventricles, atria, atrioventricular valves, interventricular and interatrial septum. To increase the detection rate of fetal heart anomalies, several studies suggested combining the four-chamber view with left outflow tract view (Kirk et al., 1994) or combining both left and right outflow tract (Devore, 1992; Bromley et al., 1992; Kirk et al., 1997; Stoll C et al., 2002; Carvalho et al., 2002; Ogge et al., 2006) or adding other cardiac views (Wigton et al., 1993; Yoo SJ et al., 1997; Yoo SJ, et al., 1999; Yagel et al., 2001; Yagel et al., 2002; Barboza et al., 2002;) and got satisfactory results.

1.1.1.1 Using four-chamber view alone to screen the fetal cardiac defects

Four-chamber view is the basis of the cardiac scan for fetal CHDs and many major CHDs can be detected in the four-chamber view. The visualization of the four-chamber view was usually suggested to be an important method to reveal the fetal congenital defects (DeVore, 1985; Copel et al., 1987; Tegnander et al., 1994). However, the detection rate of fetal congenital heart defects by using the

four-chamber view alone was quite different in different centers, ranging from 5% to 92% (Copel et al., 1987; Rustico et al., 1995; Tegnander et al., 1995; Stumpflen et al., 1996; Buskens et al., 1996; Yagel et al., 1997; Todros et al., 1997). The detection rates among non-referral centers or in the low-risk population remain low (Wong et al., 2003; Tegnander et al., 1995). Many studies emphasized the importance of fetal cardiac screening, but the widespread improvements in detection rate were not achieved (Copel et al., 1987; Rustico et al., 1995; Tegnander et al., 1995; Stumpflen et al., 1996; Buskens et al., 1996; Yagel et al., 1997; Todros et al., 1997).

Professor Chaoui summarized four reasons for the significant differences in the detection rate in different centers (Chaoui, 2003).

The first reason was inadequate examination. Inadequate examination is probably the main cause of congenital heart defects being missed in the four-chamber view. There are two major problems often encountered when performing the fetal heart screening. One is that the examiner may not have the ability to obtain an adequate four-chamber view with different fetal position, and the other is that the image is not optimized for detecting the fetal heart anomalies.

The second reason was that the four-chamber view is visualized but the heart defects are not detected. Some heart defects not detectable in the four-chamber view usually have the four-chamber structures and thus can be missed in the four-chamber view.

And also some factors, such as transducer frequency, insonation angle, gestational age and maternal obesity, may play an important role in determining whether a defect exists or not. Additionally, if the defects are small for the gestational age when the fetal heart screening performs, the defects may go undetectable.

The third reason was that the anomaly evolves *in utero*. It was known that not all the heart anomalies present in the early pregnancy. They may evolve *in utero*. Some heart defects, such as aortic and pulmonary valve obstruction, will progress *in utero* (Hornberger et al., 1995; Simpson et al., 1997; Maeno et al., 1999). Deterioration *in utero* is an important factor to decide to decrease ventricular damage by balloon valvuloplasty *in utero* in fetuses with critical semilunar stenosis (Allan et al., 1995; Kohl et al., 2000; Tulzer et al., 2002). Additionally, rhabdomyoma is another cardiac anomaly which is usually present in late pregnancy (Chaoui, 2003). Therefore, early fetal heart screening by two-dimensional ultrasonography may be reliable but not as accurate as mid-trimester ultrasound screening and cannot replace it.

The fourth reason was that some congenital heart defects cannot be detected in the four-chamber view. It is known that not all the congenital heart disease can be detected in the four-chamber view (Allan et al., 2001). Many conotruncal anomalies, such as tetralogy of Fallot, transposition of great arteries, double-outlet right ventricle (DORV) and truncus arteriosus, usually have the normal four-chamber view and thus these lesions are often missed when using the four-chamber view alone to

screen the fetal heart defects. Additionally, a few other heart defects, such as some types of secundum atrial septal defect and patent ductal arteriosus, can only be detected postnatally.

Therefore, some suggestions were given to increase the detection rate of congenital heart detects when using the four-chamber view alone (Chaoui, 2003). For example, examination of the fetal heart at 20-22 weeks of gestation, using a 5MHz transducer, magnifying and optimizing the image adequately, using a checklist and applying color Doppler flow imaging when available. However, there are still some congenital heart defects which cannot be detected by using the four-chamber view alone.

1.1.1.2 Using four-chamber view combining outflow tract view to screen the fetal cardiac defects

Because many conotruncal anomalies and some other congenital heart defects could not be detected in the four-chamber view, many doctors suggested combining the four-chamber view and left or both outflow tract view to screen the fetal heart defects (Devore, 1992; Bromley et al., 1992; Kirk et al., 1994; Kirk et al., 1997; Stoll C et al., 2002; Carvalho et al., 2002; Ogge et al., 2006) and the majority of investigators agreed to use the four-chamber view combining both left and right outflow tracts view to screen the fetal cardiac defects. The outflow tract view can interrogate the great artery origins and orientation, together with the two approximately equally

sized great arteries crossing at the normal angle after their origins. Carvalho (Carvalho et al., 2002) and Ogge (Ogge et al., 2006) proved that combining the four-chamber view and both outflow tract view was an effective method to detect fetal congenital heart defects prenatally, which increased the detection rate significantly and allowed the detection of cardiac malformations not recognizable in the four-chamber view. Many conotruncal anomalies, such as tetralogy of Fallot, transposition of the great arteries (TGA), truncus arteriosus, et al., could be detected in the left and right outflow tract views.

However, the fetal heart examination was generally regarded as a difficult work (Crane et al., 1994; Rustico et al., 1995; Tegnander et al., 1995; Garne et al., 2001; Wong et al., 2003). Visualization of the four-chamber view is relatively easy and the success rate is relatively high. However, the detection rate of major CHDs was not as high as expected (Tegnander et al., 1994; Isaksen et al., 1999; Hunter et al., 2000) and a number of CHDs involving the great arteries were often missed by using the four-chamber view alone (Constantine et al., 1991; Achiron et al., 1992; Shirley et al., 1992). Adding left and right outflow tract view to the four-chamber view is a valid method to screen the cardiac defects involving the great arteries and greatly increases the detection rate of CHDs, but the visualization of the left and right outflow tract is not easy, which is experience-dependent and needs systematical training. When properly trained and practiced, acquisition of the four-chamber view and ventricular outflow tract views may be sufficient to detect the majority of major CHDs (Allan,

2000; Tegnander and Eik-Nes, 2006). Thus, if technically feasible, left and right outflow tract view should be added into routine fetal heart screening program.

1.1.1.3 Adding the three-vessel view (3VV) and three-vessel and trachea view (3VT) in the routine screening program

Although combining the four-chamber view and left and right outflow tract view can detect the majority of fetal CHDs, there are still some CHDs not detectable or not easily recognizable, especially the ductal-dependant lesions without hypoplastic great arteries or the lesions involving the aortic arch. Furthermore, it is not easy to teach and to learn, and is a time-consuming and operators' skill-dependent procedure (Rustico et al., 1995). Therefore, it is beyond the capability of the majority of operators performing routine fetal heart screening (Allan et al., 2001).

Yoo et al. suggested that using three-vessel view (3VV) to detect the ductal-dependent lesions or aortic arch abnormalities (Yoo et al,. 1997 and 1999). 3VV view is a transverse view of the fetal upper mediastinum, where normally the oblique view of pulmonary artery and transverse view of aorta and superior vena cava (SVC) are arranged in a straight line from left to right with a decrease in their diameter, and can be acquired as simple as the four-chamber view. Due to nearly parallel to the four-chamber view, 3VV can be acquired by slightly sliding the transducer toward the fetal head. In their study, 28 of 29 cases involving the

ventricular outflow tract or/and great arteries had the abnormal three-vessel view (Yoo et al., 1997). With the help of color Doppler, 3VV view can help us to reveal the ductal-dependent lesions easily (Vinals et al., 2002). In their 43 cases of cardiac defects, 5 cases of ductal-dependant lesions, including 4 cases of hypoplastic left heart syndrome and 1 case of pulmonary atresia, have the reverse flow in the aortic arch or ductus arteriosus in addition to the severe abnormalities of the outflow tract. Therefore, the 3VV view is an important section to detect the fetal CHDs involving the ventricular outflow tract or/and great arteries, which can implement the weakness of using the four-chamber view alone to screen the fetal cardiac anomalies, especially for the ductal-dependant lesions and aortic arch abnormalities.

However, 3VV view reveals the relationship of ascending aorta and pulmonary artery and the aortic arch is not included. It is well known that visualization of the aortic arch is difficult and time-consuming. Therefore, some investigators attempted three-vessel and trachea view (3VT) to replace the 3VV view to detect the aortic arch anomalies because the 3VT view demonstrates the relationship of aortic arch with pulmonary artery and superior vena cava and its location in relation to the trachea (Yagel et al., 2002; Vinals et al., 2003; Yoo et al., 2003).

A standard 3VT view is defined as a cross-sectional view of the fetal upper mediastinum just cranial to the 3VV view. The 3VT view is also easy to be acquired and it visualizes the pulmonary artery, aortic arch and SVC from left to right, with

their diameter decreasing gradually. In the 3VT view, it can also reveal the relationship of aortic arch with the trachea, which is the key point to diagnose the right-sided aortic arch. Additionally, the 3VT view is also the key plane to detect the persistent left superior vena cava. Therefore, 3VT view can detect not only the cardiac defects involving the ventricular outflow tract but also the aortic arch and superior vena cava abnormalities. Therefore, 3VT view is a reliable method to determinate the abnormalities in the upper mediastinum and adding the 3VT view into the routine screening program can help us to detect more fetal cardiac defects (Yagel et al., 2002; Vinals et al., 2003; Yoo et al., 2003).

1.1.2 Screening guidelines

For the vast majority of sonographers, midwives and obstetricians, the primary goal of fetal heart screening is to identify the cardiac anomalies existing or not. To improve the detection rate of fetal CHDs, many guidelines were published to standardize the performance of fetal heart screening (AIUM, 1998; AIUM, 2003; ACOG, 2004; ISUOG, 2006). These guidelines specified how to perform the ultrasound screening, including the gestational age and the technical factors, and classified the prenatal cardiac ultrasound screening into 'basic' and 'extended basic' examination.

The 'basic' ultrasound examination is the visualization of the four-chamber view.

However, performing the 'basic' screening should not be mistaken for a simple chamber count because the observation of the four-chamber view involves a set of specific criteria. In the four-chamber view, we should observe the situs, axis, rhythm, rate and size of the heart, together with the symmetry of atria and ventricles, the intact interventricular septum, the contribution of atrial septum, the motion and insertion of atrioventricular valves, et al (ISUOG, 2006).

The 'extended basic' examination combines the four-chamber view with the ventricular outflow tract views and 3VT view, which can increase the detection rates of major CHDs compared to using the four-chamber view alone. These additional views have the ability to detect more conotruncal anomalies, aortic arch abnormalities and other cardiac defects involving the great arteries and veins.

Therefore, it is recommended by most guidelines that, if technically feasible, 'extended basic' ultrasound examination should be used as routine prenatal screening program. At least, the 'basic' ultrasound examination should be performed on each pregnancy woman attending the routine prenatal ultrasound screening at 18-23 weeks of gestation. If there are any abnormalities found or there are any referral indications existed, suspected cases should be referred to the specialists of fetal echocardiography.

1.2 Prenatal diagnosis of fetal congenital heart diseases by two-dimensional echocardiography

Some investigators attempted to use detailed fetal echocardiography to screen the fetal heart (Stumpflen et al., 1996). However, it requires that the operators have experienced skills and adequate knowledge about fetal CHDs and it is time-consuming. Most of the operators have no capability to perform detailed fetal echocardiography and thus it is impossible to be applied in low-risk populations. Their major goal is to suspect the cardiac anomalies and then refers to the fetal cardiologist for further diagnosis. Therefore, the practitioners, who performed the prenatal ultrasound screening, should be familiar with the indications for detailed fetal echocardiography.

The specific indications include maternal and fetal factors (Small and Copel, 2004). The maternal factors include family history of congenital heart disease, maternal metabolic disease (diabetes mellitus, phenylketonuria), maternal infections (Rubella, Coxsackie or Parvovirus B19, et al), maternal antibodies (Anti-Ro and Anti-La) and Cardiac teratogen exposure (Retinoids, Phenytoin, Carbamazepine, lithium carbonate, and valproi acid etc); the fetal factors include suspected fetal heart anomaly, abnormal fetal karotype, major extra-cardiac anomalies, increased nuchal translucency, abnormal fetal heart rate or arrhythmia. However, some studies showed that the most effective indication is suspected fetal cardiac defects referred from the

routine obstetrical screening program (Cooper et al., 1995). In their study, overall 915 fetuses referred for detailed fetal echocardiography were enrolled. However, 307 (34%) were referred for family history and only 2 CHDs (0.7%) were detected; 253 maternal diabetes were referred and the detection rate of CHDs is only 1.2%; 48 maternal teratogen exposures were included but no CHD detected. However, 23 cases of CHDs were detected in 34 cases referred for suspected CHDs by the routine ultrasound screening program, but it only accounted for 4% of referred fetal echocardiogram. Their overall detection rate of CHDs for referred fetal echocardiogram was 15%. Therefore, the most effective method to increase the detection rate of fetal CHDs is to increase the suspected fetal heart defects on a routine obstetrical screening program.

A detailed fetal echocardiogram should be performed by the specialists (fetal echocardiographers who may be the cardiologist, radiologist or perinatologist) who are familiar with the fetal cardiology, if there existing the indications raising the likelihood of fetal congenital heart defects. A detailed fetal echocardiography should involve visceroatrial situs, systematic and pulmonary venous connections, foramen ovale mechanism, atrioventricular connections, ventriculoarterial connections, great arterial relationships and sagittal views of aortic and ductal arch (ISUOG, 2006). Therefore, a sequential segmental analysis of the fetal heart should be performed for the detailed fetal echocardiography, which will bring the excellent diagnostic accuracy in expert hands (Perolo et al., 2001; Gottliebson et al., 2006). It usually uses

a six basic planes for the sequential segmental analysis of the fetal heart, including the four-chamber view, left and right ventricular outflow tract view, three-vessel and trachea view, sagittal view of the ductal and aortic arch (Yoo et al., 1999).

However, although the diagnostic accuracy of fetal CHDs is extremely high, there are still some difficulties in prenatal diagnosis of fetal congenital cardiac defects. For example, the entire fetal interventricular septum is still difficult for us to evaluate which makes small ventricular septal defects (VSD) easily missed in prenatal period. The exact relationship of semilunar valves, which is important for us to determine the relationship of great arteries, and the origins of great arteries are also not easy to determinate in some occasions. These may be partly explained to the limitation of current ultrasound technology. With the development of new ultrasonographic technology, these difficulties may be resolved in near future. Three-dimensional and four-dimensional echocardiography are promising new technologies.

1.3 Effect of prenatal diagnosis of fetal congenital heart diseases on fetal outcome

The prenatal diagnosis of fetal CHDs on the final outcome is debated. A few studies showed that the prenatal diagnosis of fetal CHDs did not alter the perinatal outcome of congenital heart defect fetuses (Crane et al., 1994). However, most studies found that the prenatal diagnosis has important impacts on the outcome of CHD fetuses, at

least for the severe cardiac anomalies requiring intrauterine intervention, such as hypoplastic left heart syndrome (HLHS) and coarctation of aortic arch (Tworetzky et al., 2001; Franklin et al., 2002; Tworetzky et al., 2004). Prenatal diagnosis of these lesions will improve survival and reduce morbidity and mortality. It has the similar impact on the prenatal diagnosis of transposition of great arteries (Bonnet et al., 1999). Therefore, efforts must be made to increase the prenatal detection of life-threatening cardiac malformations in neonates. Accurate prenatal diagnosis of fetal CHDs will benefit not only the outcome of fetuses with severe cardiac defects but also parental counseling, even for no life-threatening cardiac defect fetuses.

Chapter 2 Fetal three-dimensional echocardiography (Literature review)

2.1 Introduction of fetal three-dimensional echocardiography

Although the diagnostic accuracy of fetal CHDs by two-dimensional echocardiography is extremely high, there are still some difficulties in making precise diagnosis of spatially complex fetal congenital cardiac defects, such as the entire interventricular septum and exact relationship of great arteries. With the development of new ultrasound technology, these difficulties may be resolved in near future. Fetal three-dimensional echocardiography is a promising new technology. It had been proved that three-dimensional echocardiography can enhance the diagnosis of congenital heart disease in infants, children and adult (Vogel et al., 1994; Marx et al., 1995; Salustri et al., 1995). With the use of three-dimensional ultrasound, the whole fetal heart can be encompassed in a volume dataset, which can be used for storage and offline analysis.

2.1.1 Evolution

Over the past three decades, three-dimensional echocardiography (3DE) was used in adult and pediatric heart diseases and got a satisfactory promising result (Derker et al., 1974; Geiser et al., 1982; Vogel and Losch, 1994). Three-dimensional

echocardiography was firstly introduced for fetal heart scan by using the free-hand scanning with or without cardiac gating (Kuo et al., 1992; Merz et al., 1995; Deng et al., 1996; Meyer-Wittkopf et al., 2001). However, some difficulties were encountered by fetal three-dimensional echocardiography. Cardiac gating is one of the problems: without gating, we can only get the static three-dimensional images, which are not suitable for beating fetal heart; with gating, we can get dynamic three-dimensional pictures while it was hard to get an effective gating method because the electrocardiogram (ECG) of the fetal heart is so weak. Scanning mode is another problem. Free-hand scanning provides the freedom of moving the transducer. However, it is of little clinical significance without digital control of image acquisition. With the advent of volume transducer, the image quality of three-dimensional echocardiography was greatly improved, although it was still inferior to conventional two-dimensional echocardiography (Bega et al., 2001). Investigators had attempted three-dimensional echocardiography to visualize the screening sections of the fetal heart and explored its potential clinical application.

Very recently, some three-dimensional echocardiographic techniques were offered by many ultrasound manufactures, including the technique called 'Spatiotemporal image correlation' (STIC) and real-time three-dimensional echocardiography, which provided exciting acquisition method and image quality of a beating fetal heart (Devore et al., 2003; Vinals et al., 2003; Goncalves et al., 2003; Maulik et al., 2003; Acar et al., 2005). Until now, more technical modalities are available to image the

fetal heart and most of them are still in improvement (Devore et al., 2005; Paladini et al., 2006; Messing et al., 2007; Uittenbogaard et al., 2008 and 2009).

2.1.2 Category

Three-dimensional echocardiography can be classified into two forms: reconstructive and real-time. Reconstructive three-dimensional echocardiography, including static three-dimensional echocardiography and spatiotemporal image correlation (STIC), generates volume data from a series of two-dimensional planar images, while real-time 3D echocardiography acquires three-dimensional volume data directly with the use of a new matrix array transducer. Nowadays, reconstructive 3D echocardiography was widely used in fetal heart scanning since its relatively higher image quality and abundant image modalities (Devore et al., 2005; Paladini et al., 2006; Messing et al., 2007; Uittenbogaard et al., 2008 and 2009). However, random fetal or maternal motion artifacts limited the application of reconstructive 3D echocardiography. Real-time 3D echocardiography can acquire the volume data instantaneously without cardiac gating, which limits the motion artifacts generated by concerning the fetal and maternal motion and avoiding inaccurate and complicated calculation related to gating and position-sensing algorithms (Sklansky et al., 1999). Therefore, it is believed that real-time three-dimensional echocardiography will play an important role in fetal heart scanning in near future with the improvement made by the manufactures, although the image quality is still

relatively inferior and no more image modalities can be used now.

2.1.3 Advantages

Although fetal three-dimensional echocardiography currently encounters many difficulties, including relatively inferior image quality and fetal motion artifacts, it still has the potentials in improving both detection rate and diagnosis of fetal congenital heart defects. It is well known that two-dimensional echocardiography is an effective tool to screen and diagnose the fetal cardiac defects. However, the detection rate of fetal CHDs varies greatly in different centers (Copel et al., 1987; Rustico et al., 1995; Tegnander et al., 1995; Stumpflen et al., 1996; Buskens et al., 1996; Yagel et al., 1997; Todros et al., 1997). The detection rate and diagnostic accuracy of fetal CHDs is operator experience-dependent (Tegnander et al. 2006). In the expert's hand, the detection rate and diagnostic accuracy is high while it is relatively low for the trainee. The main advantage of fetal 3D echocardiography is that it can reduce the scanning time and operator dependence by acquiring the volume data within a few seconds from a single window (Sklansky et al., 1997). Moreover, 3D echocardiography may improve interpretation and comprehension of fetal cardiac images by extracting any image plane within the volumetric data.

2.2 Static three-dimensional echocardiography

Static three-dimensional ultrasound was usually used for surface rendering view of fetal face, spine, limb, etc. However, it can be used for fetal heart scanning in some extents, especially for the ventricular outflow tracts. Static three-dimensional echocardiography can be acquired by two methods without cardiac gating. One method uses conventional two-dimensional transducer (free-hand scanning) and the other uses mechanical volume transducer which make the three-dimensional data acquisition more stable and easy (Deng et al., 1996; Nelson et al., 1996; Sklansky et al., 1997; Sklansky et al., 1998; Leventhal et al., 1998; Sklansky et al., 1999; Meyer-Wittkopf et al., 2000). Some researches demonstrated that static three-dimensional echocardiography can help us to visualize more structures and sections of the fetal heart (Sklansky et al. 1997; Bega et al., 2001). Three-dimensional echocardiography offered the advantages in obtaining and visualizing the cardiac planes from the stored volume data. In a study conducted by Zosmer and his colleagues, they visualized the four-chamber and left ventricular outflow tract view in 93% (15/16) cases and they identified the aortic arch view in 87% (14/16) cases (Zosmer et al., 1996). They also found that the aortic arch can be acquired by angling approximate 35? from ductal arch view which could help us to understand the anatomical structures more comprehensively. However, although static three-dimensional echocardiography could improve screening the fetal heart defects, it has the obvious limitations in imaging the fetal heart due to the inferior image quality and more motion artifacts. Static image is inadequate to interpret the beating fetal heart.

2.3 Dynamic three-dimensional echocardiography

With the help of cardiac gating, dynamic three-dimensional echocardiography can demonstrate higher resolution of structures of the fetal heart (Sklansky et al., 1997). Fetal dynamic three-dimensional echocardiography can be acquired either by free-hand scanning or by mechanical volume transducer. However, obtaining the gated fetal heart data is still challenging due to the fetal electrocardiac activity is too weak. Many attempts had been made to find the feasible and effective cardiac gated method, including temporal Fourier transform, M-mode gated, Doppler gated, tissue Doppler gated, or external trigger devices (Deng et al., 1996; Nelson et al., 1996; Meyer-Wittkopf et al., 2001; Brekke et al., 2004; Herberg et al., 2005). Using the dynamic three-dimensional echocardiography, we can also extract the cardiac views from stored 3D volume data and reconstruct the rendering view of cardiac structures. Gated three-dimensional echocardiography had been shown to be of particular use in fetal heart diseases. However, either the Doppler gated or M-mode gated or other cardiac gated dynamic three-dimensional echocardiography is too complicated and complex to be used for routine clinical practice. Furthermore, image quality and motion artifacts are still the problems for fetal dynamic three-dimensional echocardiography. A simple-to-use and effective fetal three-dimensional echocardiography will benefit the fetal heart scan. Spatiotemporal imaging correlation (STIC) and real-time three-dimensional echocardiography were

developed quickly in last few years and became the promising solution for the fetal heart scanning.

2.4 Spatiotemporal image correlation (STIC)

Spatiotemporal image correlation is a kind of reconstructive gated dynamic 3D echocardiography. It uses the average heart rate from systolic incursion peaks to gate the fetal heart. This new technology was introduced in fetal heart scanning in the year 2003 and seemed to be the most effective modality of gated dynamic three-dimensional echocardiography (Goncalves et al., 2003; DeVore et al., 2003; Vinals et al., 2003). Since then, a lot of studies were performed using STIC technology in fetal heart scanning (Goncalves et al., 2004; Yagel et al., 2006; Paladini et al., 2006; Vinals et al., 2006; Meyers et al., 2007; Hata et al., 2008; Gindes and Achiron, 2008).

2.4.1 Mechanism

In the past few years, efforts were made to establish an effective and promising method to simplify the fetal echocardiography and to combine it into routine fetal heart examinations. STIC is an automated volume acquisition of the entire fetal heart by using a mechanical volume transducer and specific software. The principle used by the STIC technology to synchronize spatial and temporal information into a

volume dataset of the fetal heart is the average heart rate from systolic incursion peaks. After the average heart rate is calculated, beat-to-beat changes of about 10% variations are detected and the 2D images are rearranged accordingly to ensure that images from the same time are merged into one volume (Goncalves et al., 2003; DeVore et al., 2003; Vinals et al., 2003). Therefore, the STIC algorithms can not calculate the average heart rate correctly when there are some changes in the fetal heart rate, which will cause the artifacts due to the errors in rearranging the according two-dimensional (2D) images. In that condition, however, we can re-acquire the volume dataset.

After many years' development, there are abundant image modalities with STIC technologies. Multiplanar display and rendering display are the initial and basic image modalities with STIC technology. Multiplanar display can demonstrate three orthogonal images at the same time, while rendered view can visualize any intracardiac structure with a depth perspective view. The both image display formations can be examined as a cine loop or as a still image. Nowadays, with the tremendous progress in the development of STIC technology, there are a lot of ultrasound techniques can be combined with STIC technology, including inversion mode, color Doppler, Power Doppler, tomographic ultrasound image (TUI) and B-flow, to evaluate the beating fetal heart.

2.4.2 Clinical applications

2.4.2.1 Multiplanar display

The most basic method of STIC examination of the fetal heart is to simply scroll through the volume dataset to visualize the four-chamber view, the ventricular outflow tract view, and three-vessel and trachea view (Goncalves et al. 2006). By moving the reference point, the operator can manipulate the volume dataset to display any plane within the volume (Devore et al., 2004; Yagel et al., 2007; Uittenbogaard et al., 2008). Therefore, it is possible to add this technology into the routine fetal heart scanning. With STIC, we can systematically evaluate the relationship of the great arteries by manipulating the volume dataset (Goncalves et al., 2003; Vinals et al., 2006). Moreover, this technology provides an easy-to-manipulate and simple approach to visualize the aortic and ductal arches (Goncalves et al., 2006; Espinoza et al., 2007) and the lateral view of interventricular septum (IVS) which allows observation of the entire IVS (Myers et al., 2007).

2.4.2.2 Rendering view

Rendering view can provide a depth perspective view of any cardiac structures and planes being examined, such as the perspective four-chamber view and overriding aorta of conotruncal anomalies, which allows data acquired from multiple planes to

be displayed on a rendering display (Goncalves et al., 2006; Gindes and Achiron, 2008). With rendering view, the en face view of atrioventricular valves and IVS could be observed from the ventricular chambers, which are not accessible by standard 2D ultrasound (Chaoui et al., 2004; Vinals et al., 2006; Yagel et al., 2006).

2.4.2.3 Tomographic ultrasound imaging (TUI)

TUI is a new display format of the three- and four-dimensional ultrasound, which allows demonstration of multiple sections of the beating fetal heart at the same time. TUI can simultaneously display 4 to 8 parallel sections. TUI provides a novel and simple method to simultaneously display the four-chamber view, three-vessel and trachea view, and both ventricular outflow tract view after acquisition of a good STIC volume dataset (Espinoza et al., 2006). With TUI and STIC technologies, we can even perform the systematical sequential analysis of fetal congenital heart disease (Paladini et al., 2006).

2.4.2.4 Rendering techniques of STIC for visualizing the great arteries

It is known that visualization of the four-chamber view is relatively easy, but it cannot detect the CHDs involving the outflow tract. However, visualizing the ventricular outflow tract is not easy. The most impressive thing of three-dimensional

echocardiography is that it allows simply visualization of spatial crisscrossing relationship of great arteries. This can be realized by acquiring the volume data combined STIC with color Doppler, power Doppler, B-flow, and inversion mode (Goncalves et al., 2006; Yagel et al., 2007).

Color Doppler and power Doppler can be used effectively in three-dimensional echocardiography combined with STIC technology, which is sensitive for detecting the intracardiac flows. Therefore, it can easily reveal the crisscrossing of the great arteries. Color Doppler STIC has the potential to detect mild regurgitation jet, venous streams and location and extent of ventricular septal defect (Chaoui et al., 2004; Goncalves et al., 2004; Yagel et al., 2005). This technique can also assist the diagnosis of some rare fetal CHDs (Chaoui et al., 2003).

Inversion mode (IM) is another post-processing image modality, which was originally proposed by Nelson et al., and can be used combined with STIC (Nelson et al., 1996; Goncalves et al., 2004; Espinoza et al., 2005; Yagel et al., 2007). This algorithm transforms the anechoic structures into solid patterns. Thus anechoic organs appear echoic while normally echoic structures look like anechoic. This technique allows visualization of aortic and ductal arch with the digital cast mode from acquisition volumes, which can assist evaluating the spatial relationship of the great arteries.

B-flow can also be combined with STIC, which can enhance weak blood signals and suppress the surrounding tissue signals (Pooh, 2000). B-flow does not use the Doppler principles and thus it has no angle-dependent as much as color Doppler and power Doppler. Therefore, it is more sensitive to detect the great arteries and venous return to the heart. B-flow combined STIC technique provides a means to evaluate fetal intracardiac and extracardiac hemodynamics (Volpe et al., 2006; Hata et al., 2008).

2.4.2.5 Automated sonography

Automated sonography is a new technique based on STIC technology, which can automatically extract the standard screening planes from the acquired volume dataset (Abuhamad et al., 2007). When we perform the extended basic screening of the fetal heart using this novel technique, the only thing to do is to acquire a good STIC volume and other things will be done by the specific software. Several investigates had been done to use this technique in screening and diagnosis of the fetal CHDs. Uittenbogaard et al. tested its feasibility to be used in routine fetal cardiac screening (Uittenbogaard et al., 2009) and Rizzo et al. used it to detect the transposition of the great arteries (Rizzo et al., 2008). Therefore, this novel technique may be of great use in improving the detection rate of fetal CHDs and decreasing the operator-dependence in fetal heart screening in near future.

2.4.2.6 Volume measurement techniques

STIC technology is a kind of three-dimensional echocardiography and thus it has the ability to calculate the volumetry of cardiac chambers. Sonographic automatic volume calculation (SonoAVC) and virtual organ computer-aided analysis (VOCAL) are two three-dimensional volume measurement techniques (Raine-Fenning et al., 2008; Deb et al., 2009; Cheong et al., 2009). They are able to automatically calculate fetal volumes and seem to be reliable and feasible for the measurement of fetal volumes. Therefore, the STIC technology has the potential to evaluate the fetal heart function more accurately and represent the trends for future. However, there are still a large amount of studies needed to test its feasibility in routine clinical application.

2.4.3 Advantages and disadvantages

STIC technology has abundant image modalities and has the potentials to enhance the detection rate of fetal cardiac defects. The most promising aspect of STIC technology is that the volume dataset can be stored or transferred through the internet for later offline evaluation by experienced experts (Michailidis et al., 2001; Vinals et al., 2003). It may simplify and standardize the procedure of fetal heart screening and thus decrease the operator's dependence. It would play an important role in reducing the operator-dependence of detecting the fetal heart defects, particularly the conotruncal anomalies (Vinals et al., 2006; Espinoza et al., 2007; Rizzo et al., 2008).

However, the STIC acquisition is not a direct scanning and it is still a kind of motion-gated three-dimensional echocardiography. There are some limitations and artifacts (Chaoui et al., 2004). Fetal motion and arrhythmias are the main cause of artefacts. The acquisition time is still long, making fetal movement artefacts a major problem during the acquisition process. Acquiring a perfect volume dataset is not easy yet.

2.5 Real-time three-dimensional echocardiography

Real-time 3D echocardiography is now possible with the development of 2D matrix-array probe technology (Acar et al., 1999; Sugeng et al., 2003). Unlike 3D echocardiography using STIC technology, which is still a reconstructed 3D ultrasound, real-time 3D echocardiography using a matrix-array probe enables visualization of the pulsating fetal heart in real time without the need of cardiac gating, just as in real-time gray-scale echocardiography (Scharf et al., 2000; Maulik et al., 2003; Sklansky et al., 2005; Acar et al., 2005; Hata et al., 2006; Acar et al., 2007). The use of real-time 3D echocardiography has been extensively reported in adult and pediatric cardiology, and has been shown to be particularly useful in the assessment of valvular diseases and congenital heart diseases, as well as the evaluation of cardiac function (Acar et al., 1999; Scharf et al., 2000; Jenkins et al., 2004).

2.5.1 Mechanism

Real-time 3DE data volumes are based on 2D matrix probe technologies. The matrix probe utilizes approximate 3000 elements, resulting in image quality that is comparable with traditional 2D array transducers, and it uses all the channels to transmit and receive ultrasound pulses (Sugeng et al., 2003). These enables the real-time generation of 3D images, which can be manipulated real-time or after the images were frozen. With real-time 3D echocardiography, we could freeze the 3D images and perform "cine" function in the same way as what we do with 2D echocardiography using conventional ultrasound transducers. In addition, we could rotate and crop these frozen 3D volumes as much as necessary.

There are two major methods in displaying the volume information generated by real-time 3D echocardiography – the live 3D imaging and the live xPlane imaging (biplane imaging). The term "live 3D imaging" and "live xPlane imaging" are used by the manufacturer to describe this particular technology. The live 3D imaging provides a real-time volumetric examination of the target organ, while the live xPlane imaging displays two high-resolution real-time views of the target organ. Unlike the multiplanar view of 3D volumes acquired by conventional mechanical 3D probes, in which only the primary plane is acquired with full resolution while the other two planes are reconstructed, both views acquired by live xPlane imaging are

of high resolution displayed in real time, due to the use of the matrix-array probe.

2.5.2 Clinical potentials

Compared to the reconstructive three-dimensional echocardiography, there are few studies performed for fetal heart due to the relatively low image quality and less imaging modalities (Scharf et al., 2000; Maulik et al., 2003; Sklansky et al., 2005; Acar et al., 2005; Hata et al., 2006; Acar et al., 2007). Real-time 3D echocardiography could be used to instantaneously visualize the normal and abnormal structures of the fetal heart, including the rendered view of four-chamber view, outflow tract view, sagittal view of aortic arch and coronal view of atrioventricular valves. Additionally, real-time 3D echocardiography can help us to image the structures which are difficult or even not to be imaged by two-dimensional ultrasound and it can be applied to visualize the new inside 3D views of intracardiac defects and tumors. Most studies stated that real-time 3D echocardiography is the promising solution of fetal cardiac imaging with tremendous clinical potentials. However, no more details were available.

2.5.3 Advantages and disadvantages

Real-time three-dimensional echocardiography is theoretically the promising and suitable solution for fetal cardiac scanning. It has obvious advantages. First,

acquisition is simple and quick. Second, fetal movement artefacts are not the problem. The volumes can be manipulated real-time or after the volumes were frozen.

Nowadays, Real-time three-dimensional echocardiography has obvious limitations as well. Relatively low image resolution is the main limitation. Less image post-processing function and image modality is another important limitation. For example, color Doppler is not available for the real-time three-dimensional echocardiography yet, which has been used in adult and pediatric real-time 3D echocardiography. However, it is believed that the image quality and modalities of fetal real-time three-dimensional echocardiography will be greatly improved after the optimization by the manufacturers and it will become the dominant fetal three-dimensional echocardiograph in near future. A large number of studies need to be done with this promising three-dimensional ultrasound technology. There is a long way for the fetal real-time three-dimensional echocardiography.

2.6 Summary

The development of fetal three-dimensional echocardiography was greatly improved in recent years. STIC technology seems to be the most effective gated fetal three-dimensional echocardiography and is widely applied for fetal heart scanning. Any other gated three-dimensional echocardiography is of historical interest.

Real-time three-dimensional echocardiography represents the future of fetal 3D echocardiography. It will become the dominant fetal 3D echocardiography and play an important role in fetal heart scanning.

Chapter 3 Screen the fetal heart with live xPlane imaging

3.1 Introduction

Congenital heart disease (CHD) is the most leading cause of neonatal morbidity and mortality (Meberg et al., 2000; Cuneo et al., 2004). However, the detection rate in different medical centres varied greatly (Tegnander et al., 1995; Wong et al., 2003; Simpson, 2004). This is mainly caused by the complex anatomy of the fetal heart and operators' experience has a significant impact on the prenatal detection rate of CHDs (Tegnander and Eik-Nes, 2006). Various ways were suggested to improve the detection rate, including the four-chamber view, the great arteries, the three-vessel and trachea view, systematic training program, and three-dimensional ultrasound (Allan et al., 1985; Tegnander et al., 1994; Yoo et al., 1997; Hunter et al., 2002; Yagel et al., 2002; Devore et al., 2003; Ogge et al., 2006). Some guidelines suggested the 'extended basic' examination of fetal heart, including combination of the four-chamber view, left and right outflow tract view and three-vessel and trachea view, if the technique is feasible (AIUM, 2003; ISUOG, 2006). Visualizing these views, however, is not easy to teach and to learn, and is also time-consuming and strongly depends on operators' skills and experience (Wigton et al., 1993; Rustico et al., 1995; Tegnander and Eik-Nes, 2006). Therefore, it is of great benefit to find a simple way to screen the fetal heart, which would improve the detection rate of fetal CHDs and make the training program much easier.

Real-time three-dimensional echocardiography (3DE) is based on 2D matrix-array probe technologies. The matrix probe utilizes approximate 3000 elements, resulting in image quality that is comparable with traditional 2D array transducers, and it uses all its channels to transmit and receive ultrasound pulses (Sugeng et al., 2003). There are two image modalities of real-time 3DE – the live 3D imaging and the live xPlane imaging. The live xPlane imaging can simultaneously visualize two high resolution views in real time. The primary image plane is the reference plane, displayed on the left side of the screen. The secondary image plane can be selected by rotation through a full 360° around the reference plane, together with a lateral tilt of −45° to +45° around the primary image plane at a reference line which can be determined by the operator, or by tilting (elevation) from −30° to +30°.

The objective of this study was to describe methodology of live xPlane imaging in the screening and visualization of the fetal heart in detail.

3.2 Patients and Methods

Fifty-one pregnant women with uncomplicated singleton pregnancies who had their routine mid-trimester scan in a university teaching hospital were invited to participate in this observational study. The local ethics committee approved the research protocol. Informed consent was obtained in all cases.

All real-time 3DE examinations were performed using an iU-22 ultrasound scanner (Philips Medical System, Bothell, Washington, USA) with a 7-2MHz matrix transducer (X7-2) by one operator using the manufacturer's Fetal Echo preset. No special patient preparation was required.

According to the ISUOG guidelines (ISUOG, 2006), four fetal heart screening planes recommended by ISUOG, including four-chamber view, left outflow tract view (LVOT), right outflow tract view (RVOT), three-vessel and trachea view (3VT) were acquired by live xPlane imaging. We use the four-chamber view and fetal mid-sagittal view of upper thorax as the reference plane to acquire these planes, respectively. Firstly, we acquire an apical four-chamber view of the fetal heart with spine posterior (the apex at about 45° to the midline of fetal thorax) and then activate live xPlane imaging function to visualize the LVOT, RVOT and 3VT view. Secondly, we acquire the mid-sagittal view of fetal upper thorax and move the reference line to image the four screening planes of fetal heart. The acquisition time was also recorded since the fetus was in proper position and the time continued to be recorded for each starting plane once the acquisition of the screening planes started.

3.3 Results

A total of 51 cases were scanned by live xPlane imaging. The mean maternal age was

28.5±4.1 (range 18 to 38) years with a mean Body Mass Index (BMI) of 21.7±2.7 (range 16.1 to 29.7). All the cases were scanned between 19 to 23 weeks (mean 20.3 ±0.5 weeks).

The visualization rate of each screening plane displayed by live xPlane imaging was described in Table 3.1. The acquisition time of using four-chamber view and fetal mid-sagittal view of upper thorax was also stated in Table 3.1 as well. The specified methodology of visualizing each screening plane was described as follow.

3.3.1 Using the four-chamber view as the starting plane

Firstly, we displayed an apical four-chamber view and then use live xPlane function to visualize the LVOT, RVOT and 3VT views. LVOT can be visualized by slightly titling the reference plane (four-chamber view) towards the fetal head (Figure 3.1). RVOT can be imaged by using the reference line through the right ventricle, criss-cross, left atrium and descending aorta, i.e. using the reference line across the mediastinum and descending aorta (Figure 3.2). 3VT can also be displayed by titling the reference plane (four-chamber view) more cephaly than that of imaging the LVOT (Figure 3.3). In this study, the visualization rate of LVOT, RVOT and 3VT was 94.1% (48/51), 100% (51/51) and 98.0% (50/51). The mean acquisition time is 530? 97s (median 303s, range from 149s to 2112s).

3.3.2 Using the mid-sagittal view of fetal upper thorax as the starting plane

Secondly, we acquired the mid-sagittal view of fetal upper thorax and activated the live xPlane imaging to visualize the four-chamber, LVOT, RVOT and 3VT views. When we put the reference line through the root of aorta, LVOT can be acquired simultaneously (Figure 3.4). Four-chamber view could be visualized by putting the reference line just below the aorta at the mid-sagittal view (Figure 3.5) and 3VT could be imaged in the same way by putting the reference line through the upper thorax (Figure 3.6). The visualization rate of LVOT, four-chamber and 3VT was 100% (51/51), respectively. However, RVOT was difficult to be imaged when using the mid-sagittal view as the starting plane. It could be displayed by rotating the reference plane around the root of aorta but the visualization rate was only 41.2% (21/51) (Figure 3.7). The mean acquisition time was 320? 16s (median 206s, range from 60s to 2366s).

Therefore, the most effective solution of using live xPlane imaging to acquire the screening view of the fetal heart was that: 1) the four-chamber view is the essential and basic view; 2) when acquiring the LVOT view, use the mid-sagittal view of fetal upper thorax as the starting plane and put the reference line through the root of aorta; 3) when visualizing the RVOT view, use the four-chamber view as the starting plane and put the reference line across the right ventricle, criss-cross, left atrium and

descending aorta, i.e. put reference line across the mediastinum and descending aorta; 4) when imaging the 3VT view, we can either use the midsagittal view as the starting plane, putting the reference line across the upper thorax, or we can use the four-chamber view as the starting plane, titling the reference plane (four-chamber view) slightly towards the feta head.

3.4 Discussion

Although the fetal heart screening developed greatly in recent years, it is hard to detect the fetal CHDs prenatally, especially for the non-experienced operators. Due to the random fetal positions, the training program is difficult to teach and to learn, and is also time-consuming and operators' skills dependent (Wigton et al., 1993; Rustico et al., 1995). Therefore, many solutions were applied to improve the detection rate, including using the four-chamber view alone, using the four-chamber combined left and right ventricular outflow tract view, and using the four-chamber combined the great arteries (Allan et al., 1985; Tegnander et al., 1994; Yoo et al., 1997; Hunter et al., 2002; Yagel et al., 2002). In recent years, many guidelines were published to standardize the screening program (AIUM, 200 3; ISUOG, 2006). It was recommended that the 'extended basic' screening program should be performed for the fetal heart screening, if technically feasible. It combined four sections: the four-chamber view, LVOT, RVOT and 3VT view. The four-chamber view is the most basic screening plane. It is easy to acquire and was enrolled in all the screening

programs. Three-vessel and trachea view is parallel to the four-chamber view and is also easy to be imaged by just pushing the transducer slightly towards the fetal head. However, acquiring the LVOT and RVOT is not an easy commission. It needs systematical training and is an operator dependent procedure.

Many new technologies, including spatiotemporal image correlation (STIC) and real-time three-dimensional echocardiography, were attempted to improve the detection rate of fetal CHDs recently.

STIC is a kind of reconstructive three-dimensional echocardiographic technique. Using this approach, four screening sections of the fetal heart can be easily visualized. With the STIC technique, it is possible to use this technology into the routine fetal heart scanning. The most basic method of STIC examination of the fetal heart is to simply scroll through the volume dataset to visualize the four-chamber view, the ventricular outflow tract view, and three-vessel and trachea view (Goncalves et al. 2006). By moving the reference point, the operator can even manipulate the volume dataset to display any plane within the volume (Devore et al., 2004; Yagel et al., 2007; Uittenbogaard et al., 2008). STIC technique has a certain procedure to visualize the fetal heart screening planes and has the potentials to reduce the operators' dependence in screening the fetal heart. However, there are several limitations of these STIC-based approaches. First, acquiring a good STIC volume is not easy and is still in the hands of the experts only. Second, generation of

the rendered view and multiplanar view are performed as post hoc volume analysis and therefore movement artefact may not be easily appreciated.

Real-time 3DE using a matrix-array probe enables visualization of the pulsating fetal heart in real time just as real-time gray-scale echocardiography (Scharf et al., 2000; Maulik et al., 2003; Sklansky et al., 2005; Acar et al., 2005; Hata et al., 2006; Acar et al., 2007). With the live xPlane imaging, we can display two high-resolution real-time views of the target organ, due to the use of the matrix-array probe. The main advantage of live xPlane imaging in fetal heart screening is that only the four-chamber and the mid-sagittal view is needed and the RVOT, LVOT and 3VT view can be visualized by moving the reference line or tilting the reference plane.

The application of matrix probe in fetal heart had been reported by several researchers (Scharf et al., 2000; Maulik et al., 2003; Sklansky et al., 2005; Acar et al., 2005; Hata et al., 2006; Acar et al., 2007). They reported that live xPlane imaging could be used to visualize the normal and abnormal structures of the fetal heart, including the four-chamber view, outflow tract view, sagittal view of aortic arch. However, no further details were available, in particular the protocol and methodology.

In this study, we developed and reported the methodology of acquiring and examining the screening planes of the fetal heart with live xPlane imaging. The

procedure was simple and straight. When performing the fetal heart screening with live xPlane imaging, we just need display the four-chamber view and mid-sagittal view of fetal upper thorax and other thing could be done by moving the reference line.

There are several limitations of this study. First, this was only a feasibility study, and the definitive role of this new technology required further study in a large population. Second, color Doppler has not been used in the study because we just describe the methodology of using live xPlane imaging to acquire the fetal heart screening planes, although color Doppler flow imaging of this new matrix probe has been available with this new technique. Third, the reference line can be only come from the midline of transducer and can not be manipulated from all directions, which made the acquisition time much longer if the fetus was in non-proper position. It is envisaged that such capability will be available in the future, which might simplify the training program and then reduce the operator-dependent. Nonetheless, we have demonstrated that screening the fetal heart with live xPlane imaging is feasible.

In conclusion, live xPlane imaging can be used to visualize the screening views of the fetal heart, and potentially may be a useful tool for the assessment and diagnosis of fetal CHDs.

Chapter 4 Live xPlane imaging display of ductal and aortic arch

4.1 Introduction

Congenital heart disease (CHD) is the most common form of congenital anatomical anomalies (Grandjean et al., 1999). Antenatal diagnosis of fetal CHDs is important for proper perinatal and neonatal management (Bonnet et al., 1999; Mahle et al., 2001). With increased experience and development of ultrasonographic technologies, more major fetal congenital cardiac anomalies can be detected prenatally, with the higher detection rate in referral centers (Tegnander and Eik-Nes, 2006). However, the detection rate among the non-referral centers remains low (Wong et al., 2003; Tegnander et al., 1995). This is mainly due to the complex anatomy of the fetal heart, which is operators' experience dependency when performing the fetal heart screening (Tegnander and Eik-Nes, 2006).

The four-chamber view is the basis of the cardiac scan for fetal CHDs (Vinals et al., 2003; Allan et al., 1986; Copel et al., 1987). Many major CHDs can be detected by the four-chamber view. However, some specific fetal cardiac abnormalities (e.g. transposition of great arteries or coarctation of aortic arch) may not be detected on the four-chamber view (ISUOG guideline, 2006). CHDs involving the ventricular outflow tract or great arteries usually have the normal four-chamber view (Sharland

and Allan, 1992; Benacerraf, 1994). To compensate for this weakness of the use of a four-chamber view alone, some doctors extended the examinations to include the left and right outflow tracts (Achiron et al., 1992; Kirk et al., 1999). Visualizing the left and right outflow tracts, however, is not easy to teach and to learn, and is also time-consuming and operators' skills dependent (Wigton et al., 1993; Rustico et al., 1995). Therefore, prenatal screening of conotruncal anomalies or coarctation of aortic arch is still one of the most challenging topics and this condition is frequently missed in routine screening program (Bull et al., 1999; Garne et al., 2001), which is mainly due to the difficulties in displaying the two ventricular outflow tracts and showing the parallel arrangement of the great arteries. Furthermore, the ductal arch and aortic arch often extend in the abnormal way in conotruncal anomalies. Therefore, it is extremely difficult to observe the whole course of the arches, which is of great use for accurate diagnosis and classification of conotruncal anomalies and will benefit the outcome of the fetus.

The ductal arch view is extremely useful in screening the conotruncal anomalies and coarctation of aortic arch (Allan, 2004; Espinoza et al., 2007). The ductal arch view is also called long-axis view of the arterial duct or the sagittal view of the ductal arch, which visualizes the right ventricle in continuity with the main pulmonary artery, ductus arteriosus, descending aorta, together with the transverse view of ascending aorta (Allan, 2004). The ductal arch view reveals not only the relationship between pulmonary artery and ascending aorta, but also the relationship between the

pulmonary and aortic valve. The aortic arch view can directly display the longitudinal view of the aortic arch, which is useful for the identification of the aortic arch abnormalities. Methods able to help us to easily image these views would be extremely beneficial for the detection of fetal cardiac defects.

Real-time three-dimensional echocardiography (3DE) using a matrix-array probe enables the visualization and examination of the pulsating fetal heart at real-time without the need for gating, just like real-time grey-scale scanning (Maulik et al., 2003; Acar et al., 2005). There are two modalities of real-time 3DE with the matrix-array technology – the live 3D imaging and the live xPlane imaging. The term "live 3D imaging" and "live xPlane imaging" are used by the manufacturer to describe this particular technology. The live 3D imaging provides a real-time volumetric examination of the target organ, while the live xPlane imaging displays two high-resolution real-time views.

The objective of this study was to develop a novel and simple method to image the ductal arch and aortic arch by real-time 3DE with live xPlane imaging and to explore its potential application.

4.2 Patients and Methods

One hundred women with singleton pregnancies who attended their routine

mid-trimester scan in the Department of Obstetrics and Gynaecology of a university teaching hospital were invited to participate in this observational study. The local ethics committee approved the research protocol. Informed consent was obtained in all cases. Additional 7 cases with suspected fetal congenital heart defects were also recruited.

All subjects had an additional 3DE examination and all examinations were performed using an iU-22 ultrasound scanner (Philips medical system, Bothell, Washington, USA) with a 7-2MHz matrix-array probe (X7-2). No special patient preparation was required. All 3DE examinations were performed by one operator.

The fetal heart scanning was performed using the manufacturer's Fetal Echo preset. We firstly acquired an apical four-chamber view of the fetal heart, with the spine at 6 o'clock position (fetal spine posterior). Next, push the transducer towards the fetal head to visualize the three vessels and trachea view (3VT) and then activated live xPlane imaging function. Two real-time planes were displayed. By moving the reference line on the primary plane, a secondary image plane cutting across the reference line was displayed on the right window. By default, the secondary plane was at 90? rotation to the reference plane. In our study, the 3VT plane was displayed on the left side. The reference line was adjusted in the reference plane to be placed across the continuity of pulmonary artery and descending aorta in the 3VT view, and the ductal arch view was immediately displayed and visualized in the right window.

Slightly adjust the primary image plane to make the reference line go through the transverse view of aortic arch and descending aorta, the aortic arch view were then displayed in real time on the right window.

4.3 Results

A total of 107 cases were studies, included 7 cases with congenital cardiac defects. The mean maternal age was 27.9? .1 (range 18 to 38) years with a mean BMI of 21.9? .5 (range 16.1 to 29.9). The mean gestational week was 21.2? .3 (range 18 to 23).

The ductal arch view and aortic arch view were successfully visualized by real-time 3DE using live xPlane imaging in all 100 normal cases (Figure 4.1 and Figure 4.2). Once the 3VT view was obtained, the use of live xPlane imaging enables an acquisition and display of ductal arch view and aortic arch view in real time. The visualization rate of the ductal arch view and aortic arch view was 100%.

There were 7 cases with congenital heart defects (Table 4.1), including one case of truncus arteriosus with VSD, two cases of complete transposition of great arteries without VSD, one case of corrected transposition of great arteries with VSD, one case of double outlet of right ventricle (DORV), one case of coarctation of aortic arch, and one case suspicious of truncus or DORV. It showed that abnormal 3VT view and

abnormal ductal arch view in truncus and complete TGA cases by live xPlane imaging (Figure 4.3). It is noted that in the case of corrected TGA and DORV, it showed the normal three-vessel and trachea view. However, live xPlane imaging revealed the abnormal sign. In the case of corrected TGA, it showed the aortic arch when we placed the reference line across left vessel on the 3VT view (originally the pulmonary artery in the normal fetus), and it demonstrated the pulmonary artery when the reference line was put across the middle vessel, which is originally the aortic arch in the normal cases (Figure 4.4 and Figure 4.5). In the case of DORV, it also showed abnormal ductal arch and aortic arch (Figure 4.6 and Figure 4.7). For the case of coarctation of aortic arch, it showed the narrow isthmus of aortic arch on the aortic arch view (Figure 4.8). For the last case which was suspicious of truncus or DORV, it showed the normal ductal arch view and aortic arch view by the live xPlane imaging. This sign made us have the evidence to exclude the diagnosis of truncus and DORV and this case was prenatally diagnosed for abnormal course of aorta caused by diaphragmatic eventration. The first 5 cases were confirmed by autopsy and the last 2 cases were confirmed by postnatal echocardiography.

4.4 Discussion

Prenatal diagnosis of conotruncal anomalies and aortic arch abnormalities was still the challenge for the obstetric sonography (Bull, 1999; Garne et al., 2001). Accumulating evidence showed that these anomalies were diagnosed prenatally

would reduce neonatal morbidity and mortality (Bonnet et al., 1999; Franklin, et al., 2002). The performance of using the four-chamber view alone to screen the fetal heart anomalies was relatively good. However, it had certain limitations in detection of the abnormalities involving the ventricular outflow tract and great arteries (Sharland and Allan, 1992; Wigton et al., 1993). Therefore, some investigators added two ventricular outflow tract views in routine screening program (Achiron et al., 1992; Kirk et al., 1999). Visualizing the left and right outflow tracts, however, is not easy to teach and to learn, and is also operators' skills dependent (Wigton et al., 1993; Rustico et al., 1995). Some doctors used the three-vessel view (3VV) or three vessels and trachea view (3VT) as the additional view to address the weakness of the four-chamber view (Yoo et al., 1997; Yagel et al., 2002; Vinals et al., 2003). The 3VV and 3VT view are both easy to obtain by simply sliding the transducer cephaly from the four-chamber view toward the fetal upper mediastinum. Therefore, we can easily obtain the 3VV and 3VT just like the four-chamber view. As we know, however, 3VV reveals the relationship of pulmonary artery and ascending aorta which do not include the aortic arch, and 3VT reveals the relationship of pulmonary artery and aortic arch, not including the ascending aorta. It is not as directly as displaying the longitudinal view of ductal and aortic arch.

Ductal arch view allows the visualization of continuity of right ventricle, pulmonary valve, pulmonary artery, ductus arteriosus and descending aorta, which provides important information to screen the conotruncal anomalies. It not only reveals the

relationship between pulmonary and aortic valve, but also reveals the crossing of the great arteries. Therefore, the ductal arch view is of great use in screening the conotruncal anomalies and a detailed scan of the fetal heart has been proposed to include the ductal arch view (Allan, 2004).

Aortic arch view can display the whole course of the ascending aorta, aortic arch, aortic isthmus and descending aorta, which provides direct sign in screening and diagnosing aortic arch abnormalities, including the coarctation and interruption of aortic arch.

However, it is not easy to obtain these two views by two-dimensional echocardiography. Like the left and right outflow tract view, it is dependent of operators' skill and need the systematic training. Even for the experienced operators, it is impossible to get these two sections in every situation. Some researchers explored to get these views using three-dimensional echocardiography, including spatiotemporal image correlation (STIC) and automated four-dimensional echocardiography (Goncalves et al., 2006; Espinoza et al., 2006 and 2007; Rizzo et al., 2008). By simply manipulating the acquired 3D volumes, it is easy to visualize the ductal arch view and aortic arch view. Some researches using STIC technique revealed that the ductal arch view was not visualized in most conotruncal anomalies. Thus, examination of the fetal heart played an important role in screening the conotruncal defects with the use of STIC technology (Goncalves et al., 2006;

Espinoza et al., 2006 and 2007; Rizzo et al., 2008).

However, STIC technology is a kind of reconstructed 3D echocardiography. Therefore there are several limitations of these STIC-based approaches. Firstly, the acquisition of a good STIC volume is not easy and is still in the hands of the experts only. Second, generation of the rendering view and multiplanar view are performed as post hoc volume analysis. Third, the multiplanar view is a reconstructed view and therefore any "defect" created by movement artefact may not be easily appreciated.

Live xPlane imaging, based on the real-time 3D technique, allows the scanning of two imaging planes of the fetal heart at different angles in real time. The live xPlane imaging of the fetal heart has been reported by Acar et al (Acar et al., 2005), who successfully used the imaging method to simultaneously visualize the four-chamber view and the great arteries in 60 cases. Although the visualization of ductal arch view and aortic arch view was commented to be possible, no further details were available.

We can easily get the ductal arch view by placing the reference line through pulmonary artery and descending aorta on the 3VT view using real-time three-dimensional echocardiography with live xPlane imaging. Similarly, we can acquire the aortic arch view by putting the reference line through the aortic arch and descending aorta on the 3VT view. Both ductal arch view or aortic arch view and the 3VT view were obtained simultaneously, without the need of transducer movement,

by simply moving the reference line on the 3VT view. As the 3VT view can be obtained as easily as the four-chamber view (Yagel et al., 2002; Vinals et al., 2003), it is possible for less experienced operators to obtain these planes with live xPlane imaging. Furthermore, imaging of ductal and aortic arch view can be used as a compensation of the 3VT view. In this study, one corrected TGA case and one DORV case showed the normal 3VT view but the abnormal ductal and aortic arch view.

There are two obvious advantages of this approach. First, acquisition is simple and quick because both reference and secondary image planes are real-time. Second, movement artefact is not a problem because the manipulation of live xPlane imaging is real-time just like two-dimensional ultrasound. Unlike the multiplanar view of 3D volumes acquired by STIC with the conventional mechanical 3D probes, in which only the primary plane was acquired with full resolution while the other two planes were reconstructed, the two planes acquired by live xPlane imaging are both of high resolution.

In this study, we have shown that the ductal arch view and aortic arch view can be easily and successfully visualized using the live xPlane imaging. The procedure was direct and simple. The operator only needs to obtain a good 3VT view and the ductal and aortic arch view can be obtained simply by activating the live xPlane function and placing the reference line along the according structures on the reference image.

The major limitation is that obtaining the ductal arch view and aortic arch view using live xPlane imaging would not be possible if the reference line cannot be put through the target structures. However, this is not a problem in our experience because fetal movement will bring the fetus in a favorable position for imaging. In our study, the visualization rate of the ductal arch view and aortic arch view is 100% by asking the mothers walking outside for the favorable fetal position. It is believed that, with the development of this newer technology, the reference line could be placed in 360? directions in near future, making the image planes be obtained more easily and simply, which now can only be placed along the ultrasound beam.

In conclusion, live xPlane imaging is an easy and feasible method for real-time imaging of the ductal and aortic arch, and potentially may be a useful tool for the assessment and screening of conotruncal anomalies and aortic arch abnormalities.

Chapter 5 Live xPlane imaging of interventricular septum

5.1 Introduction

The detection rate of structural fetal cardiac abnormalities is much higher in expert hands and referral centers than in non-experienced operators and non-referral centers (Tegnander et al., 1995; Wong et al., 2003; Tegnander and Eik-Nes, 2006). Many subtle abnormalities, including ventricular septal defects (VSDs) in particular, remains low (Myers et al., 2007). VSDs are among the CHDs most often missed at prenatal scanning (Yagel et al., 1997; Hoffman and Kaplan, 2002).

At present, two-dimensional (2D) ultrasound is the main method for the screening and diagnosis of congenital malformations. In order to increase the detection rate of CHD, various views have been proposed, including the four-chamber, outflow tract and three vessels and trachea views (Allan et al., 1986; Carvalho et al., 2002; Zalel et al., 2004). However, none of these methods provides comprehensive visualization of the interventricular septum (IVS), and the four-chamber view provides only a cross-sectional image. The introduction of three-dimensional (3D) echocardiographic techniques using spatiotemporal image correlation (STIC) enabled the acquisition of a heart volume which could then be manipulated to demonstrate cardiac structures that are otherwise difficult to show, such as the IVS (Goncalves et al., 2003; Yagel et al., 2006). However, STIC technology is not real-time, which requires offline

analysis, and the acquisition time is long, making fetal movement artifacts a major problem during the acquisition process.

Real-time 3D echocardiography using a matrix-array probe enables visualization and examination of the pulsating fetal heart in real time, just as real-time two-dimensional echocardiography (Maulik et al., 2003; Acar et al., 2005). There are two major applications of matrix-array probe technology: live 3D imaging and live xPlane imaging. Live xPlane imaging can simultaneously acquire two high resolution views in real time, due to the use of the matrix-array probe. Images are displayed using a split-screen format, with the primary image plane as the reference plane, displayed on the left side of the screen. The secondary image plane can be selected by rotation through a full 360° around the reference plane, together with a lateral tilt of −45° to +45° around the primary image plane at a reference line which can be determined by the operator, or by tilting (elevation) from −30° to +30°.

The objective of this study was to explore the potential use of live xPlane imaging in the visualization and assessment of the IVS, and in particular to describe the methodology.

5.2 Patients and Methods

One hundred and fifty-four women with singleton pregnancies who attended their

routine mid-trimester ultrasound examination in the department of obstetrics and gynecology of a university teaching hospital were invited to participate in this observational study. Informed consent was obtained in all cases. All patients had an additional 3D echocardiographic examination for the purposes of the study. Initially, the examination was arranged at 25–30 weeks of gestation. Towards the end of the study, the examination was arranged at 19–24 weeks of gestation. All examinations were performed using an iU-22 ultrasound machine (Philips Medical Systems, Bothell, WA, USA) equipped with a 7–2 MHz matrix probe (X7-2). No special patient preparation was required. All 3D echocardiography examinations were performed by one operator.

The fetal heart examination was performed using the manufacturer's Fetal Echo preset. First, we acquired an apical four-chamber view of the fetal heart, with the apex either at the 12 o'clock position (if the fetal spine was posterior) or at the 6 o'clock position (fetal spine anterior). Next, the xPlane imaging function was activated. The primary image plane was the apical four-chamber view, displayed on the left side of the screen. By moving the reference line on the primary image plane, a secondary image plane cutting across the reference line was displayed on the right side of the screen. By default, the secondary plane was rotated +90° with respect to the reference plane. For the purposes of this study, this rotation was satisfactory and required no adjustment. The reference line was adjusted within the reference plane to lie along the IVS in the four-chamber view, and the in-plane view of the IVS was

displayed in the right window.

5.3 Results

A total of 154 cases were studied, including four cases with congenital cardiac defects. The mean ? SD maternal age was 32.0 ? 4.2 (range, 21–40) years and the mean ? SD maternal body mass index (BMI) was 21.2 ? 2.8 (range, 16.3 to 32.1). Fifty-five (36.4%) cases were examined between 19 and 24 weeks and 96 were examined between 25 and 30 weeks.

The in-plane view of the IVS was visualized successfully by real-time 3D echocardiography using live xPlane imaging in 153 (99.4%) cases. The cardiac apex was at the 12 o'clock position in 85 (55.6%) cases and at the 6 o'clock position in 68 (44.4%) cases (Figures 5.1 and 5.2). Once an apical four-chamber view was obtained, the use of live xPlane imaging enabled almost immediate acquisition and display of the in-plane view of the IVS. In the case in which visualization of the IVS failed, this was because we could not obtain a satisfactory apical four-chamber view after repeated attempts. The patient had a gestational age of 20 weeks, a normal BMI of 20.2 and a Cesarean section scar.

The seven cases with CHD included isolated VSD, one case of atrioventricular septal defect (AVSD), three cases of truncus arteriosus with VSD, one case of tetralogy of

Fallot, and one case of transposition of great arteries without VSD. The VSDs in the first six cases were clearly displayed in the in-plane view of the IVS using live xPlane imaging (Figure 5.3, Figure 5.4 and Figure 5.5), as was the intact IVS in the last case. The abnormalities of all seven cases were confirmed either by autopsy (two cases with truncus) or postnatal echocardiography and surgery (the remaining 5 cases).

5.4 Discussion

Isolated VSD accounts for 30% of all pediatric cardiac defects and it is commonly found associated with other cardiac anomalies (Wren et al., 2000), yet it is the type of CHD most commonly missed on prenatal screening (Yagel et al., 1997; Hoffman and Kaplan, 2002). The main reason for such poor detection is probably the fact that there is no simple way to examine the IVS in its entirety; the four-chamber view provides only a limited assessment in a cross-sectional image. The ability to visualize the entire IVS in one single image could potentially improve the detection rate of VSD.

Paladini et al. first reported the examination of the entire IVS in the so-called 'in-plane' view using 2D sonographic techniques (Paladini et al., 2003). By careful manipulation and tilting of the ultrasound probe, starting from the long-axis view of the left ventricle, the operator attempted to orientate the IVS in the same plane as the

ultrasound beam, thus displaying the whole IVS, or the 'in-plane' view. However, image acquisition could be difficult and was strongly influenced by fetal position. The overall success rate was 65.8%, this rate being 100%, 36% and 0% when the fetal spine was posterior, lateral and anterior, respectively. Similar findings were reported by Lau, who had an overall success rate of 46% (Lau, 2006).

Another way of visualizing the IVS is by using the rendered view on 3D echocardiographic volumes acquired using STIC technology; using this approach, prenatal identification of VSDs and atrial septal defects has been reported (Yagel et al., 2006; Uittenbogaard et al., 2008). More recently, Myers et al. described another method to rapidly access the in-plane view of the IVS on STIC volumes using multiplanar views instead of the rendered view (Myers et al., 2007). However, there are several limitations of these STIC-based approaches. First, the acquisition of good STIC volumes is not easy and is still in the hands of the experts only. Second, generation of the rendered and multiplanar views is performed as post-hoc volume analysis. Third, the rendered view is a reconstructed 'surface' view and therefore any 'defect' created by overlying shadowing or movement artifacts may not be easily recognized. The last limitation can be partly overcome by directing the STIC acquisition to the plane of the IVS such that the enface view of the septum is in the acquired plane of the STIC acquisition.

The live xPlane imaging method reported here allowed simultaneous visualization of

two different imaging planes of the fetal heart in real time: the four-chamber view and the in-plane view of the IVS. This was achieved without moving the transducer, simply by placing the sample line along the interventricular septum in the four-chamber view. There are three obvious advantages of this approach. First, acquisition is simple and quick because both reference and secondary image planes are real-time. Second, movement artifacts are less of a problem than they are using 3D STIC technology because the acquisition and freezing of an image is similar to that in 2D scanning. Third, the IVS plane is an ordinary ultrasound image rather than a reconstruction and therefore any structure that causes acoustic shadowing will be shown on the same image, making assessment simple and straightforward.

Live xPlane imaging (or 'biplane imaging') of the fetal heart has been attempted (Acar et al., 2005), which indicated that simultaneous visualization of the four-chamber view and the great vessels in 60 cases. However, although they commented that visualization of the IVS was possible, they provided no further details.

In this study we have shown how the in-plane IVS view can be visualized easily and successfully using live xPlane imaging. The procedure is simple; all that is required is a good four-chamber view for the reference image. The in-plane IVS view can then be obtained simply by activating the live xPlane function and, while maintaining the probe's position, placing the reference line along the IVS on the reference image.

We have shown that the in-plane IVS view can be obtained successfully even if the fetal spine is anterior. However, obtaining the in-plane view using live xPlane imaging would not be possible if the axis of the IVS was not parallel to the ultrasound beam. This was not a major problem in our experience because fetal movement usually brought the fetal heart into a favorable position for imaging.

There are several limitations of this study. First, this was only a feasibility study, and establishing a definitive role for this new technology requires further comparative studies with alternative methods of examining the fetal IVS. Second, color Doppler was not used because the color setting of matrix probes remains to be optimized for fetal cardiac examination. Nonetheless, we have demonstrated that examination of the fetal IVS by the live xPlane imaging is both feasible and easy.

In conclusion, live xPlane imaging is an easy method for real-time imaging of the IVS, and potentially may be a useful tool for the assessment and diagnosis of VSD. However, further studies are required to evaluate the sensitivity and reproducibility of this technique in a large population.

Chapter 6 Assessment of interventricular septum with live 3D imaging

6.1 Introduction

Congenital heart disease (CHD) is the most common form of congenital anatomical anomalies (Grandjean et al., 1999). However, the detection rate among the non-referral centres or in the low-risk populations in general remains low, in particular the more subtle abnormalities, including ventricular septal defects (Tegnander et al., 1995; Wong et al., 2003). Many normal and anomalous fetal cardiac structures have not been fully delineated by two-dimensional echocardiography (2DE), such as the lateral view of the interatrial septum and interventricular septum (Yagel et al., 2006).

Ventricular septal defect (VSD) is one of the most missed CHDs at prenatal scanning (Yagel et al., 1997; Hoffman and Kaplan, 2002). Four-chamber view of the heart with color Doppler mapping is often not sufficient to detect VSDs, as the lesions can lie at any level of the three-dimensional septum, and blood flow across the lesion can be intermittent or absent depending on the characteristics of fetal hemodynamics. Various techniques have been proposed to screen the fetal heart (Allan et al., 1986; Carvalho et al., 2002; Zalel et al., 2004). However, none of these provides a proper assessment of the complete interventricular septum (IVS) in its entirety, and the

four-chamber view provides only a cross-sectional image of the IVS.

Paladini et al firstly reported the examination of the entire IVS in the so-called "in-plane" view using 2D ultrasound (Paladini et al., 2003). By careful manipulation and tilting of the ultrasound probe from the long-axis view of the left ventricle, the operator attempted to image the IVS on the same plane as the ultrasound beam to display the "in-plane" view. However, image acquisition could be difficult and strongly influenced by the fetal position. The overall success rate was 65.8% and the rate was 100%, 36% and 0% when the fetal spine was posterior, lateral and anterior, respectively, and similar finding was reported by Lau et al with an overall success rate of 46% (Lau, 2005).

The introduction of three-dimensional echocardiography (3DE) using spatiotemporal image correlation (STIC) enables the acquisition of a heart volume which could then be manipulated to demonstrate cardiac structures otherwise difficult to show, such as the IVS (Goncalves et al., 2003; Yagel et al., 2006). However, the two major limitations of the STIC technology are that the image is not real-time but requires off-line analysis, and the acquisition time is still long which makes fetal movement artefact a major problem during the acquisition.

Real-time 3DE are based on 2D matrix-array probe technologies. The matrix probe utilizes approximately 3000 elements, resulting in image quality that is comparable

with traditional 2D array transducers, and it uses all its channels to transmit and receive ultrasound pulses (Sugeng et al., 2003). These enables the real-time generation of 3D images, which can be manipulated either at real-time or after the images were frozen, and enables the visualization and examination of the pulsating fetal heart at real-time, just like real-time grey-scale scanning (Maulik et al., 2003; Acar et al., 2005 and 2007). We could freeze the 3D images and perform "cine" function in the same way as what we do with 2DE using conventional ultrasound transducers.

There are two major image modalities of real-time 3DE – the live 3D imaging and the live xPlane imaging (biplane imaging). The live 3D imaging provides a real-time volumetric examination of the target organ. In live 3D imaging, it provides a maximum acquisition angle of 72? x 90? to image the fetal heart.

The objective of this study was to explore the potential use of live 3D imaging in the visualization and assessment of the en face view of IVS. The methodology was developed and reported in this study.

6.2 Patients and Methods

One hundred and fifty-four pregnant women with uncomplicated singleton pregnancies who attended their routine mid-trimester scan in a university teaching

hospital were invited to participate in this observational study. The local ethics committee approved the research protocol. Informed consent was obtained in all cases.

Consented subjects were invited back for an additional 3DE examination at a gestation between 19-30 weeks. All examinations were performed using an iU-22 ultrasound scanner (Philips Medical System, Bothell, Washington, USA) with a 7-2MHz matrix-array transducer (X7-2). No special patient preparation was required. All real-time 3DE examinations were performed by one operator.

The fetal heart scanning was performed using the manufacturer's Fetal Echo preset. We firstly acquired a four-chamber view of the fetal heart, with spine either posterior (the apex at about 12 o'clock) or anterior (at about 6 o'clock position) (Figure 6.1a). Next, the live 3D function was activated. The acquisition angle was adjusted to 72? to cover the whole fetal heart and the volume was then cropped by the green box (along the z-axis) to display the 3D imaging of the four-chamber view (Figure 6.1b). When the fetus remained quiescent for 1 to 2 seconds, the "freeze" button was pressed. This produced a cine-loop of real-time 3D volumes. By using the "cine" function, the best volume was chosen. The volume was then cropped along the x-axis by moving the red box to the right side of the IVS on the four-chamber view (Figure 6.1c). The resultant volume was then turned 90? along the y-axis to make the right side of IVS facing the operator (Figure 6.1d). The last step was to perform additional

cropping of the volume dataset along the original z-axis which was accomplished by scrolling back the green box (Figure 6.1e).

In the first 20 cases, we also attempted to visualize the en face IVS view by using a subcostal 4-chamber view approach. However, the image quality of the en face view obtained using live 3D imaging was found to be inferior to that obtained from an apical 4-chamber view, mainly because of the acoustic shadowing caused by the overlying rib cage (Figure 6.2). Therefore, the apical 4-chamber view approach alone was adopted for the rest of the study.

6.3 Results

A total of 154 cases were studies, included 7 cases with CHDs. The mean maternal age was 32.0? .2 (range 21 to 40) years with a mean Body Mass Index (BMI) of 21.2? .8 (range 16.3 to 32.1). Overall, 58 (37.7%) cases were at or before 24 weeks, and 96 (62.3%) were between 25 to 30 weeks.

An en face view of the interventricular septum was successfully visualized by real-time 3DE using live 3D imaging in 153 cases except one. The cardiac apex was at about 12 o'clock position in 85 cases (55.6%), and was at about 6 o'clock in 68 cases (44.4%). Once an apical four-chamber view was obtained, the use of live 3D imaging enables a quick volume-rendered display of the en face view of the IVS

(Figures 6.3 and 6.4).

In one case, visualization of IVS was failed because the operator was unable to obtain a satisfactory apical four-chamber view after repeated attempts and manipulation. The patient was at 20 weeks of pregnancy, with a BMI of 20.2 and a prior caesarean section scar.

There were 7 cases with CHDs, including one case of isolated VSD, one case of atrioventricular septal defect (AVSD), three cases of truncus arteriosus with VSD, one case of tetralogy of Fallot, and one case of transposition of great arteries without VSD. The VSDs in the first 6 cases were successfully displayed in the en face view of the IVS using live 3D imaging (Figure 6.5 and 6.6). In the last case without VSD, the intact IVS was clearly shown in the volume-rendered en face view. The abnormalities of all seven cases were confirmed either by autopsy (two cases with truncus) or postnatal echocardiography and surgery (the remaining 5 cases).

6.4 Discussion

VSD is present isolated in 30% of all pediatric cardiac defects and commonly found as part of a cardiac anomaly (Wren et al., 2000), and yet is easily missed on prenatal screening (Yagel et al., 1997; Hoffman and Kaplan, 2002). The main reason for such poor detection rate is probably due to the fact that there is no simple way to examine

the whole IVS. The four-chamber view provides a limited assessment of the IVS in a cross-sectional image. The ability to visualize the entire IVS in one single image could potentially improve the detection rate.

The en face view (or surgeon's eye view) of the IVS extends our understanding and capabilities of arriving at optimal diagnostic accuracy, and of optimizing imaging for management teams and parental counselling. Visualization of the IVS increases diagnostic accuracy of the size and functionality of VSDs. The ability to differentiate between the right and left faces of the IVS adds to our fuller evaluation of the defect, and may add to our understanding of the pathophysiology of these lesions.

The en face view of IVS can be visualized by STIC technology (Yagel et al., 2006; Uittenbogaard et al., 2008). Using this approach, prenatal identification of VSDs and atrial septal defects has already been reported. However, there are several limitations of these STIC-based approaches. First, the acquisition of good STIC volumes is not easy and is still in the hands of the experts only. Second, generation of the rendered view and multiplanar view are performed as post hoc volume analysis. Third, the rendered view is a reconstructed "surface' view and therefore any "defect" created by overlying shadowing artefact or movement artefact may not be easily appreciated.

The live 3D imaging reported in this study allowed the rapid volume-rendered display of the en face view of IVS without the need of transducer movement, by

rotating and cropping the volumes along the interventricular septum on the four-chamber view. There are two obvious advantages of this approach. First, acquisition is relatively easy and quick. The matrix probe enables the acquisition and display of volume data "real-time", just like conventional 2D imaging. Second, Movement artefact is not a problem because it takes little time to take an image shot. Once the "freeze" button is pressed, the volume data cine loop will be stored and available for review and analysis. The en face view of IVS can then be rapidly visualized.

The use of matrix probe had been reported for 3D fetal echocardiography by several researchers (Scharf et al., 2000; Maulik et al., 2003; Sklansky et al., 2005; Acar et al., 2005; Hata et al., 2006; Acar et al., 2007). They reported that live 3D imaging could be used to instantaneously visualize the normal and abnormal structures of the fetal heart, including the rendered view of four-chamber view, outflow tract view, sagittal view of aortic arch and coronal view of atrioventricular valves. Although the visualization of en face view of ventricular septum was commented to be possible, no further details were available, in particular the protocol and methodology. Moreover, most studies used lower frequency matrix probes (frequency range 4 to 2MHz) and ultrasound scanners (SONOS 7500 live 3D Echo, Philips Medical Systems, Andover, WA, USA) which were optimized for adult or pediatric heart scanning.

In this study, we have developed and reported in detail the methodology of acquiring and examination the en face view of the fetal IVS by real-time 3DE with live 3D imaging. We have shown that the en face view of IVS could be easily and successfully visualized using the live 3D imaging. The procedure was simple. The operator firstly obtained a good four-chamber view, and then froze the volume sequence by pressing the "freeze" button. The en face view of IVS was then obtained by cropping the 3D volumes along the x-axis and then rotating the 3D volumes along the IVS according to standardized steps. In this study, we have shown that the en face view of IVS could be successfully obtained even if the fetal spine is anterior.

There are several limitations of this study. First, this was only a feasibility study, and the definitive role of this new technology required further comparative studies with alternative methods of examining the fetal IVS, in particular the accuracy in the prenatal diagnosis of fetal VSD. Second, color Doppler has not been used in the study because the color Doppler flow imaging of this new matrix probe has not been available with live 3D imaging for fetal cardiac examination yet. It is envisaged that such capability will be available in the future, which might further improve the accuracy of assessment of IVS and prenatal diagnosis of VSD. Nonetheless, we have demonstrated that examination of the fetal IVS by the live 3D imaging is feasible.

In conclusion, live 3D imaging can be used to display the en face view of fetal IVS,

and potentially may be a useful tool for the assessment and diagnosis of fetal VSDs. However, further studies are required to evaluate the sensitivity and reproducibility of this technique in a large population.

Chapter 7 Comparison of real-time 3DE and STIC in assessment of fetal interventricular septum

7.1 Introduction

Fetal ventricular septal defect (VSD) is one of the most missed congenital heart diseases prenatally (Yagel et al., 1997; Hoffman and Kaplan, 2002). This is mainly because conventional 2D ultrasound cannot examine the fetal interventricular septum (IVS) in entirety and color Doppler flow imaging is often not sufficient to detect VSDs due to the similar pressure between two ventricles (Yagel et al., 2006). Although some researchers found that the whole fetal IVS can be visualized by the so-called 'in-plane' view of fetal IVS, this technique was still at the hands of experts and greatly affected by fetal position (Paladini et al., 2003; Lau et al., 2006).

Three-dimensional echocardiography provides the solution to visualize the IVS from the lateral view, which can easily assess the whole fetal IVS in entirety (Yagel et al., 2006; Meyer et al., 2007). Nowadays, there are two types of 3D ultrasound, STIC and real-time 3DE, can be used to image the beating fetal heart (Goncalves et al., 2003; DeVore et al., 2003; Vinals et al., 2003; Maulik et al., 2003; Goncalves et al., 2004; Acar et al., 2005; Yagel et al., 2006; Paladini et al., 2006; Vinals et al., 2006; Meyers et al., 2007; Hata et al., 2008; Gindes and Achiron, 2008). They can visualize the fetal IVS in either rendered or multiplanar mode.

Spatiotemporal image correlation (STIC) is a kind of reconstructive 3D ultrasound. STIC is an automated volume acquisition of the entire fetal heart by using a mechanical volume transducer and specific software. It uses the average heart rate from systolic incursion peaks to gate the fetal heart; thereby it can not be acquired and manipulated in real time. Multiplanar display and rendered display are the initial and basic image modalities with STIC technology. Multiplanar display can demonstrate three orthogonal images at the same time. By moving the reference point, the operator can manipulate the volume dataset to display any plane within the volume (Devore et al., 2004; Yagel et al., 2007; Uittenbogaard et al., 2008). Rendered view can visualize any intracardiac structure with a depth perspective view. Therefore, the fetal IVS can be assessed from the lateral view with either multiplanar or rendered display mode. After many years' development, there are a lot of ultrasound techniques can be combined with STIC technology, including inversion mode, color Doppler, Power Doppler, tomographic ultrasound image (TUI) and B-flow, to evaluate the beating fetal heart.

Real-time 3DE is another kind of 3D techniques using a matrix-array transducer, which can visualize the beating fetal heart in real time (Acar et al., 1999; Sugeng et al., 2003). It also has two image modalities: live xPlane imaging and live 3D imaging. Live xPlane imaging can simultaneously visualize two high resolution views in real time. The primary image plane is the reference plane, displayed on the left side of the

screen. The secondary image plane can be selected by rotation through a full 360◦ around the reference plane, or by a lateral tilt of −45? to +45? around the primary image plane at a reference line which can be determined by the operator, or by tilting vertically (elevation) from −30? to +30? Live 3D imaging provides a real-time volumetric examination of the target organs. Live 3D imaging can display the fetal IVS in rendered mode. We had reported the methodology of how to imaging the fetal IVS with real-time 3DE (Xiong et al., 2009 and 2010).

In our best knowledge, there is no study to compare these two 3DE technologies. The objective of this study was to compare the role of real-time 3DE and STIC technology in assessment of the fetal IVS.

7.2 Patients and Methods

7.2.1 Patients

50 pregnant women with singleton pregnancies who had their routine mid-trimester scan were invited to attend this study. The research protocol was approved by local ethics committee and informed consent was obtained in all cases. These fetuses were scanned and diagnosed by two experienced operators in fetal cardiology. The final diagnosis was made if the diagnosis of fetal heart by each operator was the same. If the diagnosis of the two operators is different, the patients would be referred to

another experienced doctor. The fetus would be rescanned by these experienced doctors to make the final diagnosis and judged whether the VSD existed or not. Follow-up were made to confirm the diagnosis.

7.2.2 IVS displayed by STIC

All STIC examinations were performed by using either Voluson 730 or E8 ultrasound scanner (GE Medical System, Kretz, Austria) with a 6-2MHz mechanical volume transducer (RAB8-4) by one operator using the manufacturer's Fetal Echo preset.

Volume dataset were acquired by using apical four-chamber view and the sagittal view of fetal thorax with the fetal spine posterior as the starting plane, respectively. The acquisition angle was set to 20? 30? to cover the entire fetal heart and acquisition time was set to 10 seconds. When the fetus was still, the acquisition was activated after asking the mother to hold her breath for 10 seconds. The volume dataset were stored for further offline analysis after acquisition of a satisfactory volume. The satisfactory volumes were defined as no obvious motion artefacts in the B-plane.

The offline analysis of the volume dataset to visualize the fetal IVS was performed using 4D VIEW® 9.0 (GE Medical system, Kretz, Austria) software. When assessing the volumes acquired with apical four-chamber view as the starting plane, we firstly

rotated the volumes to make the IVS parallel to y-axis and then put the reference dot at the right side of the fetal IVS in the A-plane. The lateral view of the fetal IVS (so-called 'in-plane' view of IVS) was displayed in the B-plane (Figure 7.1). Thereafter, activated the rendered mode and adjusted the rendered box to observe the volumes from the right side of the fetal IVS in the A-plane. The rendered view from the lateral side of IVS (so-called 'en face' view of IVS) can be visualized by moving the green line of ROI to the right side of the IVS in the A-plane (Figure 7.2).

When assessing the volumes acquired with the sagittal view of the fetal thorax as the starting plane, we firstly moved the reference dot just below the aortic valve and the four-chamber view was displayed in the B-plane and then rotated the volume to make the axis of the fetal heart parallel to the y –axis in the B-plane. The in-plane view of IVS was displayed in the A-plane by putting the reference dot at the right side of IVS in the B-plane (Figure 7.3). Activated the rendered view and adjusted the rendered box to observe the volumes from the right side of fetal IVS in the four-chamber displayed in the B-plane. The en face view of IVS could be displayed by putting the green line of rendered box to the right side of the IVS (Figure 7.4).

7.2.3 IVS displayed by real-time 3DE

All real-time 3DE examinations were performed using an iU-22 ultrasound scanner (Philips Medical System, Bothell, Washington, USA) with a 7-2MHz matrix

transducer (X7-2) by another operator using the manufacturer's Fetal Echo preset. No special preparation was required.

We had reported the methodology of how to image the lateral view of fetal IVS using real-time 3DE with live xPlane imaging and live 3D imaging (Xiong et al., 2009 and 2010). The in-plane view of IVS could be visualized by acquiring an apical four-chamber view and putting the reference line along the right side of IVS (see Figure 5.1). The en face view (i.e. rendered view) of IVS could be acquired by rotating and cropping the volumes. The methodology of how to image the en face view of fetal IVS was described in detail in Chapter 6 (see Page 64, 65 and Figure 6.1).

7.2.4 Score the images of IVS

There were totally six images of IVS obtained for each fetus: live xPlane image, live 3D image, multiplanar image and rendered image with the four-chamber view as the starting plane, multiplanar image and rendered image with the sagittal view of the fetal thorax as the starting plane. Therefore, these images were grouped into six groups and randomized them in sequence for the further analysis, respectively. The images were scored by another doctor, who was familiar with fetal 3DE and blinded to the results of the fetus, according to the image quality, the outline of the fetal IVS and motion artefact. Good image quality and clear outline of IVS was scored 1,

whereas was scored 0. No motion artefact was scored 1, whereas was scored 0. Thereafter the overall score was calculated by adding the score of image quality, the outline of IVS and motion artefact. The operator was also asked to judge whether VSD existed or not and the results were compared with the final diagnosis. The sensitivity, specificity, false positive percentage, positive likelihood ratio, false negative percentage and negative likelihood ratio of each group was also calculated.

The score was then compared between each group using one-way ANOVA test. All statistical analyses were performed using the Statistical Package for Social Sciences for Windows 15.0 (SPSS Inc, Chicago, IL, USA).

7.3 Results

Fifty cases, including 31 cases of normal fetus and 19 cases of fetal CHDs, were scanned by both STIC and real-time 3DE. The mean maternal age was 29.2? .6 (range 21 to 42) years with a mean Body Mass Index (BMI) of 23.2? .4 (range 19.8 to 31.6). All the cases were scanned between 21 to 28 weeks (mean 23.3? .8 weeks).

There were 15 cases with VSD and 4 cases without VSD in CHD fetus and 31 cases of normal fetus in this study (Table 7.1). The Sensitivity, specificity, false positive, false negative, positive likelihood ratio and negative likelihood ratio of each modality in assessment of fetal VSDs were calculated and describe in Table 7.2. Live

xPlane imaging of the fetal IVS has the highest specificity and the highest positive likelihood ratio, while its sensitivity is relatively low. The IVS images obtained from the STIC technique with the four-chamber view as the starting plane have relatively higher sensitivity while the specificity and positive likelihood ratio is relatively low. The IVS images acquired with multiplanar view of STIC from the sagittal view as the starting plane has the similar sensitivity and specificity to real-time 3DE.

A total 300 images of the lateral view of fetal IVS were obtained and grouped into six groups: live xPlane image (Group 1), live 3D image (Group 2), multiplanar view of STIC from four-chamber view (Group 3), rendered view of STIC from four-chamber view (Group 4), multiplanar view of STIC from the sagittal view (Group 5), rendered view of STIC from the sagittal view (Group 6). The score of each group was described in Table 7.3. It showed significant difference between groups for all the parameters ($P<0.01$). There was no significant difference between Group 1, 2, 5, 6 and between Group 3, 4 ($P>0.05$). There was significant difference between group 3, 4 and group 1, 2, 5, 6 ($P<0.05$). It means that the image quality of real-time 3DE (Group 1, 2) and STIC with the sagittal view as the starting plane (Group 5, 6) is significantly superior to that of STIC with the four-chamber view as the starting plane (Group 3, 4) ($P<0.05$).

7.4 Discussion

Although the fetal heart screening techniques developed greatly in last two decades, it is difficult to detect the fetal CHDs prenatally yet. Many new technologies, including real-time 3DE and STIC technique, were attempted to improve the detection rate of fetal CHDs recently.

Both real-time 3DE and STIC technique can assess the fetal IVS in entirety, which have the potentials to improve the detection rate of fetal VSD (Yagel et al., 2006; Meyer et al., 2007, Xiong et al., 2009). The methods are relatively simple and easy to understand.

In this study, fifty cases were examination by real-time 3DE and STIC technique. The image quality in the group of STIC from the four-chamber view (Group 3, 4) is much worse than other groups ($P<0.05$). This was because the lateral view of IVS acquired with the four-chamber view as the starting plane is perpendicular to the four-chamber view, thereby producing more motion artefacts. The lateral view of IVS acquired by STIC with the sagittal view as the starting plane has the better image quality, which is due to that the IVS view is parallel to the starting plane, therefore less motion artefact produced. As to real-time 3DE, motion artefact is no more the problem. There were no significant differences in image quality between Group 1, 2, 5, 6. It indicated that we should use the sagittal view as the starting plane or use real-time 3DE to assess the entire IVS. Real-time 3DE has the similar effect to the STIC volume with the sagittal view as the starting plane in evaluating the fetal

IVS.

However, there are several limitations of the STIC technique. First, acquiring a good STIC volume is not easy and is still in the hands of the experts. Second, manipulating the volumes is not easy when using the sagittal view as the starting plane, while the manipulation of the volume is easy but lower image quality and more motion artefacts might affect the diagnosis when using the four-chamber view as the starting plane.

The methodology of real-time 3DE is simple and easy to understand and also has the high efficacy. In our study, the visualization rate was as high as 100% in both normal case and abnormal cases. The detection rate of fetal VSD in this study is only about 53.3% with no positive false rate and 16.7% negative false rate for live xPlane imaging and with a positive false rate of 27.3% and a negative false rate of 17.9% for live 3D imaging. The low detection rate of fetal VSD by real-time 3DE may be due to two reasons. One is that the image of 3D ultrasound is quite different as conventional 2D ultrasound. Therefore, interpretation of 3D images need re-consideration. The other is that the score is made by the observer after the observation of still images, not the beating fetal heart. Nonetheless, we compared the six modalities of 3DE and demonstrated that real-time 3DE evaluation of the fetal VSD is feasible and its effect is similar to the STIC volume acquired from the sagittal view and superior to the STIC volume acquired from the four-chamber view.

The main limitation of this study is that the still images, not the videos, is available to the observer to make the diagnosis. Additionally, only fifty cases were involved in this study. Further study need to evaluate the sensitivity and reproducibility in a large population.

In conclusion, the image quality of real-time 3DE is similar to the images acquired by STIC from the sagittal view and superior to that obtained by STIC from the four-chamber view. Real-time 3DE can be used to assess the fetal IVS with the higher image quality and specificity compared to the STIC technique, which has the potentials to improve the detection rate of fetal VSD.

Chapter 8 A novel way to screen the fetal conotruncal anomalies with live xPlane imaging

8.1 Introduction

Conotruncal anomalies are the leading causes of cyanotic congenital heart disease characterized by the abnormal development of conotruncal septum (Paladini et al., 1996; Tometzki et al., 1999; Sivanandam et al., 2006). These anomalies include tetralogy of Follot, absent pulmonary valve syndrome, double outlet right ventricle (DORV), transposition of the great arteries (TGA), malposition of great arteries and truncus arteriosus. Although the screening techniques of fetal congenital heart disease were greatly improved, the detection rate of conotruncal anomalies was still low (Smith et al., 1995; Sivanandam et al., 2006). This is mainly because these anomalies usually have the normal four-chamber view. Thus, using four-chamber view to screen the fetal heart will miss some outflow tract anomalies prenatally.

The solution to resolve the problems is to use screening method recommended by most guidelines to screen the fetal heart (AIUM, 2003; ISUOG, 2006). It includes four cardiac planes: the four-chamber view, left and right outflow tract view and three-vessel and trachea view. However, visualizing these four views is not easy. It needs systematic training and depends on the operators' experience (Tegnander and Eik-Nes, 2006). Therefore, finding a simple way to screen the fetal heart will bring

great benefit, which would improve the detection rate of fetal conotruncal anomalies and make the training program much easier.

Some researchers attempted to use spatiotemporal image correlation (STIC) to improve the detection rate of fetal conotruncal anomalies (Devore et al., 2003; Goncalves et al., 2003 and 2006; Yagel et al., 2007; Espinoza et al., 2006 and 2007). Most of them tried to detect the fetal conotruncal anomalies by visualizing the left and right outflow tract view. The procedure was relatively complex which was not fit for routine application. Espinoza et al. reported that using the ductal arch view alone can be used to detect the fetal conotruncal anomalies and the detection rate was as high as 94.4% (Espinoza et al., 2007). The ductal arch view allows visualization of right ventricle in continuity with the pulmonary artery, ductus arteriosus and descending aorta, together with the transverse view of the ascending aorta (Allan, 2004). However, STIC technique is a kind of reconstructed three-dimensional echocardiography. It can not be acquired and manipulated in real time.

The live xPlane imaging, a kind of real-time 3DE techniques using a matrix-array transducer, can simultaneously visualize two high resolution views in real time (Sugeng et al., 2003). The primary image plane is the reference plane, displayed on the left side of the screen. The secondary image plane can be selected by rotation through a full 360° around the reference plane, or by a lateral tilt of −45° to +45° around the primary image plane along the reference line which can be determined by

the operator, or by tilting vertically (elevation) from −30◦ to +30◦.

The objective of this study was to evaluate the role of live xPlane imaging visualization of ductal arch view in the screening of fetal conotruncal anomalies.

8.2 Patients and Methods

200 pregnant women with uncomplicated singleton pregnancies who had their routine mid-trimester scan were enrolled in this observational study. The research protocol was approved by local ethics committee and informed consent was obtained in all cases.

All real-time 3DE examinations were performed using an iU-22 ultrasound scanner (Philips Medical System, Bothell, Washington, USA) with a 7-2MHz matrix transducer (X7-2) by one operator using the manufacturer's Fetal Echo preset. No special patient preparation was required.

All the cases were firstly scanned by one operator to visualize the ductal arch view with live xPlane imaging and judge whether it is the conotruncal anomalies or not. All the patients were then scanned by the same operator with conventional two-dimensional transducer and referred to another experienced doctor in fetal echocardiography, who was blind to the results scanned with live xPlane imaging, to

make the diagnosis. If the results were different, another experienced expert in fetal echocardiography would perform the scan again to decide which type of CHDs it is. Finally, the results were compared to evaluate the effect of live xPlane imaging in the screening of the fetal conotruncal anomalies.

The detailed method of visualizing the ductal arch view with live xPlane imaging is described as follow. Firstly an apical four-chamber was visualized and then live xPlane imaging was activated. Put the reference line through the sternum and descending aorta (i.e. through the right ventricle, criss-cross, left atrium and descending aorta in the four-chamber view) and observe the image displayed on the right window to judge whether the ductal arch view existing or not (Figure 8.1). The ratio of inner diameter of pulmonary artery (PA) and ascending aorta (AAO) was calculated as well. PA was measured just above the pulmonary valve and AAO was measured between the anterior and posterior wall on the same plane (Figure 8.2). If the ductal arch view exists and the ratio of PA to AAO is more than 1, the conotruncal anomalies were excluded. Otherwise, the ductal arch view disappears or the ratio of PA to AAO is less than 1, the conotruncal anomalies were suspected by the live xPlane imaging.

The comparison between conotruncal and non-conotruncal anomalies was then compared using Chi-square test. All statistical analyses were performed using the Statistical Package for Social Sciences for Windows 15.0 (SPSS Inc, Chicago, IL,

USA).

8.3 Results

A total of 200 cases were enrolled in this study and scanned by both live xPlane imaging and conventional two-dimensional echocardiography. The mean maternal age was 28.6? .4 (range 19 to 39) years with a mean Body Mass Index (BMI) of 22.4? .5 (range 17.6 to 35.1). All the cases were scanned between 18 to 27 weeks (mean 23.0? .3 weeks).

There were 152 normal cases, 25 conotruncal anomalies and 23 other types of fetal CHDs were involved in this study. The visualization rate of ductal arch view displayed by live xPlane imaging was 100% (152/152) in normal cases, 8% (2/25) in conotruncal anomalies and 69.7% (16/23) in non-conotruncal CHDs, respectively. The ductal arch view usually disappears in the conotruncal anomalies cases except the tetralogy of Fallot, which has almost the normal ductal arch view except the PA/AAO ratio is less than 1 in the ductal arch view (Table 8.1). The conotruncal anomalies, such as truncus, TGA and DORV, can be easily detected by the method that the ductal arch view cannot be visualized with live xPlane imaging (Figure 8.3, Figure 8.4). Tetralogy of Fallot, however, is relatively difficult to be detected by ductal arch view, which might be detected by carefully observing the PA/AAO ratio (Figure 8.5). In this study, 2 cases with tetralogy of Fallot have the normal ductal

arch view. There were significant differences between the conotruncal and non-conotruncal anomalies ($P<0.001$). In 23 cases with other CHDs, only 7 cases had the abnormal ductal arch view, including pulmonary atresia, severe pulmonary stenosis, hypoplastic left heart syndrome and malposition of fetal heart (Table 8.2).

8.4 Discussion

Although the fetal heart screening techniques developed greatly in last twenty years, it is still difficult to detect the fetal CHDs prenatally. Screening the fetal conotruncal anomalies is still a great challenge for the non-experienced operators because fetal conotruncal anomalies usually have the normal four-chamber view. Therefore, it was recommended by many guidelines that the 'extended basic' screening program should be performed for the fetal heart screening, if technically feasible (AIUM, 2003; ISUOG, 2006). It combined four sections: the four-chamber, LVOT, RVOT and 3VT view. The four-chamber view is the most basic screening plane and is easy to acquire. Three-vessel and trachea view is parallel to the four-chamber view and is relatively easy to be imaged by just titling the transducer slightly towards the fetal head. However, acquiring the LVOT and RVOT is not easy and the training program of visualizing LVOT and RVOT is difficult to teach and to learn, and is also time-consuming (Wigton et al., 1993; Rustico et al., 1995).

Many new technologies, including spatiotemporal image correlation (STIC), were

attempted to improve the detection rate of fetal CHDs recently. With the STIC technique, the four-chamber view, the ventricular outflow tract view, and three-vessel and trachea view can be viewed by simply scrolling through the volume dataset (Goncalves et al. 2006). By manipulating the volume dataset, the operator can even display any plane within the volume (Devore et al., 2004; Yagel et al., 2007; Uittenbogaard et al., 2008). Espinoza et al. attempted to visualize the ductal arch view alone with STIC technique to detect the fetal conotruncal anomalies (Espinoza et al., 2007). This method is relatively simple and easy to understand and has a high detection rate. STIC technique has the potentials to reduce the operators' dependence in screening the fetal conotruncal anomalies. However, there are several limitations of the STIC technique. First, STIC is a kind of reconstructive three-dimensional echocardiography. Acquiring a good STIC volume is not easy and is still in the hands of the experts. Second, manipulating the volumes is performed as post hoc volume analysis and therefore it is greatly affected by the fetal motion artefact.

The application of matrix probe in fetal heart had been reported by several researchers (Scharf et al., 2000; Maulik et al., 2003; Sklansky et al., 2005; Acar et al., 2005; Hata et al., 2006; Acar et al., 2007). Live xPlane imaging can display two high-resolution real-time views of the target organ, due to the use of the matrix-array probe (Sugeng et al., 2003). The main advantage of live xPlane imaging in displaying the ductal arch view is that only the apical four-chamber view is needed and the ductal arch view will be visualized by moving the reference line through the

sternum and the descending aorta (i.e. through the right ventricle, criss-cross, left atrium and descending aorta) on the four-chamber view. This method is simple and easy to understand and also has high efficacy. In our study, the visualization rate was as high as 100% in normal case. 92% of fetal conotruncal anomalies were detected with live xPlane imaging in our study, compared to that of non-conotruncal anomalies (30.3%, $P<0.001$). The detection rate of conotruncal anomalies with visualization of ductal arch view was similar to the previous study performed with STIC technique (Espinoza et al., 2007), which the detection rate was about 94%. Therefore, it is possible to improve the detection rate of fetal conotruncal anomalies with live xPlane imaging.

The main limitation of this study is that the reference line can be only come from the midline of transducer and can not be manipulated from all directions, which made the acquisition time much longer if the fetus was in unfavourable position. It is envisaged that such capability will be available in the future, which might simplify the training program and then reduce the operator-dependent. Nonetheless, we demonstrated that screening the fetal conotruncal anomalies with live xPlane imaging is feasible and the method is easy to understand.

In conclusion, ductal arch view can be easily visualized with live xPlane imaging and this method can be used to screen the fetal conotruncal anomalies. The method is simple and feasible, which may be a useful tool for the assessment and diagnosis of

fetal conotruncal anomalies.

Chapter 9 Can live xPlane imaging of the in-plane view of interventricular septum be used to screen fetal conotruncal anomalies

9.1 Introduction

Conotruncal anomalies include tetralogy of Follot, absent pulmonary valve syndrome, double outlet right ventricle (DORV), transposition of great arteries (TGA) and truncus arteriosus. These anomalies are the main cause of cyanotic congenital heart disease characterized by the abnormal development of conotruncal septum (Paladini et al., 1996; Tometzki et al., 1999; Sivanandam et al., 2006). These anomalies usually have a normal four-chamber view and thus using the four-chamber view alone to screen the fetal heart might miss the anomalies involved the ventricular outflow tract. Therefore, we should use the four cardiac planes, including the four-chamber, ventricular outflow tract and three-vessel and trachea view, to screen the fetal heart (AIUM, 2003; ISUOG, 2006). However, visualizing these four screening views is not easy. It depends on the operators' experience and the operator needs systematic training (Tegnander and Eik-Nes, 2006). Therefore, finding a simple method to screen the conotruncal anomalies is of great benefit, which would improve the detection rate and make the training program much easier.

The in-plane view was firstly introduced by Professor Paladini in 2003 (Paladini et al.

2003). It was originally used to detect fetal ventricular septal defect (VSD). More importantly, this plane displays the longitudinal view of aorta and short axis of pulmonary artery as well. Therefore it is possible to use this view to screen the fetal conotruncal anomalies. The definition of in-plane view of interventricular septum (IVS) was a modified plane of the left outflow tract, conducted a plane perpendicular to that of long axis of left ventricle (Figure 9.1). With conventional two-dimensional ultrasound, it can be acquired by firstly obtaining a long axis view of the left ventricle as usual and then carefully rotate the transducer toward right ventricle. However, acquiring the in-plane view of IVS is still in the hands of experts in fetal echocardiography and also dependent on fetal position (Paladini et al., 2003; Lau, 2006). It is difficult for most of operators to obtain the in-plane view of IVS and the visualization rate was reported to be zero when the fetal spine was anterior (Paladini et al., 2003; Lau, 2006).

Another way of visualizing the entire IVS is using spatiotemporal image correlation (STIC) technology (Yagel et al., 2006; Uittenbogaard et al., 2008). More recently, Myers et al. attempted to rapidly obtain the in-plane view of IVS using the STIC techniques with the multiplanar views (Myers et al., 2007). However, there are several limitations of these STIC-based approaches. Firstly, the acquisition of good STIC volumes is not easy and is still in the hands of the experts only. Secondly, generation of the render view and multiplanar view are performed as post hoc analysis and not in real time. Thirdly, movement artefact is inevitable because it is

impossible to keep the fetus still and hold the breath. The above limitation using STIC may be partly overcome by starting the STIC acquisition in the plane of the IVS such that the in-plane view of the septum is in the acquired plane, which results in a high resolution in-plane view of IVS. However, the manipulation of the volume dataset is not as simple as starting the acquisition from the four-chamber view.

We had reported that the in-plane view of IVS can be easily imaged in 153 fetuses with live xPlane imaging, including 4 cases with VSD, and only one case was missed (Xiong et al., 2009). The visualization rate is as high as 99.4% (153/154) and the in-plane view of IVS can be imaged even with the spine anterior.

The objective of this study was to evaluate the feasibility of live xPlane imaging visualization of the in-plane view of IVS in the screening of the fetal conotruncal anomalies.

9.2 Patients and Methods

200 pregnant women with singleton pregnancies were enrolled in this observational study. The research protocol was approved by local ethics committee and informed consent was obtained in all cases.

All real-time 3DE examinations were performed using an iU-22 ultrasound scanner

(Philips Medical System, Bothell, Washington, USA) with a 7-2MHz matrix transducer (X7-2) by one operator using the manufacturer's Fetal Echo preset. No special patient preparation was required.

All the cases were firstly scanned by one operator to obtain the in-plane view of IVS with live xPlane imaging and judge whether it is normal or not. The normal case is described that no VSD detected and the normal relationship of aorta and pulmonary. Then all the patients were referred to another experienced doctor, which was blind to the results scanned with live xPlane imaging, to make the diagnosis. Finally, the results were compared to evaluate the feasibility of live xPlane imaging of in-plane view of IVS in the screening of the fetal conotruncal anomalies.

The detailed method of visualizing the in-plane view of IVS with live xPlane imaging is described as follow. Firstly an apical four-chamber was visualized and then live xPlane imaging was activated. Putting the reference line along the IVS on the four-chamber view and the in-plane view of IVS was immediately visualized in the right window (Figure 9.2).

The comparison between conotruncal and non-conotruncal anomalies was then compared using Chi-square test. All statistical analyses were performed using the Statistical Package for Social Sciences for Windows 15.0 (SPSS Inc, Chicago, IL, USA).

9.3 Results

A total of 200 cases were scanned with live xPlane imaging. The mean maternal age was 28.6? .4 (range 19 to 39) years with a mean Body Mass Index (BMI) of 22.4? .5 (range 17.6 to 35.1). All the cases were scanned between 18 to 27 weeks (mean 23.0? .3 weeks).

The detection rate of in-plane view of IVS displayed by live xPlane imaging was 100%. The abnormal in-plane view of IVS was described in Table 9.1 and Table 9.2. There were 25 cases of conotruncal anomalies enrolled in our study, including 9 cases of truncus, 8 cases of tetralogy of Fallot, 3 cases of DORV and 5 cases of TGA (Table 9.1). It showed abnormal in-plane view in 22 (88%) cases of conotruncal anomalies, except three cases of tetralogy of Fallot. The characteristics of truncus arteriosus and TGA in the in-plane view of IVS were that only one arterial trunk originated from the ventricles (Figure 9.3 and Figure 9.4). The characteristics of DORV were that two parallel arteries come from the ventricles (Figure 9.5). However, it showed normal in-plane view of IVS in tetralogy of Fallot except the large VSD (Figure 9.6).

There were 23 cases of other fetal CHDs enrolled in this study (Table 9.2), including 4 cases of atrioventricular septal defect (AVSD), 1 case of dextroposition, 1 case of

atrial septal defect (ASD), 1 cases of ectopia with single ventricle, 4 cases of ventricular septal defect (VSD), 1 case of right-sided aortic arch, 3 cases of persistent left superior vena cava (LSVC), 1 case of hypoplastic left heart syndrome (HLHS), 2 cases of pulmonary stenosis (PS), 3 cases of pulmonary atresia, 1 case of cardiac tumor and 1 case of pericardial perfusion. There were 6 cases showing abnormal relationship of aorta and pulmonary artery in the in-plane view of IVS, including 1 case of dextroposition, 1 case of ectopia with single ventricle, 2 cases of PS (Figure 9.7), 1 case of pulmonary atresia and 1 case of HLHS. There were significant differences of abnormal in-plane view of IVS between the conotruncal and non-conotruncal anomalies ($P<0.001$).

9.4 Discussion

Although the fetal heart screening techniques developed greatly in last two decade, detecting the fetal conotruncal anomalies is still a great challenge for the non-experienced operators. This is due to the fetal conotruncal anomalies usually have a normal four-chamber view. Therefore, screening the conotruncal anomalies should visualize the ventricular outflow tract. However, acquiring the LVOT and RVOT is not easy and the training program is difficult to teach and to learn, and is also time-consuming (Wigton et al., 1993; Rustico et al., 1995).

The in-plane view of IVS was firstly introduced to enhance the assessment of the

fetal IVS (Paladini et al., 2003). Its application often provides more additional information. According to our observation, the in-plane view can not only depict the limit of IVS to detect the VSD, but also demonstrate the relationship of aorta and pulmonary artery. In normal fetal heart, aorta is in longitudinal view and pulmonary artery in short axis. In our study, this relation exists in all 152 cases of normal fetal heart. This relationship of aorta and pulmonary artery will be lost in most fetal conotruncal anomalies. Therefore, it is possible to use this view to detect not only the VSDs but also the conotruncal anomalies.

The difficulties are that visualizing the in-plane view of IVS is not easy to each operator with conventional two-dimensional ultrasound. Acquiring the in-plane view of IVS was still in the hands of experts in fetal echocardiography and also dependent on fetal position (Paladini et al., 2003; Lau, 2006). It was reported that the in-plane view of IVS can not be displayed when the fetal spine is anterior by 2D ultrasound.

Myers et al. attempted to rapidly visualize the in-plane view of IVS using STIC technique (Myers et al. 2007). They successfully visualize the in-plane view of IVS with STIC technique in no more than 30s. Using STIC technique, the operators can even display any plane within the volume by manipulating the volume dataset (Devore et al., 2004; Yagel et al., 2007; Uittenbogaard et al., 2008). However, acquisition and manipulating the volumes data is not easy and in the experts' hands as well. Additionally, STIC is a kind of reconstructive three-dimensional

echocardiography. Movement artefacts are inevitable. Volume dataset can only be analyzed after it were acquired and stored and cannot be processed in real time.

With the advent of matrix probe, real-time three-dimensional can be applied to image the fetal heart (Scharf et al., 2000; Maulik et al., 2003; Sklansky et al., 2005; Acar et al., 2005; Hata et al., 2006; Acar et al., 2007). Nowadays, there are two main image modalities of fetal real-time three-dimensional echocardiography. One is live xPlane imaging and the other is live 3D imaging. Live xPlane imaging can display two high-resolution real-time views of the target organ (Sugeng et al., 2003). We had reported how to image the in-plane view of IVS with live xPlane imaging (Xiong et al. 2009). The method is simple and easy to understand. The thing we need to do is to visualize a good apical four-chamber view, either with the spine posterior or anterior, and then activated the live xPlane function. The in-plane view of IVS will be imaged immediately when the reference line was placed along the IVS. Four-chamber view is the basic screening plane and easy to be imaged to each operator after simple training. Live xPlane function is easy to be manipulated as well. Therefore, it is feasible to use this new technology to screen the fetal conotruncal anomalies.

There were 25 cases of conotruncal anomalies enrolled in this study and 18 cases (72%) had the abnormal relationship of aorta and pulmonary artery on the in-plane view of IVS. The other 7 cases of conotruncal anomalies were all the tetralogy of Follot. Among them, there were 4 cases can detect a VSD in the in-plane view of

IVS. Therefore, totally 22 cases (88%) in our study had the abnormal in-plane view of IVS. There were significant differences between conotruncal and non-conotruncal anomalies ($P<0.001$). In the other 23 cases of other fetal CHDs, only 6 cases (26%) had the abnormal relationship of aorta and pulmonary artery on the in-plane view of IVS. Among them, the dextroposition of fetal heart and ectopia of fetal heart had the abnormal relationship of aorta and pulmonary due to the malposition of the great arteries; HLHS had the abnormal relationship due to the very thin aorta which is difficult to be imaged; PS and pulmonary atresia had the abnormal in-plane view of IVS due to hypoplasia or dilated pulmonary artery. However, it showed the normal relationship of aorta and pulmonary artery in all the 152 cases of normal fetal heart and the other 17 non-conotruncal anomalies.

The main limitation of this study is that the reference line can be only come from the midline of transducer and can not be manipulated from all directions, which made the acquisition time much longer if the fetus was in non-proper position. It is expected that such capability will be available in near future, which would simplify the training program and then reduce the operator-dependence.

In conclusion, live xPlane imaging of the in-plane view of IVS is feasible to screen the fetal conotruncal anomalies and the method is simple and easy to understand, which may be a useful tool for the assessment of fetal conotruncal anomalies to non-experienced operators.

Chapter 10 Live xPlane imaging assists first-trimester acquisition of a true midsagittal section

10.1 Introduction

First-trimester nuchal translucency (NT) thickness measurement at 11+0 to 13+6 weeks of gestation plays an important role in prenatal screening of fetal chromosomal abnormalities (Markov et al., 2004; Kagan et al., 2006). NT is one of the best single markers for fetal trisomy 21, with a detection rate of 70–80% for a screen-positive rate of 5% (Nicolaides, 2004). The detection rate can be increased to over 90% by combining NT with first-trimester maternal serum analysis and other first-trimester ultrasound markers (Avgidou et al., 2005; Sonek et al., 2006; Falcon et al., 2006; Leung et al., 2007).

To maintain the high efficacy of NT as a screening tool, the ability of operators to achieve a reliable measurement of NT is crucial (Evans et al., 2007). This depends on proper training and strict adherence to the standard protocol and measuring technique (Monni et al., 1997). The acquisition of a true midsagittal section of the fetus is the fundamental prerequisite for a reliable NT measurement, because an oblique section will have a significant effect on the measurement. In clinical practice, such a section is obtained by manipulation of a two-dimensional (2D) ultrasound probe by the operators, who then decide whether the image represents a true midsagittal section. While it is usually easy to get a longitudinal section, to acquire a true midsagittal section is more difficult. It is generally assumed that if an image contains the fetal

nasal bone and the diencephalon (third ventricle), which are midline structures, the image will be in the true midsagittal plane. Since there is a certain degree of subjectivity in the assessment, it is expected that there is always some deviation from the real midsagittal section. Using off-line analysis of stored three-dimensional ultrasound volumes, this angle of deviation has been shown to be small among FMF (The Fetal Medicine Foundation, UK) certified operators, with a mean of 5.7? which did not significantly affect the NT measurement (Wah et al., 2008). On the other hand, this angle of deviation was significantly larger among the non-FMF certified sonographers with a mean of 14.7? (Wah et al., 2008).

Real-time 3D ultrasound is now made possible with the development of two-dimensional matrix-array probe technologies (Maulik et al., 2003; Acar et al., 2005; Gon鏰lves et al., 2006; Acar et al., 2007; Taddei et al., 2008). One application of this matrix-array probe technology is the live xPlane imaging, which enables the simultaneous display of two high-resolution real-time images of the target organ. With live xPlane imaging, the secondary image plane can be selected by rotation through a full 360? together with a lateral tilt from -45? to +45? around the reference image plane, or by tilting (elevation) from the reference image plane by -30? to +30?.

We speculate that during the acquisition of a midsagittal section of the fetus, the ability to visualize the axial section of the fetal head in the secondary plane at the same time may facilitate the acquisition of the best midsagittal plane with the least deviation. Therefore, the objective of this study was to explore the role of live xPlane imaging in the acquisition of true midsagittal section.

10.2 Patients and Methods

Eight sonographers were invited to participate in this study, four of whom were FMF-accredited for NT scanning (FMF Group) and the other four were not (non-FMF Group). All sonographers had at least 5 years' experience in obstetric ultrasound scanning. The four non-FMF certified operators were not familiar with NT measurement and were not involved in the NT screening program in the department. Women with singleton pregnancies attending the First Trimester Combined Down Syndrome Screening at the obstetric unit in our university hospital were invited to participate in this study. All pregnancies were between 11+0 and 13+6 weeks of gestation. Each of the eight sonographers was asked to perform ultrasound examinations on five patients and forty patients were examined in total. All sonographers had not used live xPlane imaging before. The study was approved by the Ethics Committee of the local institute.

All ultrasound examinations were performed using a Philips iU-22 3D ultrasound scanner (Philips, Bothell, WA, USA) equipped with a X7-2 (7–2MHz) matrix transducer. The xPlane function was activated during the whole examination. Each sonographer was instructed to obtain an image section of the fetal head and neck that they believed to represent the true midsagittal section on the left image window, based on information available to them from both the right and left image planes. During the scanning, one of the authors assisted the sonographers by putting the reference line in the left image across the fetal head, so that an axial section of the

fetal head was visualized in the right image window. Image on the right window enabled the sonographer to decide whether the image on the left side was truly midsagittal by observing (visually) the orientation of the falx cerebri, which would be parallel to the direction of the ultrasound beam if a real midsagittal section was obtained (Figure 10.1). The assistant otherwise did not give any further comment, order or assistance during the whole examination. Once the sonographer was satisfied with the image, the image was captured and stored for subsequent analysis. The time taken for each image acquisition was recorded, and there was no time limit. The operators were instructed to move the ultrasound transducer away from the maternal abdomen before another image was acquired. A total of five images of fetal sagittal section were captured for each patient.

All subsequent analysis of images was performed offline by one of the authors on the ultrasound machine. The angle between the falx cerebri and the vertical axis was measured from the image on the right window. This angle would be 0° if the original plane was truly midsagittal (Figure 10.2). The angle in each image was measured five times, while the operator was blinded to i) the sonographer who took the image and ii) the on-screen reading for each measurement. For each image, the angle of deviation was taken as the average of the three repeated measurements after exclusion of the maximum and minimum readings. The mean, SD, median and the inter-quartile range (IQR) of the angle of deviation for each sonographer and each group were calculated and compared.

The angle of deviation and the time taken for acquiring each image were compared

between FMF and non-FMF groups in this study. Wilcoxon's sign rank test was used for between-group comparisons and a *P*-value of <0.05 was considered statistically significant. All statistical analysis were performed using the Statistical Package for Social Sciences for Windows version 15.0 (SPSS Inc, Chicago, IL, USA).

The findings of the current study were compared to those from our previous study (Wah et al., 2008). In that study, operators were asked to obtain a fetal midsagittal section by using a mechanical 3D transducer as a 2D transducer. Once such an image was obtained, a static 3D volume was acquired and stored for further analysis of the angle of deviation. This angles was found to be significantly larger among the non-FMF operators compared to the FMF operators (14.7? vs. 5.7□). The fundamental difference between the current and previous study was that in the prior study operators were based on only 2D information of a single sonographic image to determine a midsagittal section, while in the current study the acquisition of the midsagittal plane was aided by the real-time information from two image planes.

10.3 Results

Of the 40 patients, there were 35 between 12+0 and 12+6 weeks' gestation. Three patients in FMF Group and two in non-FMF Group were between 13+0 and 13+6 weeks' gestation. A total of 200 images (8 operators x 5 patients per operator x 5 images per patient), including 100 images from FMF Group and 100 images from non-FMF Group, were obtained.

The median angle of deviation for each operator ranged from 1.2? to 3.4? (Table 10.1,

Figure 10.3). There was no significant difference in this angle between those who were FMF and non-FMF certified operators (median 2.0? vs. 2.2? P=0.463). The inter-quartile range of the angle of deviation was also similar among the FMF and non-FMF certified operators.

The median acquisition time of FMF Group was shorter than non-FMF Group (32.0s vs. 45.5s), but it did not reach statistical significance (P=0.107).

The performance of FMF group and non-FMF group was compared to that of our previous study as reproduced in Table 2. In that study, the median angle of deviation were 5.1癈nd 11.9癋or FMF and non-FMF operators respectively. Current study showed that, in both FMF and non-FMF group, the additional information provided by live xPlane imaging significantly reduced the angle of deviation. The median angle of deviation among the FMF-certified operators reduced from 5.1? to 2.0? (P<0.001), while the reduction was even more pronounced among the non-FMF certified operators (median 11.9? down to 2.2? P<0.001). We were unable to compare the time taken for image acquisition because this variable was not measured in the previous study.

10.4 Discussion

Acquisition of a true midsagittal section using conventional two-dimensional ultrasound remains an operator dependent and subjective assessment. A "correct" midsagittal plane is usually defined by the presence of some essential features, including the presence of the fetal nasal bone and the diencephalon (third ventricle),

but there is no other objective reference to judge. We previously demonstrated that the ability to obtain a midsagittal section is significantly better in FMF-certified operators (Wah et al., 2008), but even among these certified operators, the mean angle of deviation was 5.7? and the median was 5.1? In this study, we clearly demonstrated the added benefit if the two perpendicular planes of the target organ of interests are displayed simultaneously real-time with the live xPlane imaging technology. The use of live xPlane imaging significantly reduced the angle of deviation among the FMF operators to a median of 2.0?

More importantly, the use of live xPlane imaging significantly reduced the angle of deviation from a median of 11.9? down to 2.2? for the non-FMF certified operators. With the use of live xPlane imaging in acquiring the true midsagittal plane, there was no longer significant difference existing between the FMF certified and non-FMF certified operators (median 2.0? vs. 2.2? P=0.463). The only potential difference was that the non-FMF certified operators might need more time to acquire the true midsagittal section (median 45.5s vs. 32.0s) which nonetheless did not reach statistical significance (P=0.107).

Our findings supported our hypothesis that live xPlane imaging provides important information to assist sonographers in acquiring a true midsagittal section. Although training is important and essential to ensure an operator's competence in acquiring a true midsagittal section, the availability of live xPlane imaging was shown to shorten the learning curve of new sonographers, and increase the 'confidence' of the operators by demonstrating objectively how much the acquired plane was close to the true midsagittal plane. Moreover, the angle of deviation can be measured

immediately on the ultrasound machine, which provides objective evidence to judge how true a presumed midsagittal section is. The presumed midsagittal plane can otherwise be re-acquired immediately if it is not the true midsagittal plane.

There are fundamental differences between conventional 3D ultrasound examination with mechanical 3D probe and live xPlane imaging. With mechanical 3D transducer, one can acquire a 3D volume and display it in a multiplanar view (MPV). However, it is an offline analysis. One can confirm whether the image in the primary plane (Plane A) was a true midsagittal section by referring to the image in Plane B, retrospectively. With this approach, one cannot use the additional information from Plane B at real-time to tell whether the sagittal section was perfect midsagittal section or not. In other words, information collected by conventional 3D ultrasound can only be used retrospectively to tell how good the image plane is, but cannot be used to guide the operators during the process of image acquisition. Also, other researchers have attempted to obtain a true midsagittal plane by obtaining a 3D volume and then rotate off-line the data volume so that the image in Plane A represents a true midsagittal plane (Kurjak et al., 1999; Chung et al., 2000; Paul et al., 2001). It is certainly technically possible. However, the purpose of getting a true sagittal section in the first trimester is usually for the NT measurement. The image in A-Plane after rotation is no longer the one with the best resolution, and the delineation of the NT is expected to be worse. It is therefore not surprising that previous publications had demonstrated that such off-line manipulation and NT measurement was only successful in 60% of women, and in those cases NT was clearly demonstrated in the initial plane (Paul et al., 2001). In summary, MPV enables the confirmation of whether a midsagittal section is correct or not, but does

not assist the acquisition of a perfect image. Live xPlane imaging, on the other hand, allows the REAL-TIME simultaneous display of both Plane A and Plane B. Therefore, by reading the Plane B real-time data, one can immediately decide whether Plane A is the perfect midsagittal section. One can continue this manipulation REAL TIME until the perfect midsagittal section is obtained. At that point, the image in Plane A is also at the best possible resolution, and NT can be measured with the best axial resolution.

The major limitation of this study was that fetal position has not been controlled because fetal position could have a major influence on the time required and possibly the precision of the midsagittal plane acquisition. However, we believe that such effects were minimized by the use of multiple patients with multiple measurements. Another limitation is the relatively low spatial resolution of matrix probe in obstetric scan. The matrix probes available so far were usually optimized for cardiac examination but not for obstetric use. However, with the advent of this new X7-2 matrix probe with the higher frequency up to 7MHz, the spatial resolution of matrix probe has been greatly improved (Acar et al., 2007). In particular the spatial resolution was considered by the authors to be adequate for the demonstration of sagittal section and the measurement of angle of deviation, although it may not be good enough for NT measurement yet. It is anticipated that with further optimization, image quality will further improve for obstetric use.

In this study, we have not studied whether the reduction in angle of deviation from the midsagittal plane could be translated into an improvement in reproducibility or precision of NT measurement, because the matrix probe used is not fully optimized

for first trimester scan. However, we do believe that further optimization in the near future would enable the incorporation of live xPlane imaging into routine NT scan, which would potentially improve the precision of NT measurement.

In conclusion, real-time 3D ultrasound and live xPlane imaging technology provides valuable additional information about the orientation of the target organ, therefore significantly improving the accuracy of acquisition of a defined sonographic plane, and reducing the difference in performance between operators who are formally certified or not.

Chapter 11 General discussion and conclusion

This Ph.D thesis summarized real-time 3D ultrasound in obstetric application. With the introduction of matrix transducer, scanning the fetus in real time became available. However, few researches were performed with this novel technology.

We explored the feasibility to perform the fetal heart screening using this new technology. Fifty-one normal fetuses were scanned in this study. We developed and reported the methodology of acquiring and examining the screening planes of the fetal heart with live xPlane imaging. The procedure was simple and straight. When performing the fetal heart screening with live xPlane imaging, we just need display the four-chamber view and mid-sagittal view of fetal upper thorax and other thing could be done by moving the reference line. Using the four-chamber view as the starting plane, the visualization rate of LVOT, RVOT and 3VT view was 94.1% (48/51), 100% (51/51) and 98.0% (50/51), respectively; using the sagittal view of fetal thorax as the starting plane, the visualization rate of LVOT, four-chamber and 3VT view is 100% (51/51), respectively. However, RVOT is difficult to be imaged when using the mid-sagittal view as the starting plane. It can be displayed by rotating the reference plane around the root of aorta but the visualization rate is only 41.2% (21/51).

Therefore, the most effective solution of using live xPlane imaging to screen the fetal

heart is that: 1) acquiring the LVOT view by using the mid-sagittal view of fetal upper thorax as the starting plane and putting the reference line through the root of aorta; 2) visualizing the RVOT view by using the four-chamber view as the starting plane and placing the reference line through the right ventricle, criss-cross, left atrium and descending aorta, i.e. put reference line across the mediastinum and descending aorta; 3) imaging the 3VT view by using the mid-sagittal view as the starting plane and putting the reference line across the upper thorax, or by using the four-chamber view as the starting plane and titling the reference plane (four-chamber view) slightly towards the fetal head.

We also demonstrated a novel method to visualize the aortic and ductal arch with live xPlane imaging, which is difficult with conventional 2D ultrasound. The ductal and aortic arch view were successfully visualized by real-time 3DE using live xPlane imaging in all 100 normal cases. We can easily get the ductal arch view by placing the reference line through pulmonary artery and descending aorta on the 3VT view using real-time 3DE with live xPlane imaging. Similarly, we can acquire the aortic arch view by putting the reference line along the transverse view of aortic arch and descending aorta on the 3VT view. Imaging of ductal and aortic arch view can be used as a compensation of the 3VT view. In this study, one corrected TGA case and one DORV case showed the normal 3VT view but the abnormal ductal and aortic arch view. Therefore, live xPlane imaging is an easy and feasible method for real-time imaging of the ductal and aortic arch, and potentially may be a useful tool

for the assessment and screening of conotruncal anomalies and aortic arch abnormalities.

We explored to evaluate the entire fetal IVS by real-time 3DE with both live xPlane imaging and live 3D imaging. A total 154 fetuses were enrolled in this study. We can successfully assess the entire IVS in most fetuses (153/154). With live xPlane imaging, the in-plane view of IVS can be obtained by putting the reference line through the fetal IVS in the four-chamber; with live 3D imaging, the en face view of IVS can be visualized by cropping and rotating the volume. We also compared the images acquired by real-time 3DE and STIC in this thesis. Another fifty fetuses were enrolled to perform the comparison study between real-time 3DE and STIC. It showed that little motion artifact encounters with real-time 3DE and the image quality of real-time 3DE is similar to STIC volume acquired from the sagittal view and superior to STIC volume from the four-chamber view. Therefore, real-time 3DE can be used to display the lateral view of the fetal IVS, and potentially may be a useful tool for the assessment and diagnosis of fetal VSDs, although further studies are required to evaluate the sensitivity and reproducibility of this technique in a large population.

Conotruncal anomalies are the leading causes of cyanotic congenital heart disease characterized by the abnormal development of conotruncal septum. Although the screening techniques of fetal congenital heart disease were greatly improved, the

detection rate of conotruncal anomalies was still low (Smith et al., 1995; Sivanandam et al., 2006). This is mainly because these anomalies usually have the normal four-chamber view. Live xPlane imaging can easily visualize the ductal arch view and the in-plane view of IVS, which can help us to screen the fetal conotruncal anomalies. There were 152 normal cases, 25 conotruncal anomalies and 23 other types of fetal CHDs were involved in this study. The visualization rate of ductal arch view displayed by live xPlane imaging was 100% (152/152) in normal cases, 8% (2/25) in conotruncal anomalies and 69.7% (16/23) in non-conotruncal CHDs, respectively. The visualization rate of the normal in-plane view of IVS displayed by live xPlane imaging was 100% (152/152) in normal cases, 12% (3/25) in conotruncal anomalies and 73.9% (16/23) in non-conotruncal CHDs, respectively. The abnormal in-plane view of IVS can be detected in fetal conotruncal anomalies, including abnormal relationship of aorta and pulmonary artery or VSD. Therefore, live xPlane imaging of fetal ductal arch view and in-plane view of IVS can be used to screen the fetal conotruncal anomalies. The method is simple and feasible, which may be a useful tool for the assessment and diagnosis of fetal conotruncal anomalies.

In final, we attempted to use real-time 3D ultrasound to perform the prenatal scans outside the fetal heart. We evaluated the feasibility of using real-time 3D ultrasound to assist in obtaining a true midsagittal view in first trimester. Eight sonographers, including FMF-certified and non FMF-certified operators, were asked to perform ultrasound examinations on five patients and forty patients were examined in total. It showed that the deviation from true midsagittal view was reduced greatly with the

guidance of live xPlane imaging. Real-time 3D ultrasound provides valuable additional information about the orientation of the target organ, therefore significantly improving the accuracy of acquisition of a defined sonographic plane, and reducing the difference in performance between operators who are formally certified or not.

However, there are some limitations of this thesis. Firstly, the image quality is still relatively inferior compared to that of conventional 2D ultrasound for the reason that this transducer is originally designed for adult and pediatric cardiology and it has not fully optimized for fetus until now. Secondly, few image modalities are available with this technique. It is believed that more and more new image modalities will be produced by the manufactures. Thirdly, we only explore the feasibility of real-time 3D ultrasound in obstetric application. Further study should be performed in a large population to evaluate its sensitivity and reproducibility in obstetric scans.

In conclusion, real-time 3DE is a novel and promising technique to perform the prenatal examination, both the fetal heart and other system. It represents the future of 3D ultrasound and will become a useful tool for prenatal screening and diagnosis, which is easy to use and to teach.

Further Plan

In this thesis, we focused on the fetal heart scanning with this new matrix transducer for the reason that this transducer originally was designed for cardiology. Only one part was used outside the fetal heart with this matrix transducer. Therefore, further study will not only concentrate on fetal heart, but also outside the fetal heart.

A new matrix transducer used for obstetrics will be available in near future. We will use this new technology to image the fetal heart, such as the AV valves and fetal heart screening for non-experienced operators, and other feasible applications.

References

Acar P, Abadir S, Paranon S, Latcu G, Grosjean J, Dulac Y (2007). Live 3D echocardiography with the pediatric matrix probe. Echocardiography. 24, 750–755.

Acar P, Dulac Y, Taktak A, Abadir S (2005). Real-time three-dimensional fetal echocardiography using matrix probe. Prenat Diagn. 25, 370–375.

Acar P, Laskari C, Rhodes J, Pandian N, Warner K, Marx G (1999). Three-dimensional echocardiographic analysis of valve anatomy as a determinant of mitral regurgitation after surgery for atrioventricular septal defects. Am J Cardiol. 83, 745–749.

Achiron R, Glaser J, Gelernter I, Hegesh J, Yagel S (1992). Extended fetal echocardiographic examination for detecting cardiac malformations in low risk pregnancies. Br Med J. 304, 671–674.

Allan L (2004). Technique of fetal echocardiography. Pediatr Cardiol. 25, 223–233.

Allan L, Benacerraf B, Copel JA, Carvalho JS, Chaoui R, Eik-Nes SH, Tegnander E, Gembruch U, Huhta JC, Pilu G, Wladimiroff J, Yagel S (2001). Isolated major congenital heart disease. Ultrasound Obstet Gynecol. 17, 370–379.

Allan LD (2000). A practical approach to fetal heart scanning. Semin Perinatol. 24, 324–330.

Allan LD, Crawford DC, Chita SK, Tynan MJ (1985). Prenatal screening of congenital heart disease. BMJ. 292, 717–719.

Allan LD, Maxwell DJ, Carminati M, Tynan MJ (1995). Survival after fetal aortic balloon valvoplasty. Ultrasound Obstet Gynecol. 5, 90–91.

American College of Obstetricians and Gynecologists (2004). ACOG Practice Bulletin. Ultrasonography in pregnancy. Obstet Gynecol. 104, 1449–1458.

American Institue of Ultrasound in Medicine (1998). Performance of the basic fetal cardiac ultrasound examination. J Ultrasound Med. 17, 601–607.

American Institue of Ultrasound in Medicine (2003). Guidelines for the performance of antepartum obstetrical ultrasound examination. J Ultrasound Med. 22, 1116–1125.

Avgidou K, Papageorghiou A, Bindra R, Spencer K, Nicolaides KH (2005). Prospective first-trimester screening for trisomy 21 in 30,564 pregnancies. Am J Obstet Gynecol. 192, 1761–1767.

Barboza JM, Dajani NK, Glenn LG, Angtuaco TL (2002). Prenatal diagnosis of congenital cardiac anomalies: a practical approach using two basic views. Radiographics. 22, 1125–1137.

Benacerraf BR (1994). Sonographic detection of fetal anomalies of the aortic and pulmonary arteries: value of four-chamber view vs direct images. AJR Am J Roentgenol. 163, 1483–1489.

Bonnet D, Coltri A, Butera G, Fermont L, Bidois JL, Kachaner J, Sidi D (1999). Detection of transposition of the great arteries in fetuses reduces neonatal morbidity and mortality. Circulation. 99, 916–918.

Bromley B, Estroff JA, Sanders SP, Parad R, Roberts D, Frigoletto FD Jr, Benacerraf BR (1992). Fetal echocardiography: accuracy and limitations in a population at high and low risk for heart defects. Am J Obstet Gynecol. 166, 1473–1481.

Bull C (1999). Current and potential impact of fetal diagnosis on prevalence and spectrum of serious congenital heart disease at term in the UK. Lancet. 354, 1242–1247.

Buskens E, Grobbee DE, Frohn-Mulder IM, Stewart PA, Juttmann RE, Wladimiroff JW, Hess J (1996). Efficacy of routine fetal ultrasound screening for congenital heart disease in normal pregnancy. Circulation. 94, 67–72.

Carvalho JS, Mavrides E, Shinebourne EA, Campbell S, Thilaganathan B (2002). Improving the effectiveness of routine prenatal screening for major congenital heart defect. Heart. 88, 387–391.

Chaoui R (2003). The four-chamber view: four reasons why it seems to fail in screening for cardiac abnormalities and suggestions to improve detection rate. Ultrasound Obstet Gynecol. 22, 3–10.

Chung BL, Kim HJ, Lee KH (2000). The application of three-dimensional ultrasound to nuchal translucency measurement in early pregnancy (10-14 weeks): a preliminary study. Ultrasound Obstet Gynecol.15, 122–125.

Constantine G, McCormark J (1991). Comparative audit of booking and mid-trimester ultrasound scans in the prenatal diagnosis of congenital anomalies. Prenat Diagn. 11, 905–914.

Cooper MJ, Enderlein MA, Dyson DC, Roge CL, Tarnoff H (1995). Fetal echocardiography: retrospective review of clinical experience and an evaluation of indications. Obstet Gynecol. 86, 577–582.

Copel JA, Pilu G, Green J, Hobbins JC, Kleinman CS (1987). Fetal echocardiographic screening for congenital heart disease: the importance of the four-chamber view. Am J Obstet Gynecol. 157, 648–655.

Crane JP, LeFevre MI, Winborn RC, Evans JK, Ewigman BG, Bain RP, Frigoletto F, McNellis D, the RADIUS study group (1994). A rondomized trial of prenatal ultrasonographic screening: impact on the detection, management, and outcome of anomalous fetuses. Am J Obstet Gynecol. 171, 392–399.

Cuneo BF, Curran LF, Davis N, Elrad H (2004). Trends in prenatal diagnosis of critical cardiac defects in an integrated obstetric and pediatric cardiac imaging center. J Perinatol. 24, 674–678.

DeVore GR (1985). The prenatal diagnosis of congenital heart disease - a practical approach for the fetal sonographer. J Clin Ultrasound. 13, 229–245.

DeVore GR (1992). The aortic and pulmonary outflow tract screening in the human fetus. J Ultrasound Med. 11, 345–348.

Devore GR, Falkensammer P, Sklansky MS, Platt LD (2003). Spatiotemporal image correlation (STIC): new technology for evaluation of the fetal heart. Ultrasound Obstet Gynecol. 22, 380–387.

Devore GR, Polanco B, Sklansky MS, Platt LD (2004). The'spin'technique: a new method for examination of the fetal outflow tracts using three-dimensional ultrasound. Ultrasound Obstet Gynecol. 24, 72–82.

Espinoza J, Kusanovic JP, Goncalves LF, Nien JK, Hassan S, Lee W, Romero R (2006). A novel algorithm for comprehensive fetal echocardiography using 4-dimensional ultrasonography and tomographic imaging. J Ultrasound Med. 25, 947–956.

Espinoza J, Romero R, Kusanovic JP, Gotsch F, Erez O, Lee W, Goncalves LF, Schoen ML, Hassan SS (2007). The role of the sagittal view of the ductal arch in

identification of fetuses with conotruncal anomalies using 4-dimensional ultrasonography. J Ultrasound Med. 26, 1181–1188.

Evans MI, Van Decruyes H, Nicolaides KH (2007). Nuchal translucency measurements for first-trimester screening: the 'price' of inaccuracy. Fetal Diagn Ther. 22, 401–404.

Falcon O, Auer M, Gerovassili A, Spencer K, Nicolaides KH (2006). Screening for trisomy 21 by fetal tricuspid regurgitation, nuchal translucency and maternal serum free beta-hCG and PAPP-A at 11+0 to 13+6 weeks. Ultrasound Obstet Gynecol. 27, 151–155.

Ferencz C, Rubin JD, McCarter RJ, Brenner JI, Neill CA, Perry LW, Hepner SI, Downing JW (1985). Congenital heart disease: prevalance at livebirth. The Baltimore-Washington infant study. Am J Epidemiol. 121, 31–36.

Franklin O, Burch M, Manning N, Sleeman K, Gould S, Archer N (2002). Prenatal diagnosis of coarctation of the aorta improves survival and reduces morbidity. Heart. 87, 67–69.

Garne E, Stoll C, Clementi M, The Euroscan Group (2001). Evaluation of prenatal diagnosis of congenital heart diseases by ultrasound: experience from 20 European registries. Ultrasound Obstet Gynecol. 17, 386–391.

Gindes L, Achiron R (2008). Tetralogy of Fallot: evaluation by 4D spatiotemporal image correlation. Ultrasound Obstet Gynecol. 32, 598–599.

Gon鏘lves LF, Espinoza J, Kusanovic JP, Lee W, Nien JK, Santolaya-Forgas J, Mari G, Treadwell MC, Romero R (2006). Applications of 2-dimensional matrix array for 3- and 4-dimensional examination of the fetus: a pictorial essay. J Ultrasound Med. 25, 745–755.

Goncalves LF, Espinoza J, Lee W, Mazor M, Romero R (2004). Three- and Four-dimensional reconstruction of the aortic and ductal arches using inversion mode: a new rendering algorithm for visualization of fluid-filled anatomical structures. Ultrasound Obstet Gynecol. 24, 696–698.

Goncalves LF, Lee W, Chaiworapongsa T, Espinoza J, Schoen ML, Falkensammer P, Treadwell M, Romero R (2003). Four-dimensional ultrasonography of the fetal heart with spatiotemporal image correlation. Am J Obstet Gynecol. 189, 1792–1802.

Goncalves LF, Lee W, Espinoza J, Romero R (2006). Examination of the fetal heart by four-dimensional (4D) ultrasound with spatio-temporal image correlation (STIC). Ultrasound Obstet Gynecol. 27, 336–348.

Gottliebson WM, Border WL, Franklin CM, Meyer RA, Michelfelder EC (2006). Accuracy of fetal echocardiography: a cardiac segment-specific analysis. Ultrasound Obstet Gynecol. 28, 15–21.

Grandjean H, Larroque D, Levi S (1999). The performance of routine ultrasonographic screening of pregnancies in the Eurofetus Study. Am J Obstet Gynecol. 181, 446–454.

Hata T, Dai SY, Inubashiri E, Kanenishi K, Tanaka H, Yanagihara T, Araki S (2008). Four-dimensional sonography with B-flow imaging and spatiotemporal image correlation for visualization of the fetal heart. J clin Ultrasound. 36, 204–207.

Hata T, Kanenishi K, Tanaka H, Kimura K (2006). Real-time 3D echocardiographic evaluation of the fetal heart using instantaneous volume-rendered display. J Obstet Gynaecol Res. 32, 42–46.

Hoffman JI, Kaplan S (2002). The incidence of congenital heart disease. J Am Coll Cardiol. 39, 1890–1900.

Hornberger LK, Sanders SP, Sahn DJ, Rice MJ, Spevak PJ, Benacerraf BR, McDonald RW, Colan SD (1995). In utero pulmonary artery and aortic growth and potential for progression of pulmonary outflow tract obstruction in tetralogy of Fallot. J Am Coll Cardiol. 25, 739–745.

Hunter S, Heads A, Wyllie J, Robson S (2000). Prenatal diagnosis of congenital heart disease in the northern region of England: benefits of a training programme for obstetric ultrasonographers. Heart. 84, 294–298.

Isaksen CV, Eik-Nes SH, Blaas HG, Tegnander E, Torp S (1999). Comparison of prenatal ultrasound and postmortem findings in fetuses and infants with congenital heart defects. Ultrasound Obstet Gynecol. 13, 117–126.

Kagan KO, Avgidou K, Molina FS, Gajewska K, Nicolaides KH (2006). Relation between increased fetal nuchal translucency thickness and chromosomal defects. Obstet Gynecol. 107, 6–10.

Kirk JS, Comstock CH, Lee W, Smith RS, Riggs TW, Weinhouse E (1997). Sonographic screening to detect fetal cardiac anomalies: a five-year experience with 111 abnormal cases. Obstet Gynecol. 89, 227–232.

Kirk JS, Comstock CH, Lee W, Smith RS, Riggs TW, Weinhouse E (1999). Fetal cardiac asymmetry: a marker for congenital heart disease. Obstet Gynecol. 93, 189–192.

Kirk JS, Riggs TW, Comstock CH, Lee W, Yang SS, Weinhouse E (1994). Prenatal screening for cardiac anomalies: the value of routine addition of the aortic root to the four-chamber view. Obstet Gynecol. 84, 427–431.

Kohl T, Sharland G, Allan LD, Gembruch U, Chaoui R, Lopes LM, Zielinsky P, Huhta J, Silverman NH (2000). World experience of percutaneous ultrasound-guided balloon valvuloplasty in human fetuses with severe aortic valve obstruction. Am J Cardiol. 85, 1230–1233.

Kurjak A, Kupesic S, Ivancic-Kosuta M (1999). Three-dimensional transvaginal ultrasound improves measurement of nuchal translucency. J Perinatal Med. 27, 97–102.

Lau WL (2006). The new 'in-plane' view of the inter-ventricular septum. Prenat Diagn. 26, 90–91.

Leung TY, Chan LW, Leung TN, Fung TY, Sahota DS, Spencer K, Lau TK (2007). First-trimester combined screening for trisomy 21 in a predominantly Chinese population. Ultrasound Obstet Gynecol. 29, 14–17.

Maeno Y, Himeno W, Fujino H, Sugahara Y, Furui J, Mizumoto Y, Kato H (1999). Progression of congenital heart disease in the prenatal period. Pediatr int. 41, 709–715.

Mahle WT, Clancy RR, McGaurn SP, Goin JE, Clark BJ (2001). Impact of prenatal diagnosis on survival and early neurologic morbidity in neonates with hypoplastic left heart syndrome. Pediatrics. 6, 1277–1282.

Markov D, Chernev T, Dimitrova V, Mazne.kova V, Leroy Y, Jacquemyn Y, Ramaekers P, Van Bulck B, Loquet P (2004). Ultrasound screening and diagnosis of fetal structural abnormalities between 11–14 gestational weeks. Akush Ginekol (Sofiia). 43, 3–10.

Maulik D, Nanda NC, Singh V, Dod H, Vengala S, Sinha A, Sidhu MS, Khanna D, Lysikiewicz A, Sicuranza G, Modh N (2003). Live three-dimensional echocardiography of the human fetus. Echocardiography. 20, 715–721.

Meberg A, Otterstad JE, Froland G, Lindberg H, Sorland SJ (2000). Outcome of congenital heart defects - a population-based study. Acta Paediatr. 89, 1344–1351.

Monni G, Zoppi MA, Ibba RM, Floris M (1997). Fetal nuchal translucency test for Down's syndrome. Lancet. 350, 1631.

Myers SA, Fresquez M, Hamill N (2007). Four-dimensional sonography of the fetal heart with spatiotemporal image correlation directed at the interventricular septum. J Ultrasound Med. 26, 1071–1075.

Nicolaides KH (2004). Nuchal translucency and other first-trimester sonographic markers of chromosomal abnormalities. Am J Obstet Gynecol. 19, 45–67.

Ogge G, Gaglioti S, Maccanti S, Faggiano F, Todros T and the Gruppo Piemontese for prenatal screening of congenital heart disease (2006). Prenatal screening for congenital heart disease with four-chamber and outflow-tract views: a multicenter study. Ultrasound Obstet Gynecol. 28, 779–784.

Paladini D, Russo MG, Vassallo M, Tartaglione A (2003). The 'in-plane' view of the inter-ventricular septum. A new approach to the characterization of ventricular septal defects in the fetus. Prenat Diagn. 23, 1052–1055.

Paladini D, Rustico M, Todros T et al. (1996). Conotruncal anomalies in prenatal life. Ultrasound Obstet Gynecol. 8, 241–246

Paladini D, Vassallo M, Sglavo G, Lapadula C, Martinelli P (2006). The role of spatio-temporal image correlation (STIC) with tomographic ultrasound imaging (TUI) in the sequential analysis of fetal congenital heart disease. Ultrasound Obstet Gynecol. 27, 555–561.

Paul C, Krampl E, Skentou C, Jurkovic D, Nicolaides KH (2001). Measurement of fetal nuchal translucency thickness by three-dimensional ultrasound. Ultrasound Obstet Gynecol. 18, 481–484.

Perolo A, Prandstraller D, Ghi T, Gargiulo G, Leone O, Bovicelli L, Pilu G (2001). Diagnosis and management of fetal cardiac anomalies: 10 years of experience at a single institution. Ultrasound Obstet Gynecol. 18, 615–618.

Rizzo G, Capponi A, Cavicchioni O, Vendola M, Pietrolucci ME, Arduini D (2008). Application of automated sonography on 4-dimensional volumes of fetuses with transposition of the great arteries. J Ultrasound Med. 27, 771–776.

Rosano A, Botto LD, Botting B, Mastroiacovo P (2000). Infant mortality and congenital anomalies from 1950 to 1994: an international perspective. J Epidemiol Community Health. 54, 660–666.

Rustico MA, Benettoni A, D'Ottavio G, Maieron A, Fischer-Tamaro I, Conoscenti G, Meir Y, Montesano M, Cattaneo A, Mandruzzato G (1995). Fetal heart screening in low-risk pregnancies. Ultrasound Obstet Gynecol. 6, 313–319.

Scharf A, Geka F, Steinborn A, Frey H, Schlemmer A, Sohn C (2000). 3D real-time imaging of the fetal heart. Fetal Diagn Ther. 15, 267–274.

Sharland GK, Allan LD (1992). Screening for congenital heart disease prenatally: results of a 2 and 1/2-year study in the South East Thames region. Br J Obstet Gynaecol. 99, 220–225.

Shirley IM, Bottomley F, Robinson VP (1992). Routine radiographer screening for fetal abnormalities by ultrasound in an unselected low risk population. Br J Radiol. 65, 564–569.

Simpson JM, Sharland GK (1997). Natural history and outcome of aortic stenosis diagnosed prenatally. Heart. 77, 205–210.

Simpson LL (2004). Screening for congenital heart disease. Obstet Gynecol Clin North Am. 31, 51–59.

Sivanandam S, Glickstein JS, Printz BF, et al. (2006). Prenatal diagnosis of conotruncal malformations: dignostic accuracy, outcome, chromosomal abnormalities, and extracardiac anomalies. Am J Perinatol. 23, 241–245.

Sklansky M, Miller D, Devore G, Kung G, Pretorius D, Wong P, Chang RK (2005). Prenatal screening for congenital heart disease using real-time three-dimensional echocardiography and a novel 'sweep volume' acquisition technique. Ultrasound Obstet Gynecol. 25, 435–443.

Small M, Copel JA (2004). Indications for fetal echocardiography. Pediatr Cardiol. 25, 210–222.

Smith RS, Comstock CH, Kirk JS, Lee W, Riggs T, Weinhouse E (1999). Double-outlet right ventricle: an antenatal diagnostic dilemma. Ultrasound Obstet Gynecol. 14, 315–319.

Sonek JD, Cicero S, Neiger R, Nicolaides KH (2006). Nasal bone assessment in prenatal screening for trisomy 21. Am J Obstet Gynecol. 195, 1219–1230.

Stoll C, Dott B, Alembick Y, De Geeter B (2002). Evaluation and evolution during time of prenatal diagnosis of congenital heart diseases by routine fetal ultrasonographic examination. Ann Genet. 45, 21–27.

Stumpflen I, Stumpflen A, Wimmer M, Bernaschek CH (1996). Effect of detailed fetal echocardiography as part of routine prenatal ultrasonographic screening on detection of congenital heart disease. Lancet. 348, 854–857.

Sugeng L, Weinert L, Thiele K, Lang RM (2003). Real-Time Three-dimensional echocardiography using a novel matrix array transducer. Echocardiography. 20, 623–635.

Taddei F, Signorelli M, Prefumo F, Franceschetti L, Marasini M, Groli C (2008). Prenatal imaging of ductus venous agenesis using 4D ultrasound with a matrix array transducer. Ultrasound Obstet Gynecol. 31, 477–479.

Tegnander E and Nik-Nes SH (2006). The examiner's experience has a significant impact on the detection rate of congenital heart defects at the second-trimester fetal examination. Ultrasound Obstet Gynecol. 28, 8–14.

Tegnander E, Eik-Nes SH and Linker DT (1994). Incorporating the four-chamber view of the fetal heart into the second-trimester routine fetal examination. Ultrasound Obstet Gynecol. 4, 24–28.

Tegnander E, Eik-Nes SH, Johansen OJ, Linker DT (1995). Prenatal detection of heart defects at the routine fetal examination at 18 weeks in a non-selected population. Ultrasound Obstet Gynecol. 5, 372–380.

Tegnander E, Eik-Nes SH, Linker DT (1994). Incorporating the four-chamber view of the fetal heart into the second-trimester routine fetal examination. Ultrasound Obstet Gynecol. 4, 24–28.

The international society of ultrasound in obstetrics and gynecology guidelines (2006). Cardiac screening examination of the fetus: guidelines for performing the 'basic' and 'extended basic' cardiac scan. Ultrasound Obstet Gynecol. 27, 107–113.

Todros T, Faggiano F Chiappa E, Gaglioti P, Mitola B, Sciarrone A (1997). Accuracy of routine ultrasonography in screening heart disease prenatally. Gruppo Piemontese for Prenatal Screening of Congenital Heart Disease. Prenat Diagn. 17, 901–906.

Tometzki AJ, Suda K, Kohl T, Kovalchin JP, Silverman NH (1999). Accuracy of prenatal echocardiographic diagnosis and prognosis of fetuses with conotruncal anomalies. J Am Coll Cardiol. 33, 1696–1701.

Tulzer G, Arzt W, Franklin RC, Loughna PV, Mair R, Gardiner HM (2002). Fetal pulmonary valvuloplasty for critical pulmonary stenosis or atresia with intact septum. Lancet. 360, 1567–1568.

Tworetzky W, McElhinney DB, Reddy VM, Brook MM, Hanley FL, Silverman NH (2001). Improved surgical outcome after fetal diagnosis of hypoplastic left heart syndrome. Circulation. 103, 1269–1273.

Tworetzky W, Wilkins-Haug L, Jennings RW, van der Veide ME, Marshall AC, Marx GR, Colan SD, Benson CB, Lock JE, Perry SB (2004). Balloon dilation of severe aortic stenosis in the fetus. Potential for prevention of hypoplastic left heart syndrome: candidate selection, technique, and results of successful intervention. Circulation. 110, 2125–2131.

Uittenbogaard LB, Haak MC, Spreeuwenberg MD, Van Vugt JM (2008). A systematic analysis of the feasibility of four-dimensional ultrasound imaging using spatiotemporal image correlation in routine fetal echocardiography. Ultrasound Obstet Gynecol. 31, 625–632.

Vinals F, Heredia F, Giuliano A (2003). The role of the three vessels and trachea view (3VT) in the diagnosis of congenital heart defects. Ultrasound Obstet Gynecol. 22, 358–367.

Vinals F, Pacheco V, Giuliano A (2006). Fetal atrioventricular valve junction in normal fetuses and in fetuses with complete atrioventricular septal defect assessed by 4D volume rendering. Ultrasound Obstet Gynecol. 28, 26–31.

Vinals F, Poblete P, Giuliano A (2003). Spatio-temporal image correlation (STIC): a new tool for the prenatal screening of congenital heart defects. Ultrasound Obstet Gynecol. 22, 388–394.

Vinals F, Tapia J, Giuliano A (2002). Prenatal detection of ductal-dependent congenital heart disease: how can things be made easier? Ultrasound Obstet Gynecol. 19, 246–249

Wah YMI, Chan LWD, Leung TY, Fung TY, Lau TK (2008). How true is a 'true' midsagittal section? Ultrasound Obstet Gynecol. 32, 855–859.

Wigton TR, Sabbagha RE, Tamura RK, Cohen L, Minogue JP, Strasberger JF (1993). Sonographic diagnosis of congenital heart disease: comparison between the four-chamber view and multiple cardiac views. Obstet Gynecol. 82, 219–224.

Wong SF, Chan FY, Cincotta RB, Lee-Tannock A, Ward C (2003). Factors influencing the prenatal detection of structural congenital heart diseases. Ultrasound Obstet Gynecol. 21, 19–25.

Wren C, Richmond S, Donaldson L (2000). Temporal variability in birth prevalence of cardiovascular malformations. Heart. 83, 414–419.

Xiong Y, Wah YMI, Chen M, Fung TY, Leung TY, Lau TK (2009). Real-time three-dimensional echocardiography using a matrix probe with live xPlane imaging of the interventricular septum. Ultrasound Obstet Gynaecol. 34, 534–537.

Xiong Y, Wah YMI, Chen M, Fung TY, Leung TY, Lau TK (2010). Assessment of the fetal interventricular septum by real-time three-dimsional echocardiography with live 3D imaging. Ultrasound Obstet Gynaecol (in press).

Yagel S, Arbel R, Anteby EY, Raveh D and Achiron R (2002). The three vessels and trachea view (3VT) in fetal cardiac scanning. Ultrasound Obstet Gynecol. 20, 340–345.

Yagel S, Benachi A, Bonnet D, Dumez Y, Hochner-Celnikier D, Cohen SM, Valsky DV, Fermont L (2006). Rendering in fetal cardiac scanning: the intracardiac septa and the coronal atrioventricular valve planes. Ultrasound Obstet Gynecol. 28, 266–274.

Yagel S, Cohen SM, Achiron R (2001). Examination of the fetal heart by five short-axis views: a proposed screening method for comprehensive cardiac evaluation. Ultrasound Obstet Gynecol. 17: 367–369.

Yagel S, Cohen SM, Shapiro I, Valsky DV (2007). 3D and 4D ultrasound in fetal cardiac scanning: a new look at the fetal heart. Ultrasound Obstet Gynecol. 29, 81–95.

Yagel S, Weissman A, Rotstein Z, Manor M, Hegesh J, Anteby E, Lipitz S, Achiron R (1997). Congenital heart defects: natural course and in utero development. Circulation. 96: 550–555.

Yoo SJ, Lee H, Cho KS, et al (1999).Sequential segmental approach to fetal congenital heart disease. Cardiol Young. 9, 430–444.

Yoo SJ, Lee YH, Cho KS (1999). Abnormal three-vessel view on sonography: a clue to the diagnosis of congenital heart disease in the fetus. AJR Am J Roentgenol. 172, 825–830.

Yoo SJ, Lee YH, Kim ES, Ryu HM, Kim MY, Choi HK, Cho KS, Kim A (1997). Three-vessel view of the fetal upper mediastinum: an easy means of detecting abnormalities of the ventricular outflow tracts and great arteries during obstetric screening. Ultrasound Obstet Gynecol. 9, 173–182.

Yoo SJ, Min JY, Lee YH, Roman K, Jaeggi E, Smallhorn J (2003). Fetal sonographic diagnosis of aortic arch abnormalities. Ultrasound Obstet Gynecol. 22, 535–546.

Zalel Y, Wiener Y, Gamzu R, Herman A, Schiff E, Achiron R (2004). The three-vessel and tracheal view of the fetal heart: an in utero sonographic evaluation. Prenat Diagn. 24, 174–178.

Appendices: Tables and Figutes

Table 3.1 Visualization rate of live xPlane imaging in fetal heart screening

Starting plane	4CV	LVOT	RVOT	3VT	Time (s)
Four-chamber as the starting plane	NA	48 (94.1%)	50 (98.0%)	51 (100)	530±497
Mid-sagittal view as the starting plane	51 (100%)	51 (100%)	21 (41.2%)	51 (100)	320±416

Table 4.1 Abnormal cases in the study of live xPlane imaging of the ductal and aortic arch

No.	Prenatal diagnosis	3VT view	Ductal view	Aortic arch view	Follow up
1	Truncus arteriosus	Abnormal	Abnormal	Abnormal	Confirmed by autopsy
2	Complete TGA	Abnormal	Abnormal	Abnormal	Confirmed by autopsy
3	Complete TGA	Abnormal	Abnormal	Abnormal	Confirmed by autopsy
4	Corrected TGA	Normal	Abnormal	Abnormal	Confirmed by autopsy
5	DORV	Normal	Abnormal	Abnormal	Confirmed by autopsy
6	Coarctation of aortic arch	Abnormal	Normal	Abnormal	Confirmed by postnatal echocardiography
7	Firstly suspicious of truncus or DORV, and diagnosed for normal case by prenatal fetal echocardiography	Abnormal	Normal	Normal	Confirmed by postnatal echocardiography

3VT, three-vessel and trachea view; DORV, double outlet right ventricle; TGA, transposition of great arteries

Table 7.1 Abnormal fetuses of comparison of real-time 3DE and STIC in assessment of fetal IVS

No.	AGE	GW	BMI	Diagnosis
1	29	22	21.4	TRUNCUS
2	27	26	22.8	PS
3	35	28	22.0	AVSD
4	31	21	22.6	PS+VSD
5	28	23	21.9	TOF
6	32	24	25.9	DORV+SUBPULMONARY VSD
7	24	22	23.4	INTERRUPT OF IVC
8	32	23	31.6	TOF
9	31	21	20.4	AVSD+DORV+LSVC
10	25	26	27.7	VSD
11	42	28	26.0	LSVC
12	30	21	20.5	AVSD
13	37	24	23.8	AVSD
14	26	21	20.7	VSD
15	27	26	22.9	CORRECTED TGA+VSD
16	24	23	23.6	TOF
17	22	22	21.8	PA+TS (HRH)
18	34	24	26.0	AVSD+LSVC
19	25	23	22.9	TOF

AVSD, atrioventricular septal defect; DORV, double-outlet right ventricular; LSVC, persistent left superior vena cava; PA, pulmonary artery; PS, pulmonary stenosis; TOF, tetralogy of Follot; TOP, termination of pregnancy; TGA, transposition of great arteries; VSD, ventricular septal defect

Table 7.2 Sensitivity, specificity, false positive percentage, false negative percentage, positive likelihood ratio and negative likelihood ratio of each modality in assessment of fetal VSDs

Image modality	Sensitivity	Specificity	False positive percentage	Positive likelihood ratio	False negative percentage	Negative likelihood ratio
Live xPlane imaging	53.3% (8/15)	100% (35/35)	0% (0/8)	∞	16.7% (7/42)	0.53
Live 3D imaging	53.3% (8/15)	91.4% (32/35)	27.3% (3/11)	6.20	17.9% (7/39)	0.51
Multiplanar view of STIC from 4CV	73.3% (11/15)	80% (28/35)	38.9% (7/18)	3.67	12.5% (4/32)	0.33
Rendered view of STIC from 4CV	73.3% (11/15)	80% (28/35)	38.9% (7/18)	3.67	12.5% (4/32)	0.33
Multiplanar view of STIC from sagittal	66.7% (10/15)	97.1% (34/35)	90.9% (1/11)	23.00	12.8% (5/39)	0.34
Rendered view of STIC from sagittal	73.3% (11/15)	77.1% (27/35)	42.1% (8/19)	3.20	12.9% (4/31)	0.35

Table 7.3 Summary of image quality score of each 3DE modalities

Group	Image modality	Imaging quality	Outline of IVS	Motion artefact	Overall score
1	Live xPlane imaging	0.76±0.43	0.82±0.39	1.00±0.00	2.58±0.76
2	Live 3D imaging	0.80±0.40	0.64±0.48	0.98±0.14	2.42±0.86
3	Multiplanar view of STIC from the four-chamber view	0.32±0.47*	0.36±0.48*	0.30±0.46*	0.98±1.04*
4	Rendered view of STIC from the four-chamber view	0.38±0.49*	0.56±0.50*	0.48±0.50*	1.42±1.20*
5	Multiplanar view of STIC from the sagittal view	0.60±0.49	0.62±0.49	0.92±0.27	2.14±1.01
6	Rendered view of STIC from the sagittal view	0.70±0.46	0.80±0.40	0.88±0.33	2.38±1.00

* Compared with Group 1, 2, 5, 6, there exists significant difference ($P<0.05$). There was no significant difference between Group 1, 2, 5, 6 and between Group 3 and 4.

Table 8.1 live xPlane imaging of ductal view in 25 cases with conotruncal anomalies

No.	Diagnosis	Ductal view pattern	PA/AO	Conclusion	Follow-up
1	Truncus	Disappear	NA	Abnormal	Confirmed by autopsy
2	Truncus, SV	Disappear	NA	Abnormal	TOP refused autopsy
3	Truncus, AVSD, TAPVD	Disappear	NA	Abnormal	TOP refused autopsy
4	TOF	Existing	<1	Abnormal	TOP refused autopsy
5	TGA, SV	Disappear	NA	Abnormal	TOP refused autopsy
6	TOF	Existing	<1	Abnormal	TOP refused autopsy
7	TOF, Omphalocele	Disappear	NA	Abnormal	TOP refused autopsy
8	TGA, SV, LSVC	Disappear	NA	Abnormal	Confirmed by autopsy
9	Truncus	Disappear	NA	Abnormal	TOP refused autopsy
10	Truncus	Disappear	NA	Abnormal	Confirmed by autopsy
11	TGA without VSD	Disappear	NA	Abnormal	TOP refused autopsy
12	TGA without VSD	Disappear	NA	Abnormal	Confirmed by autopsy
13	Truncus	Disappear	NA	Abnormal	TOP refused autopsy
14	TOF, R-ARCH	Existing	<1	Abnormal	TOP refused autopsy
15	Truncus	Disappear	NA	Abnormal	Confirmed by autopsy
16	DORV, PS	Disappear	NA	Abnormal	Confirmed by autopsy
17	TOF	Existing	>1	Normal	TOP refused autopsy
18	TOF	Existing	<1	Abnormal	TOP refused autopsy
19	Corrected TGA	Disappear	NA	Abnormal	Confirmed by autopsy
20	Truncus	Disappear	NA	Abnormal	TOP refused autopsy
21	Truncus	Disappear	NA	Abnormal	TOP refused autopsy
22	TOF	Existing	<1	Abnormal	TOP refused autopsy
23	DORV	Disappear	NA	Abnormal	TOP refused autopsy

24	TOF	Existing	>1	Normal	TOP refused autopsy
25	DORV, AVSD	Disappear	NA	Abnormal	TOP refused autopsy

AVSD, atrioventricular septal defect; DORV, double-outlet right ventricular; LSVC, persistent left superior vena cava; R-ARCH, right-sided aortic arch; PS, pulmonary stenosis; SV, single ventricle; TOF, tetralogy of Follot; TOP, termination of pregnancy; TGA, transposition of great arteries; VSD, ventricular septal defect

Table 8.2 Live xPlane view of ductal view in 23 cases with non-conotruncal CHDs

No.	Diagnosis	Ductal view pattern	PA/AO	Conclusion	Follow-up
1	AVSD	Existing	>1	Normal	TOP refused autopsy
2	Dextroposition	Disappear	NA	Abnormal	TOP refused autopsy with extracardiac anomalies
3	ASD	Existing	>1	Normal	Confirmed by postnatal echocardiography
4	Ectopia, SV	Disappear	NA	Abnormal	Confirmed by autopsy
5	AVSD	Existing	>1	Normal	TOP refused autopsy
6	VSD	Existing	>1	Normal	TOP refused autopsy
7	R-ARCH	Existing	>1	Normal	Confirmed by postnatal echocardiography
8	HLHS	Disappear	>1	Abnormal	TOP refused autopsy
9	LSVC	Existing	>1	Normal	Confirmed by postnatal echocardiography
10	LSVC	Existing	>1	Normal	Confirmed by postnatal echocardiography
11	LSVC	Existing	>1	Normal	Confirmed by postnatal echocardiography
12	VSD	Existing	>1	Normal	TOP refused autopsy
13	Severe PS	Disappear	NA	Abnormal	TOP refused autopsy
14	AVSD	Existing	>1	Normal	TOP refused autopsy
15	PS	Existing	>1	Normal	TOP refused autopsy
16	Cardiac tumor	Existing	>1	Normal	TOP refused autopsy
17	AVSD	Existing	>1	Normal	Confirmed by autopsy
18	PA, TS	Disappear	NA	Abnormal	TOP refused autopsy
19	VSD	Existing	>1	Normal	Confirmed by autopsy
20	PA, VSD	Disappear	NA	Abnormal	TOP refused autopsy
21	PA, TS, TR	Disappear	NA	Abnormal	TOP refused autopsy
22	VSD	Existing	>1	Normal	TOP refused autopsy
23	Pericardial effusion	Existing	>1	Normal	IUFD without autopsy

ASD, atrial septal defect; AVSD, atrioventricular septal defect; HLHS, hypoplastic left heart syndrome; IUFD, intrauterine fetal death; LSVC, persistent left superior vena cava; R-ARCH, right-sided aortic arch; PA, pulmonary atresia; PS, pulmonary stenosis; SV, single ventricle; TOP, termination of pregnancy; TR, tricuspid regurgitation; TS, tricuspid stenosis; VSD, ventricular septal defect

Table 9.1 live xPlane imaging of in-plane view of IVS in 25 cases with conotruncal anomalies

No.	Diagnosis	Relation of AO and PA	VSD detected	Conclusion	Follow-up
1	Truncus	Abnormal	Yes	Abnormal	Confirmed by autopsy
2	Truncus, SV	Abnormal	No IVS	Abnormal	TOP refused autopsy
3	Truncus, AVSD, TAPVD	Abnormal	Yes	Abnormal	TOP refused autopsy
4	TOF	Normal	Yes	Abnormal	TOP refused autopsy
5	TGA, SV	Abnormal	No IVS	Abnormal	TOP refused autopsy
6	TOF	Normal	Yes	Abnormal	TOP refused autopsy
7	TOF, Omphalocele	Abnormal	Yes	Abnormal	TOP refused autopsy
8	TGA, SV, LSVC	Abnormal	No IVS	Abnormal	Confirmed by autopsy
9	Truncus	Abnormal	Yes	Abnormal	TOP refused autopsy
10	Truncus	Abnormal	Yes	Abnormal	Confirmed by autopsy
11	TGA without VSD	Abnormal	No	Abnormal	TOP refused autopsy
12	TGA without VSD	Abnormal	No	Abnormal	Confirmed by autopsy
13	Truncus	Abnormal	Yes	Abnormal	TOP refused autopsy
14	TOF, R-ARCH	Normal	Yes	Abnormal	TOP refused autopsy
15	Truncus	Abnormal	Yes	Abnormal	Confirmed by autopsy
16	DORV, PS	Abnormal	Yes	Abnormal	Confirmed by autopsy
17	TOF	Normal	No	Normal	TOP refused autopsy
18	TOF	Normal	Yes	Abnormal	TOP refused autopsy
19	Corrected TGA	Abnormal	Yes	Abnormal	Confirmed by autopsy
20	Truncus	Abnormal	Yes	Abnormal	TOP refused autopsy
21	Truncus	Abnormal	Yes	Abnormal	TOP refused autopsy
22	TOF	Normal	No	Normal	TOP refused autopsy
23	DORV	Abnormal	Yes	Abnormal	TOP refused autopsy

24	TOF	Normal	No	Normal	TOP refused autopsy
25	DORV, AVSD	Abnormal	Yes	Abnormal	TOP refused autopsy

AVSD, atrioventricular septal defect; DORV, double-outlet right ventricular; LSVC, persistent left superior vena cava; R-ARCH, right-sided aortic arch; PS, pulmonary stenosis; SV, single ventricle; TOF, tetralogy of Follot; TGA, transposition of great arteries; VSD, ventricular septal defect

Table 9.2 Live xPlane imaging of in-plane view of IVS in 23 cases with non-conotruncal CHDs

No.	Diagnosis	Relation of AO and PA	VSD detected	Follow-up
1	AVSD	Normal	Yes	TOP refused autopsy
2	Dextroposition	Abnormal	No	TOP refused autopsy with extracardiac anomalies
3	ASD	Normal	No	Confirmed by postnatal echocardiography
4	Ectopia, SV	Abnormal	No IVS	Confirmed by autopsy
5	AVSD	Normal	Yes	TOP refused autopsy
6	VSD	Normal	Yes	TOP refused autopsy
7	R-ARCH	Normal	No	Confirmed by postnatal echocardiography
8	HLHS	Abnormal	No	TOP refused autopsy
9	LSVC	Normal	No	Confirmed by postnatal echocardiography
10	LSVC	Normal	No	Confirmed by postnatal echocardiography
11	LSVC	Normal	No	Confirmed by postnatal echocardiography
12	VSD	Normal	Yes	TOP refused autopsy
13	Severe PS	Abnormal	No	TOP refused autopsy
14	AVSD	Normal	Yes	TOP refused autopsy
15	PS	Abnormal	No	TOP refused autopsy
16	Cardiac tumor	Normal	No	TOP refused autopsy
17	AVSD	Normal	Yes	Confirmed by autopsy
18	PA, TS	Normal	No	TOP refused autopsy
19	VSD	Normal	Yes	Confirmed by autopsy
20	PA, VSD	Normal	No	TOP refused autopsy
21	PA, TS, TR	Abnormal	No	TOP refused autopsy
22	VSD	Normal	No	TOP refused autopsy
23	Pericardial effusion	Normal	No	IUFD without autopsy

ASD, atrial septal defect; AVSD, atrioventricular septal defect; HLHS, hypoplastic left heart syndrome; IUFD, intrauterine fetal death; LSVC, persistent left superior vena cava; R-ARCH, right-sided aortic arch; PA, pulmonary atresia; PS, pulmonary stenosis; SV, single ventricle; TR, tricuspid regurgitation; TS, tricuspid stenosis; VSD, ventricular septal defect

Table 10.1 Acquisition time and Angle of deviation from the true midsagittal section for FMF and non-FMF certified operators. Each operator scanned five patients, each for five images.

	Acquisition time (s)				Angle of deviation (?			
	Mean	SD	Median	IQR	Mean	SD	Median	IQR
FMF Group: FMF certified operators								
1	69.3	114.8	17.0	8.5-70.0	1.5	1.2	1.2	0.8-2.2
2	103.3	180.4	34.0	19.5-77.0	3.0	1.8	2.7	1.5-4.3
3	70.2	75.3	34.0	23.5-104.0	3.3	2.6	2.0	1.2-5.7
4	74.3	104.2	33.0	20.5-97.5	3.7	4.5	2.3	1.1-4.6
Overall	79.3	123.6	32.0	16.3-84.5	2.9	2.9	2.0	1.1-4.2
Non-FMF Group: Non-FMF certified operators								
5	77.8	68.9	66.0	13.0-121.0	4.1	2.8	3.4	1.8-6.0
6	110.8	149.7	54.0	21.0-133.5	3.5	3.1	2.6	1.6-4.7
7	161.9	371.8	27.0	15.0-138.5	3.7	3.5	2.2	1.5-4.3
8	92.2	112.6	39.0	19.0-162.5	1.4	1.2	1.3	0.7-2.1
Overall	110.7	210.2	45.5	17.0-141.3	3.2	2.9	2.2	1.3-4.2

IQR: Inter-quartile range

Table 10.2 Summary of findings from previous study on the angle of deviation from the true midsagittal section for FMF and non-FMF certified operators using conventional approach.

	Angle of deviation (?			
	Mean	SD	Median	Interquartile range
FMF Group: FMF certified operators				
1	2.2	1.1	1.9	1.4-3.1
2	6.5	4.0	6.0	3.6-8.0
3	7.2	4.6	6.7	3.4-11.8
4	7.0	4.0	6.5	5.3-7.4
Overall	5.7	4.2	5.1	2.4-7.4
Non-FMF Group: Non-FMF certified operators				
5	10.1	9.1	6.3	3.4-14.5
6	11.1	5.4	10.8	7.4-15.9
7	22.9	13.4	25.8	8.0-30.5
8	14.5	9.2	11.9	7.7-20.0
Overall	14.7	10.8	11.9	6.1-22.2

Each operator had 25 volume datasets, five from each of five patients.

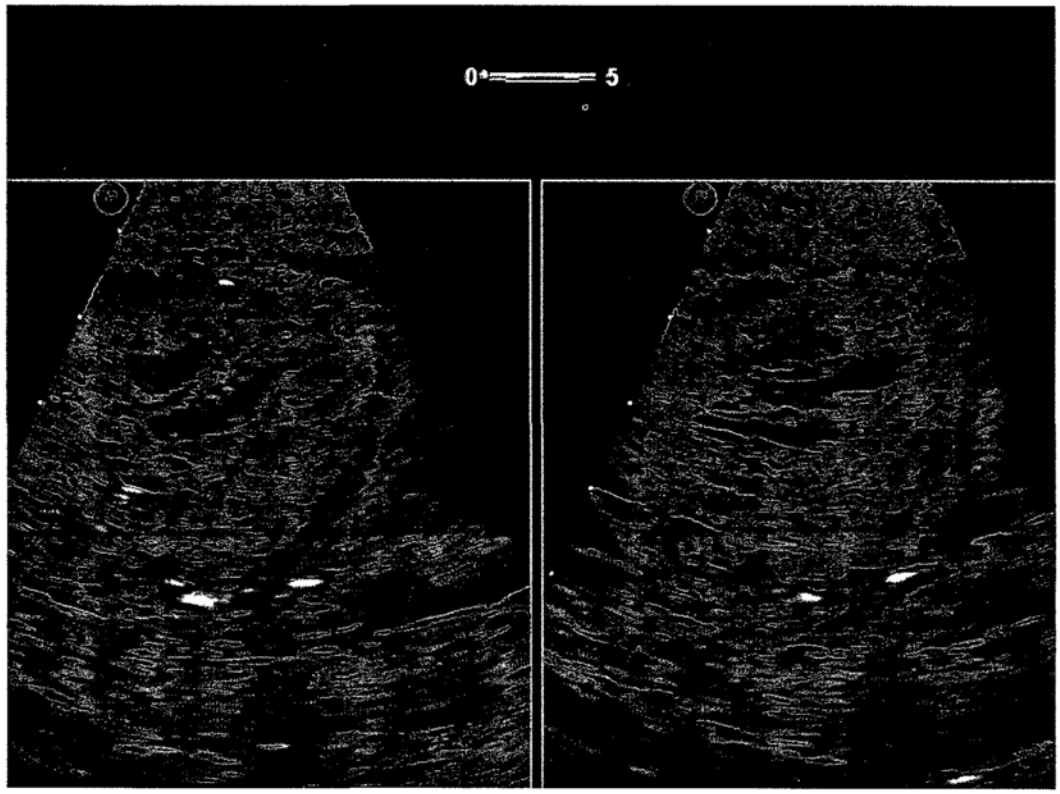

Figure 3.1 Live xPlane imaging of LVOT. Live xPlane imaging shows the LVOT using the four-chamber view as the starting plane by titling the reference plane towards the fetal head.

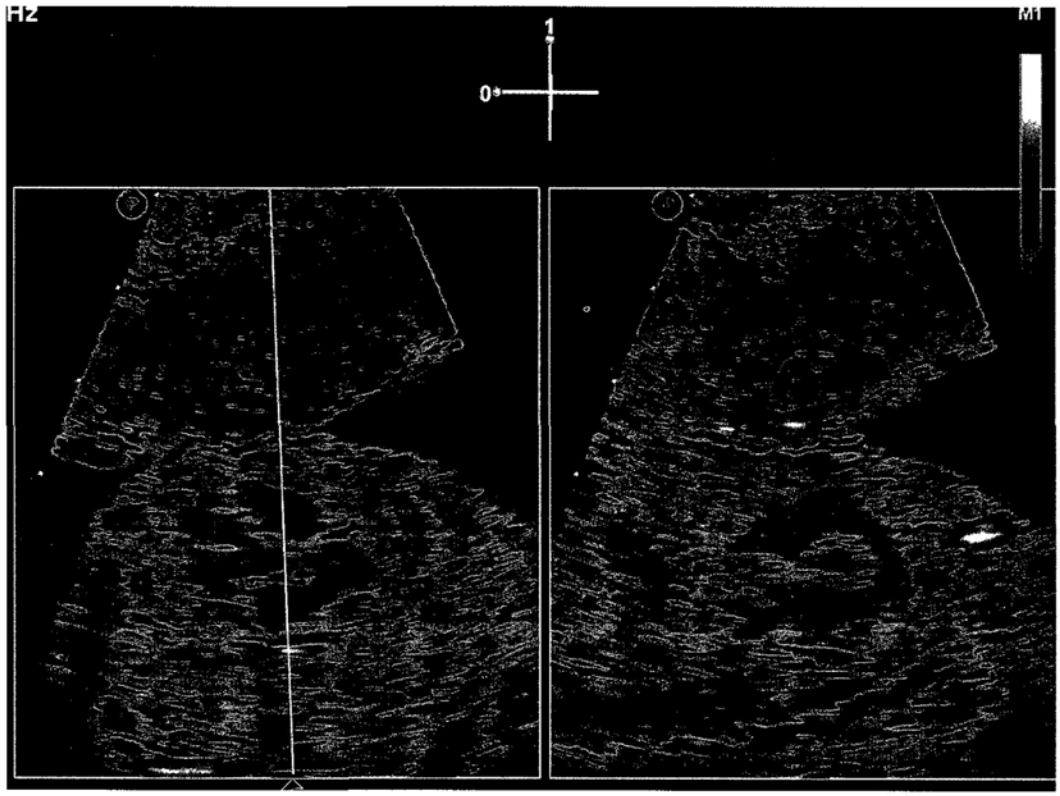

Figure 3.2 Live xPlane imaging shows the RVOT view using the four-chamber view as the starting plane by moving the reference line across right ventricle, criss-cross, left atrium and descending aorta.

Figure 3.3 Live xPlane imaging shows the 3VT view using the four-chamber view as the starting plane by titling the reference plane more cephally towards the fetal head.

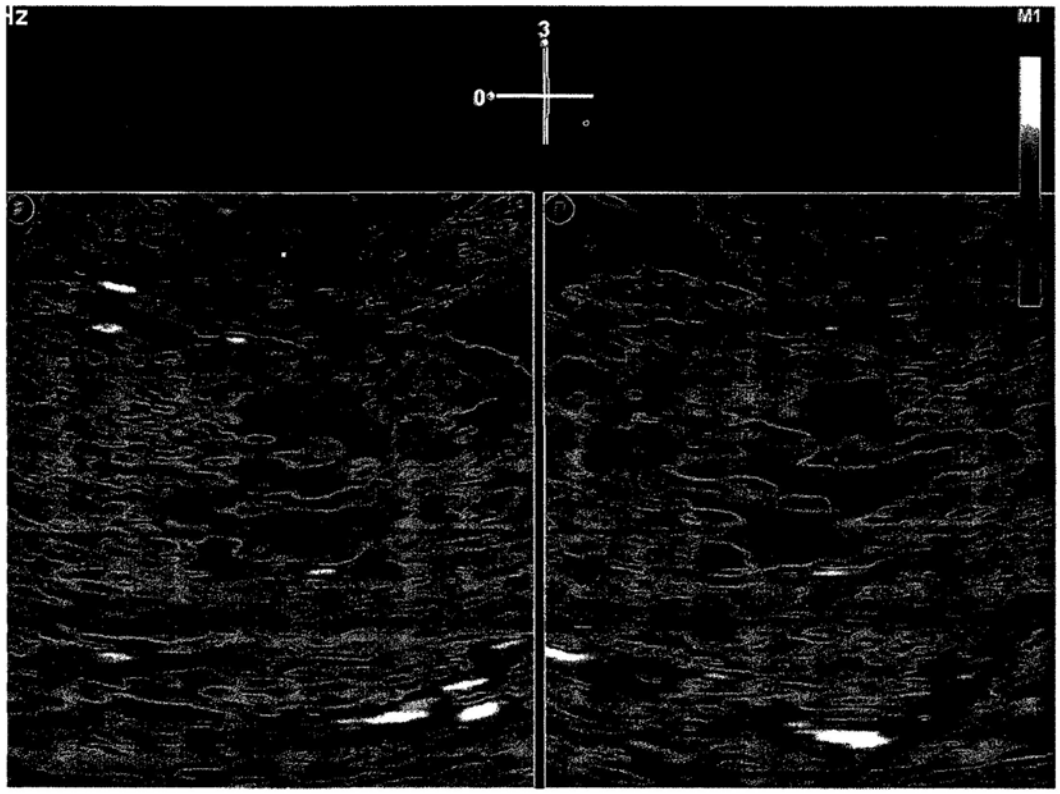

Figure 3.4 Live xPlane imaging shows the LVOT using the mid-sagittal as the starting plane by putting the reference line through the root of aorta.

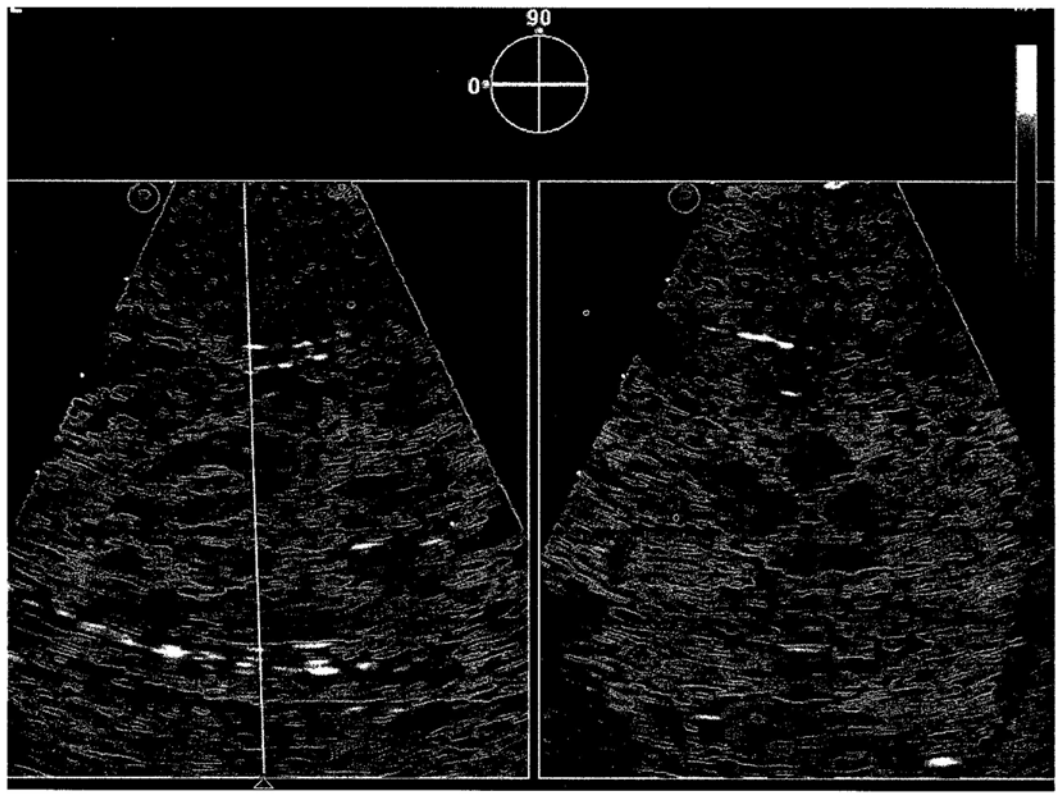

Figure 3.5 Live xPlane imaging shows the four-chamber using the mid-sagittal view as the starting plane by putting the reference just below the root of aorta.

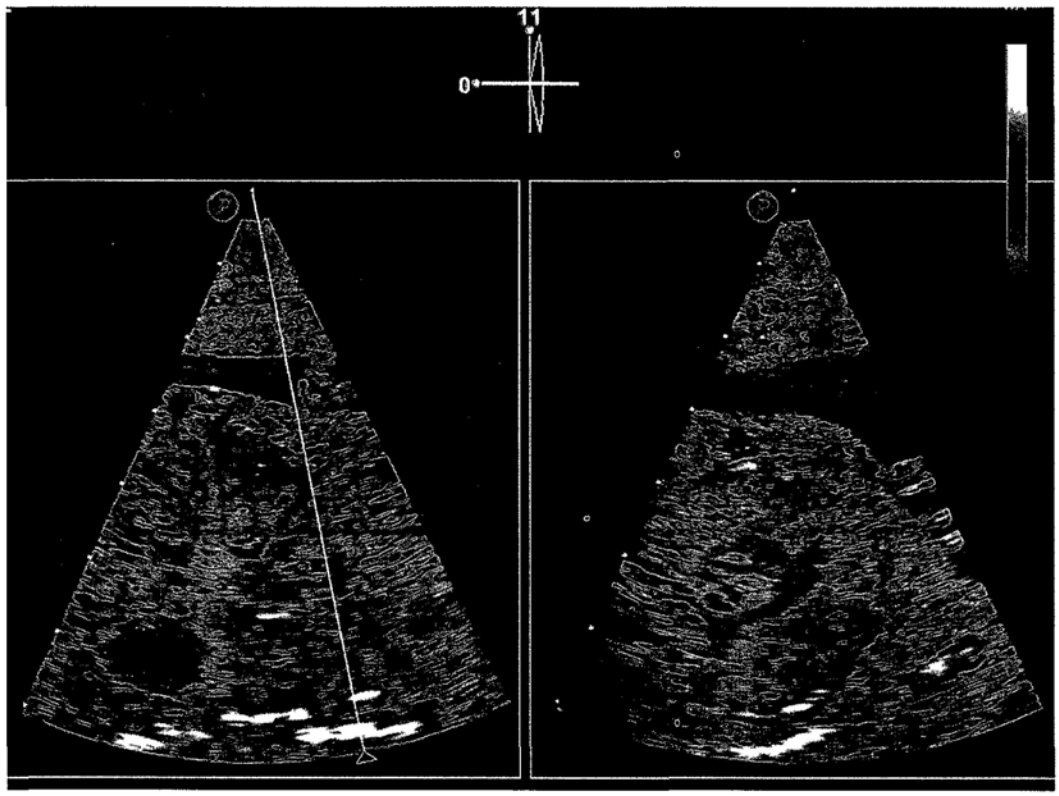

Figure 3.6 Live xPlane imaging shows the VT using the mid-sagittal view as the starting plane by putting the reference line across the upper thorax.

Figure 3.7 Live xPlane imaging shows the RVOT using the four-chamber view as the starting plane by rotating the image around the root of aorta.

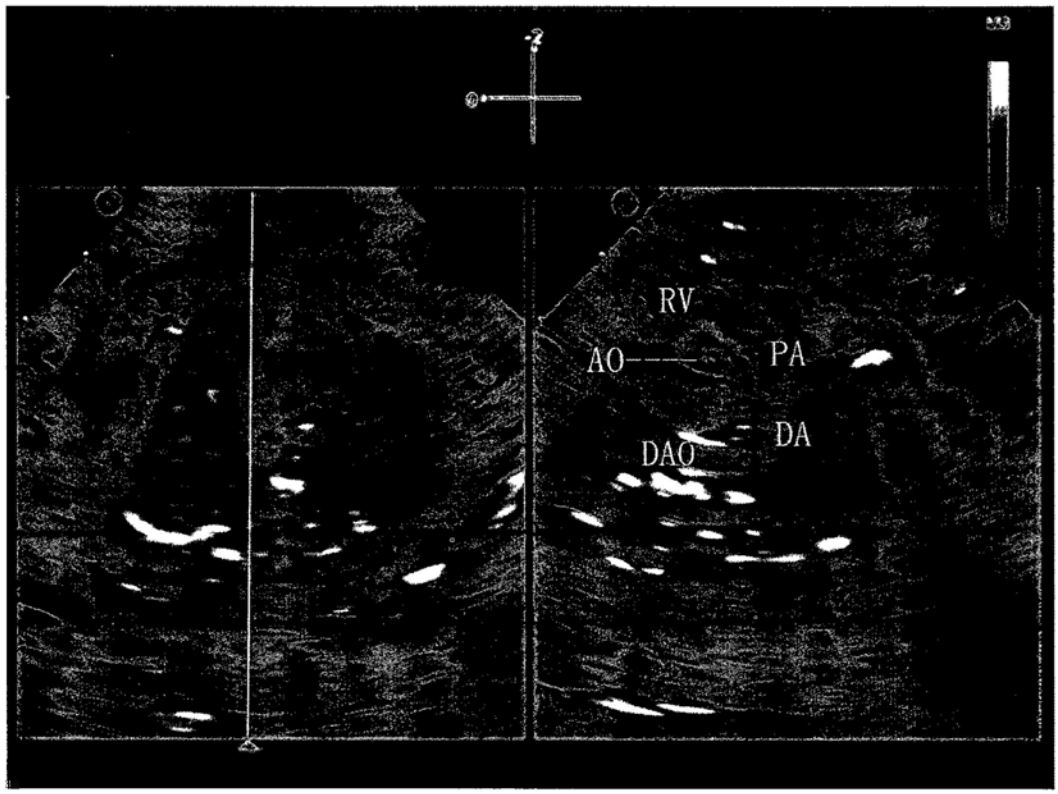

Figure 4.1 Ductal arch view shown by live xPlane imaging. A normal case is shown. 3VT view was shown on the left side and the ductal arch view displayed on the right window in real time. The original reference line in the primary image on the left side was hided after the image was frozen. The reference line shown here was added by the authors. AO, transverse view of aorta; DAO, descending aorta; DA, ductus arteriosus; PA, pulmonary artery; RV, right ventricle

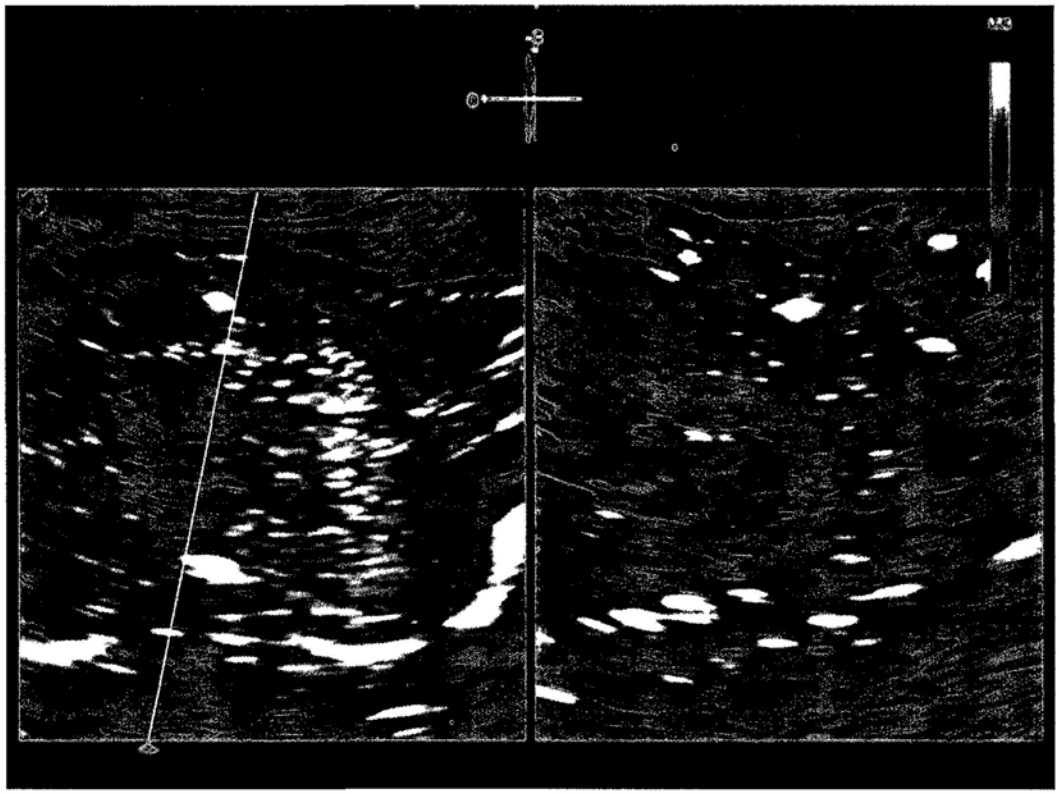

Figure 4.2 Aortic arch view displayed by live xPlane imaging. A normal case is shown. 3VT view was shown on the left side and the aortic arch view displayed on the right window in real time. The original reference line in the primary image on the left side was hided after the image was frozen. The reference line shown here was added by the authors.

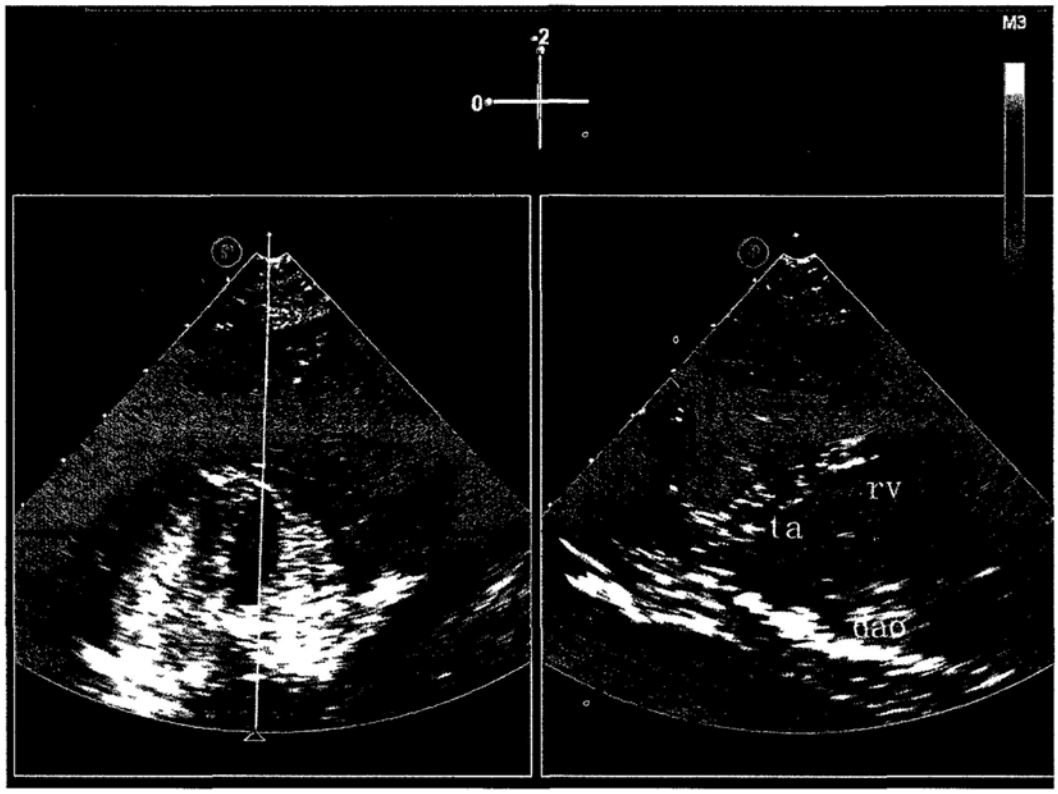

Figure 4.3 Ductal arch view of truncus arteriosus shown by live xPlane imaging. Only one artery was shown on the 3VT view on the left side. An abnormal ductal arch view was displayed on the right window. It lost the typical picture of ascending aorta surrounded by the right ventricle, pulmonary artery and ductus arteriosus. The original reference line in the primary image on the left side was hided after the image was frozen. The reference line shown here was added by the authors. dao, descending aorta; rv, right ventricle; ta, truncus arteriosus

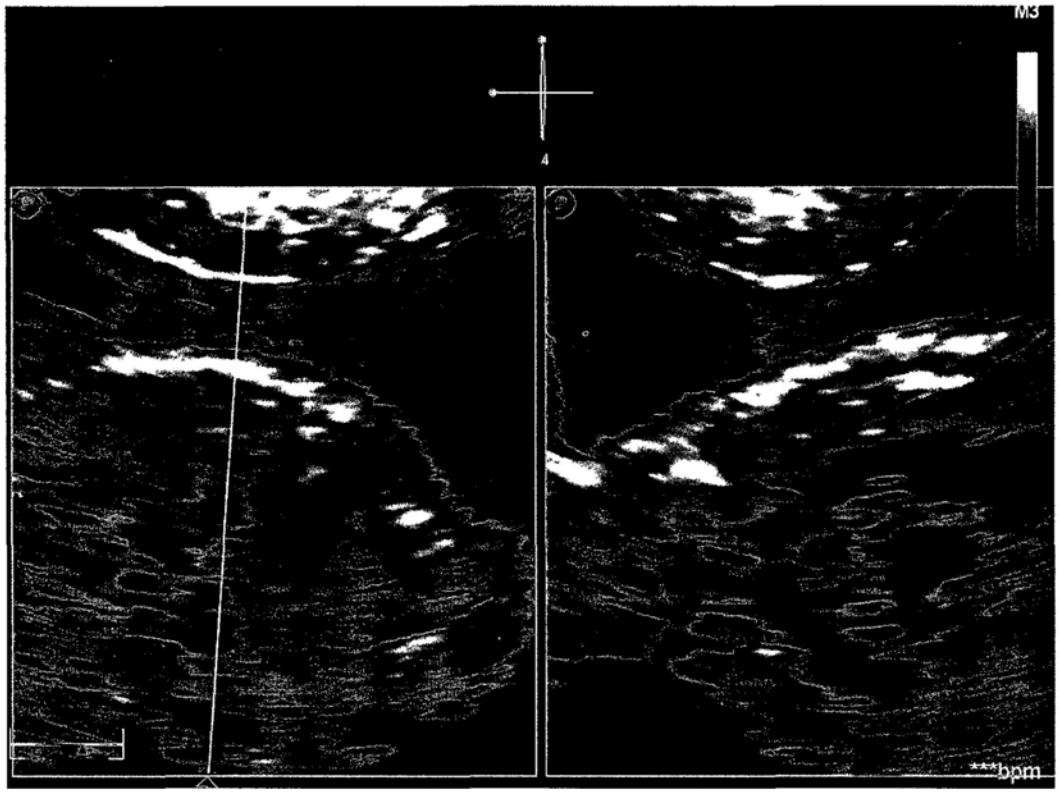

Figure 4.4 Live xPlane imaging of corrected TGA case. This case had the normal 3VT view. It showed the aortic arch when the reference line was placed across the right vessel on the 3VT view, which would be originally the pulmonary artery in the normal fetus.

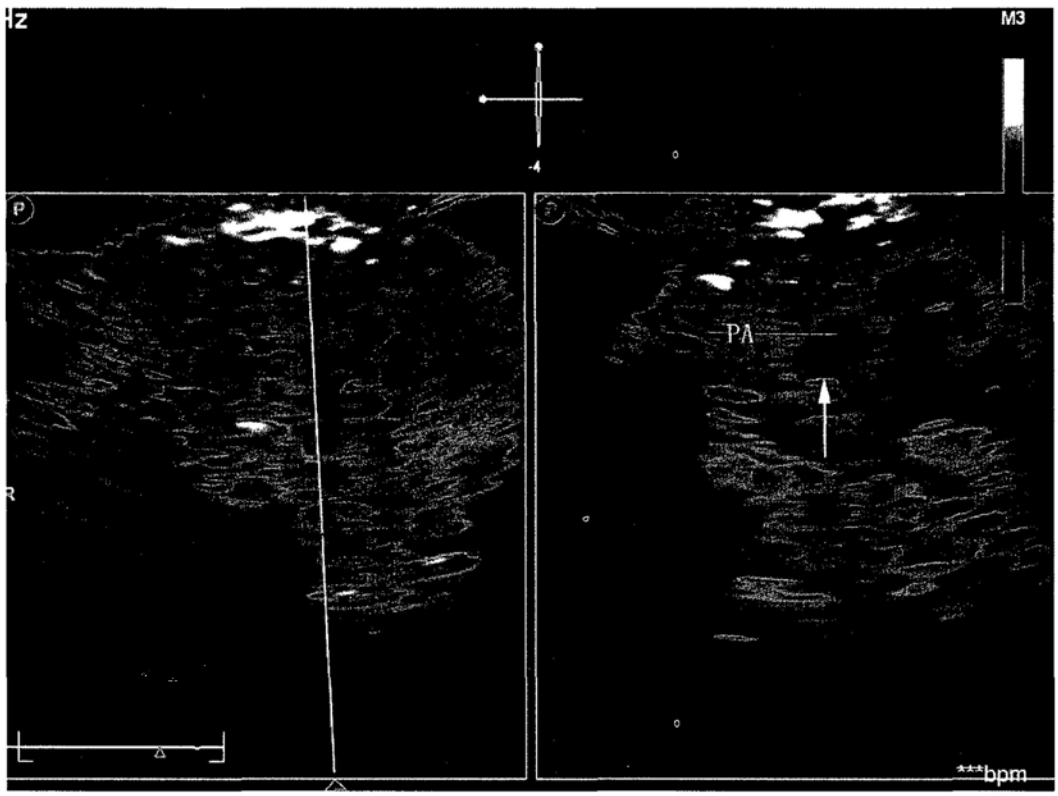

Figure 4.5 Live xPlane imaging of corrected TGA case. Figure 4.4 and Figure 4.5 are the same case. This case had the normal 3VT view. However, it showed the pulmonary artery when the reference line was placed across the middle vessel on the 3VT view, which would be originally the aortic arch in the normal fetus. The arrow showed the bifurcation of the pulmonary artery. PA, pulmonary artery

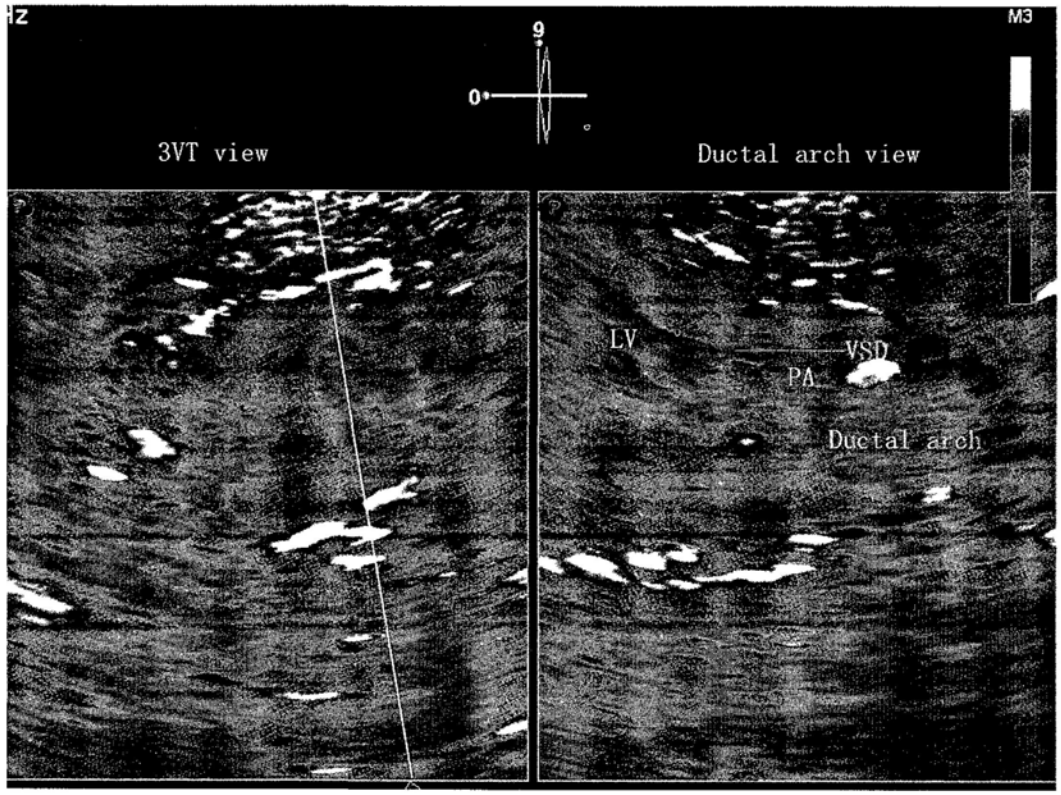

Figure 4.6 Live xPlane imaging of double outlet of right ventricle. It showed the normal 3VT view. However, it showed abnormal ductal view when the reference line was put across the pulmonary artery. The transverse view of aorta disappeared which would be exist in the normal fetus. LV, left ventricle; PA, pulmonary artery; VSD, ventricular septal defect

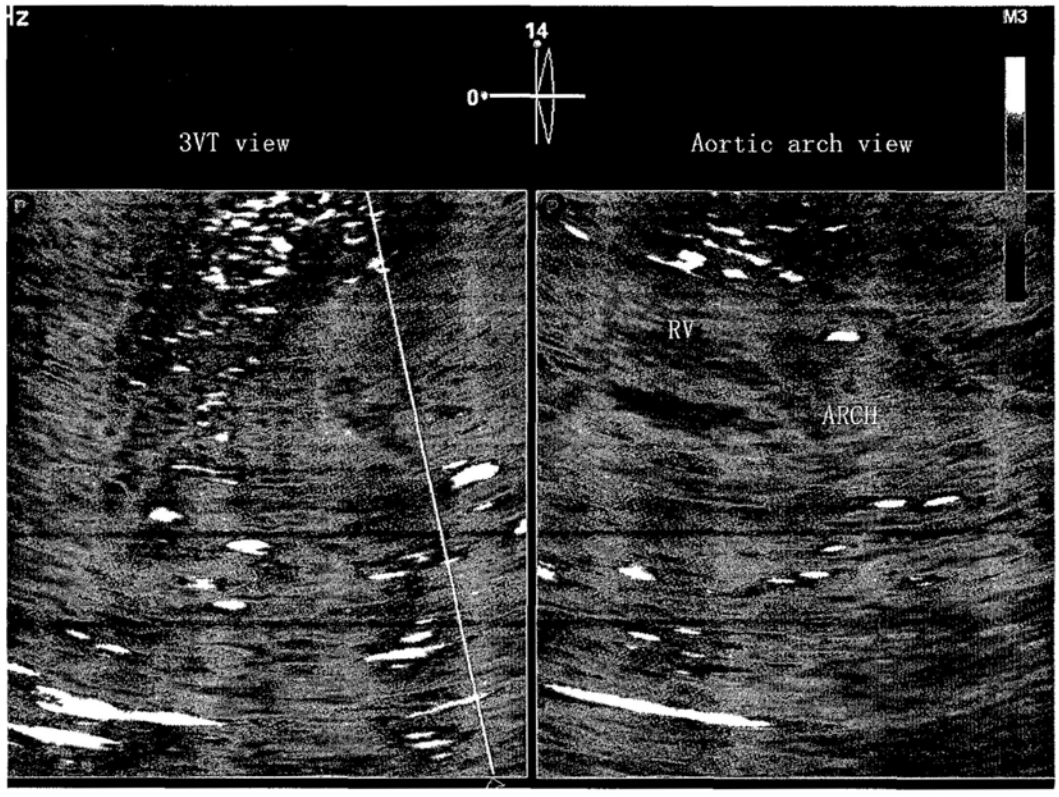

Figure 4.7 Live xPlane imaging of double outlet of right ventricle. It showed the normal 3VT view. However, it showed abnormal ductal view when the reference line was put across the transverse aortic arch. The sagittal view of aortic arch displayed. However, the aorta originated directly from the right ventricle. LV, left ventricle; PA, pulmonary artery; VSD, ventricular septal defect

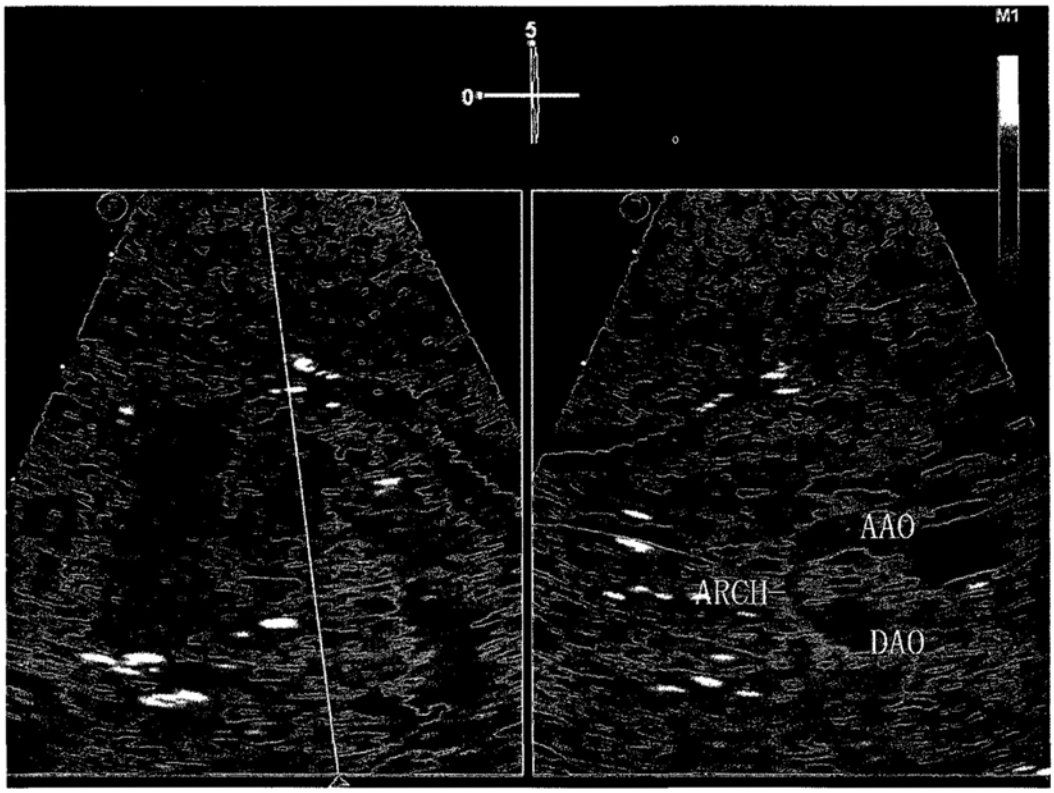

Figure 4.8 Live xPlane imaging showed narrow isthmus in the coarctation of aortic arch case. The reference line was put across the transverse aortic arch on the 3VT shown in left window and the aortic arch view shown in the right window in real time. The case was confirmed by postnatal echocardiography. AAO, ascending aorta; ARCH, aortic arch; DAO, descending aorta

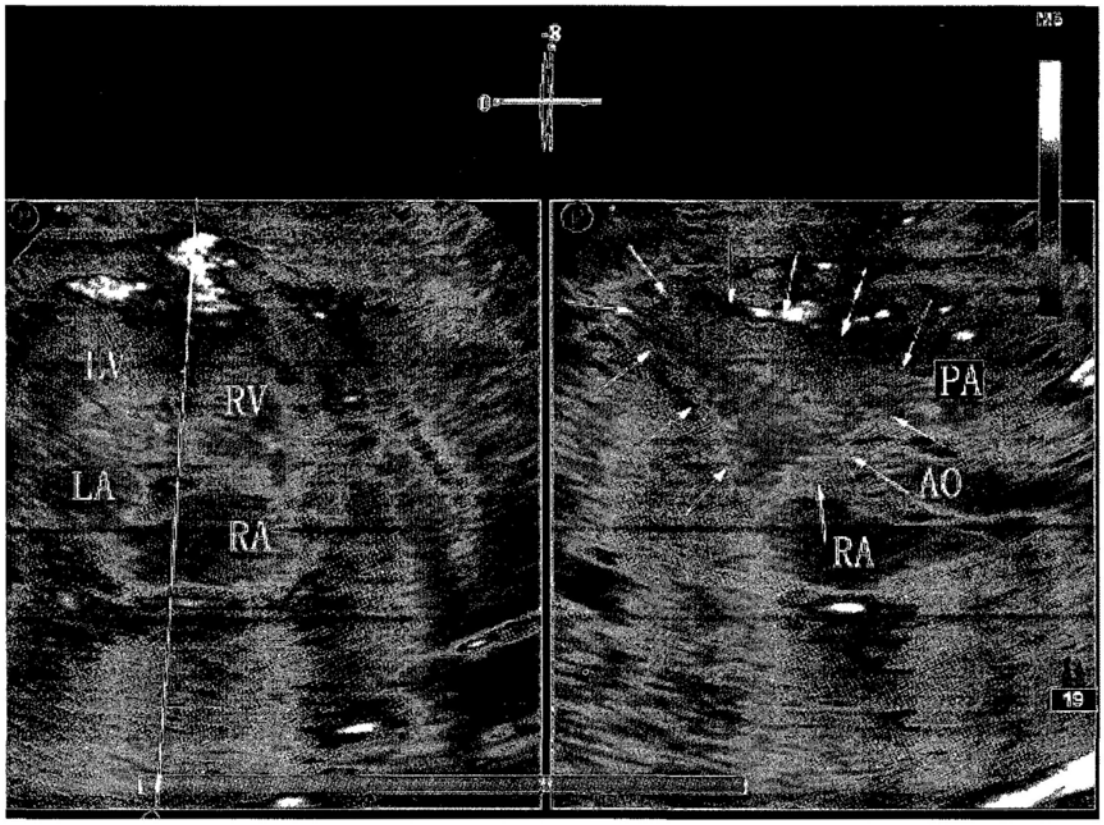

Figure 5.1 In-plane view of IVS with the fetal spine posterior displayed by the live xPlane imaging. A normal case is shown, with the outline of the septum indicated by the arrow. The original reference line in the primary image on the left side was hided after the image was frozen. The reference line shown here was added by the authors. Ao, aorta; LA, left atrium; RA, right atrium; LV, left ventricle; RV, right ventricle; PA, pulmonary artery

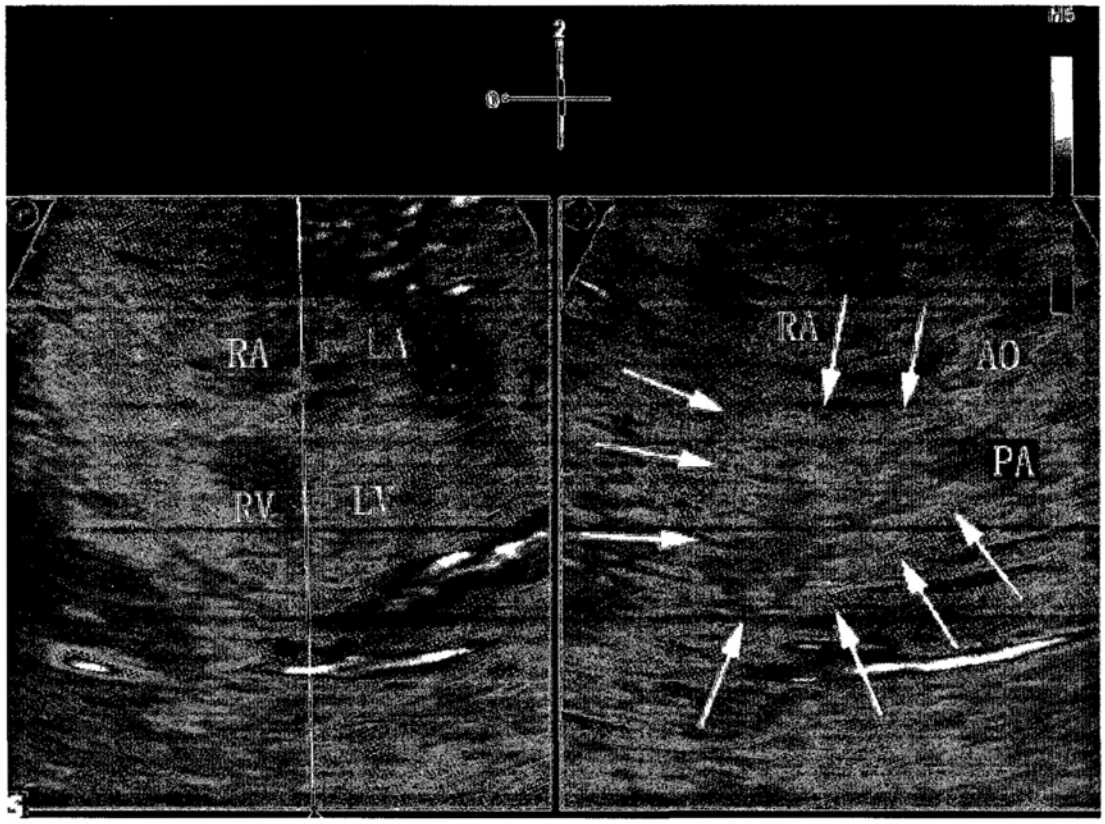

Figure 5.2 In-plane view of IVS with the fetal spine anterior displayed by the live xPlane imaging. A normal case is shown, with the outline of the septum indicated by the arrow. Ao, aorta; LA, left atrium; RA, right atrium; LV, left ventricle; RV, right ventricle; PA, pulmonary artery

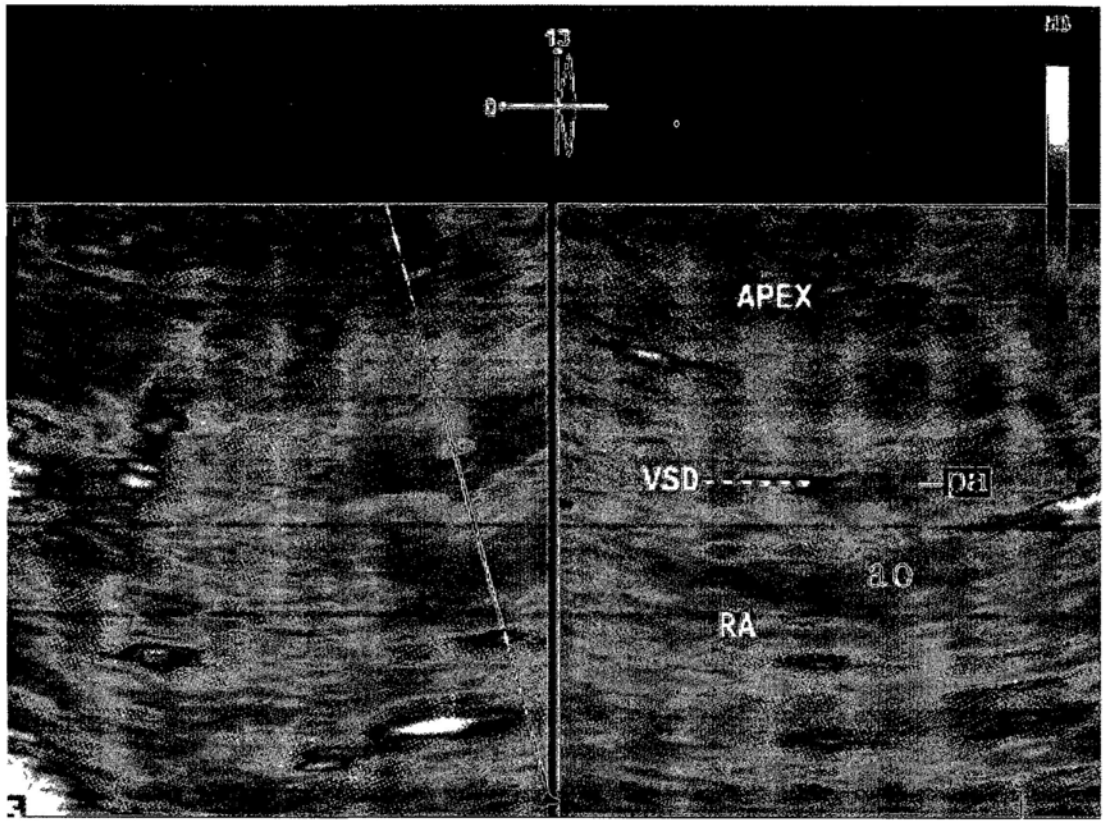

Figure 5.3 Live xPlane imaging showed VSD on the in-plane view of IVS in isolated VSD case with the fetal spine posterior. ao, aorta; RA; right atrium; PA, pulmonary artery; VSD, ventricular septal defect

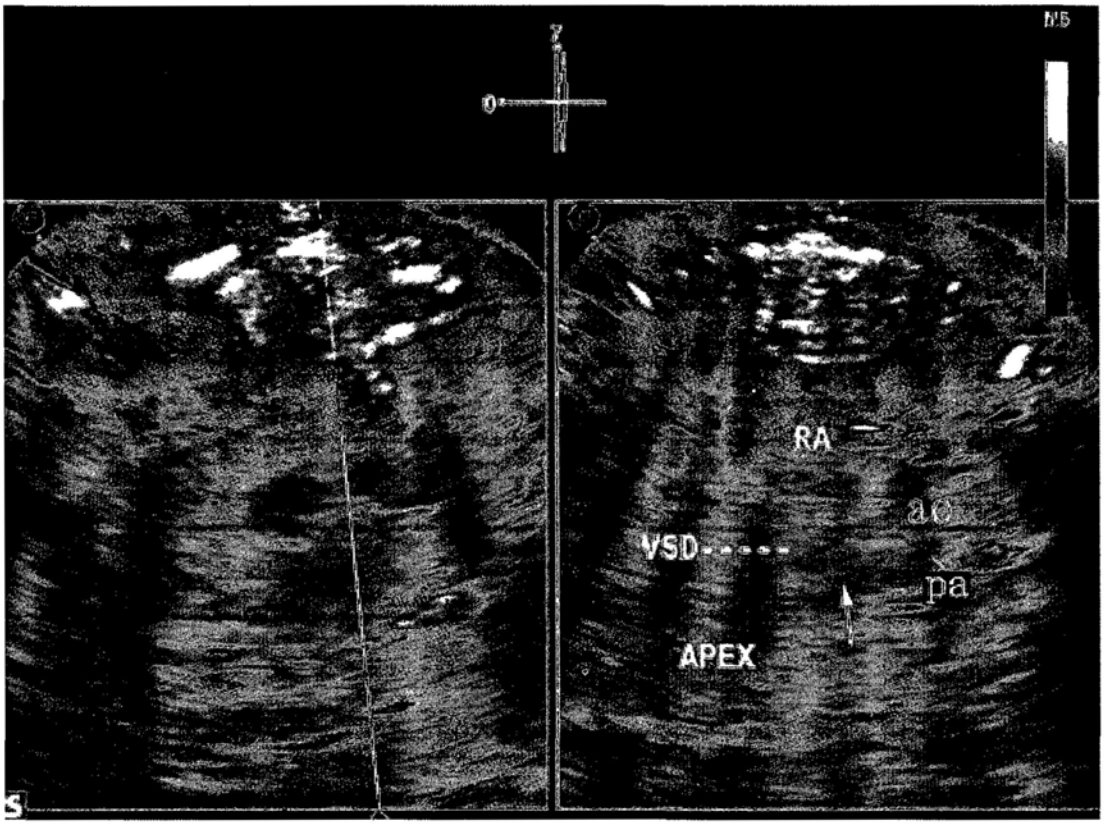

Figure 5.4 The same case as Figure 4. Live xPlane imaging showed VSD on the in-plane view of IVS in isolated VSD case with the fetal spine anterior. The VSD is indicated by the arrow. ao, aorta; RA; right atrium; PA, pulmonary artery; VSD, ventricular septal defect

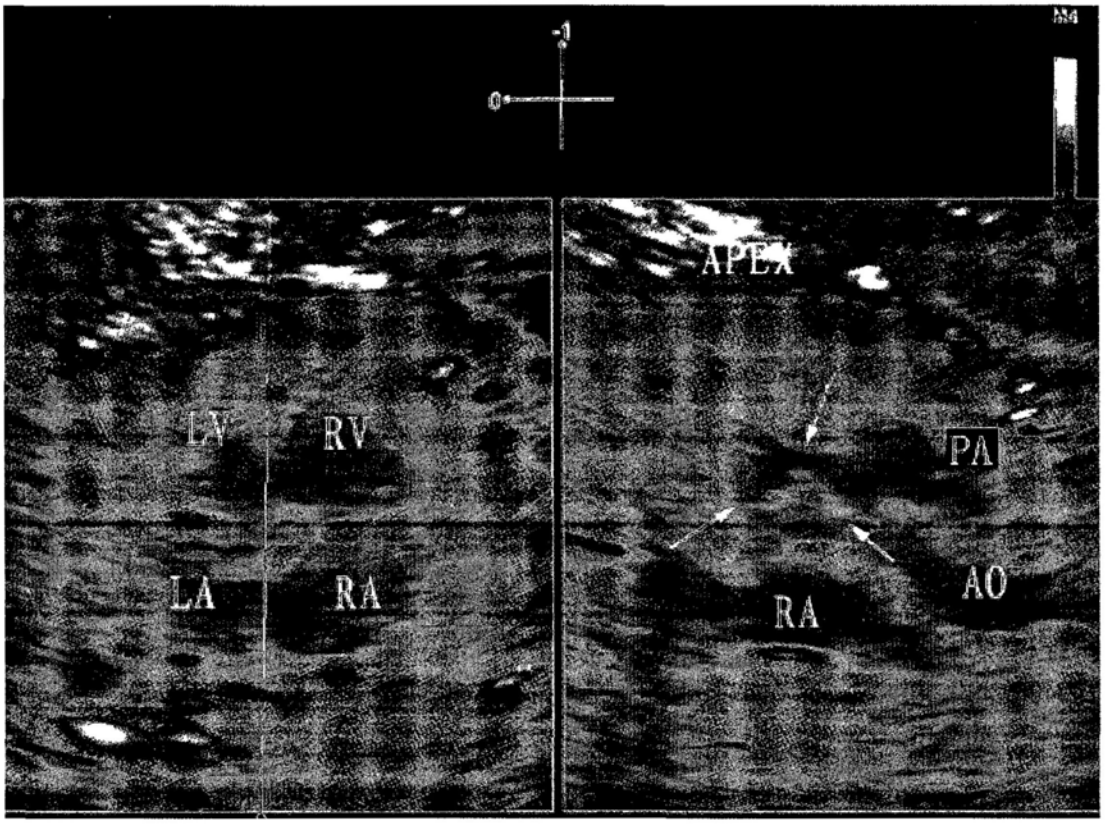

Figure 5.5 Live xPlane imaging showed VSD on the in-plane view of IVS in AVSD case. The VSD is indicated by the arrow. LA, left atrium; RA, right atrium; LV, left ventricle; RV, right ventricle; PA, pulmonary artery

Figure 6.1 Procedure of live 3D imaging in visualizing the en face view of IVS in a normal case.

Figure 6.1a Firstly acquired an apical four-chamber view of the fetal heart, with the apex pointing at about 12 o扪lock position.

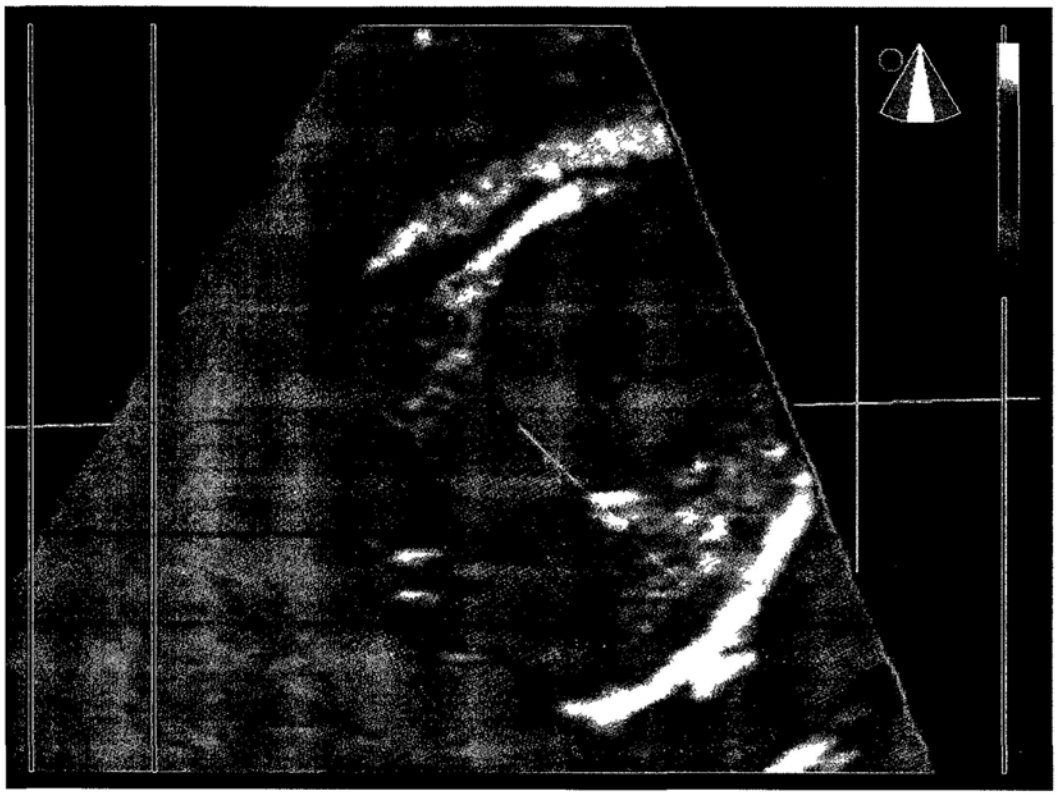

Figure 6.1b Next, the live 3D function was activated and then adjusted the acquisition angle to 72? and cropped the volume by the green box (along the z-axis) to display the 3D imaging of four-chamber view.

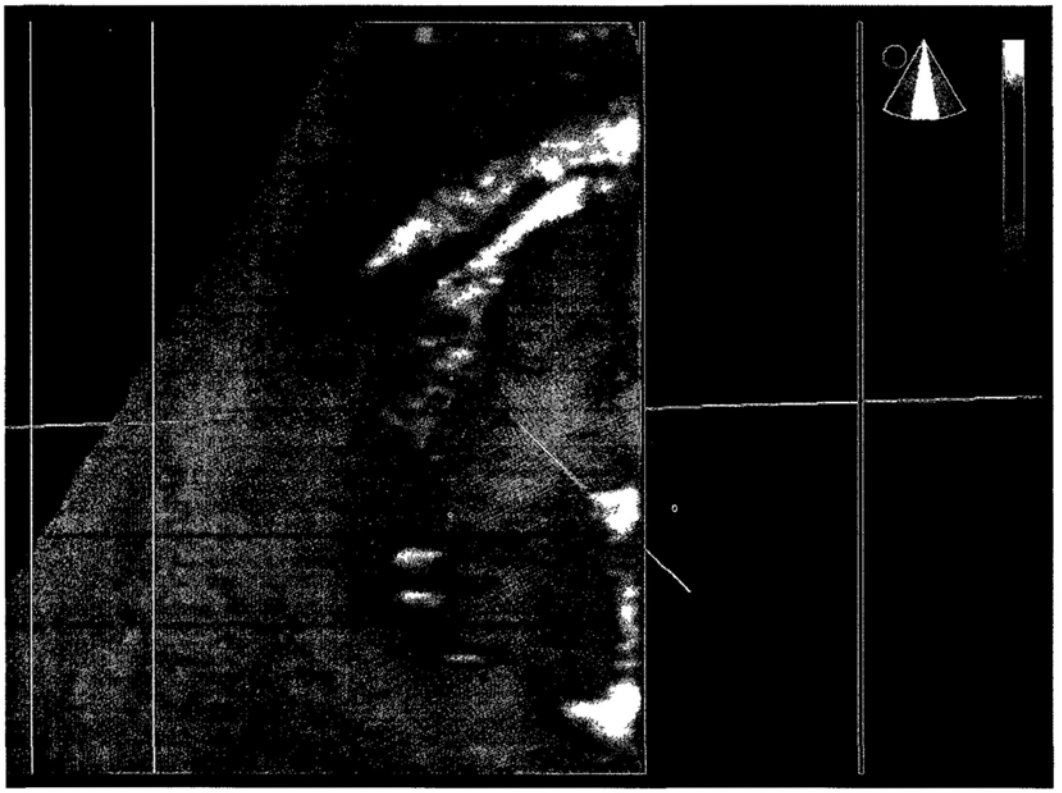

Figure 6.1c When the fetus remained quiescent for 1 to 2 seconds, the 撽reeze? button was pressed. This produced a cine-loop of real-time 3D volumes. By using the 捶ine? function, the best volume was chosen. The volume was then cropped by moving the red box along the x-axis to the right side of the IVS on four-chamber view.

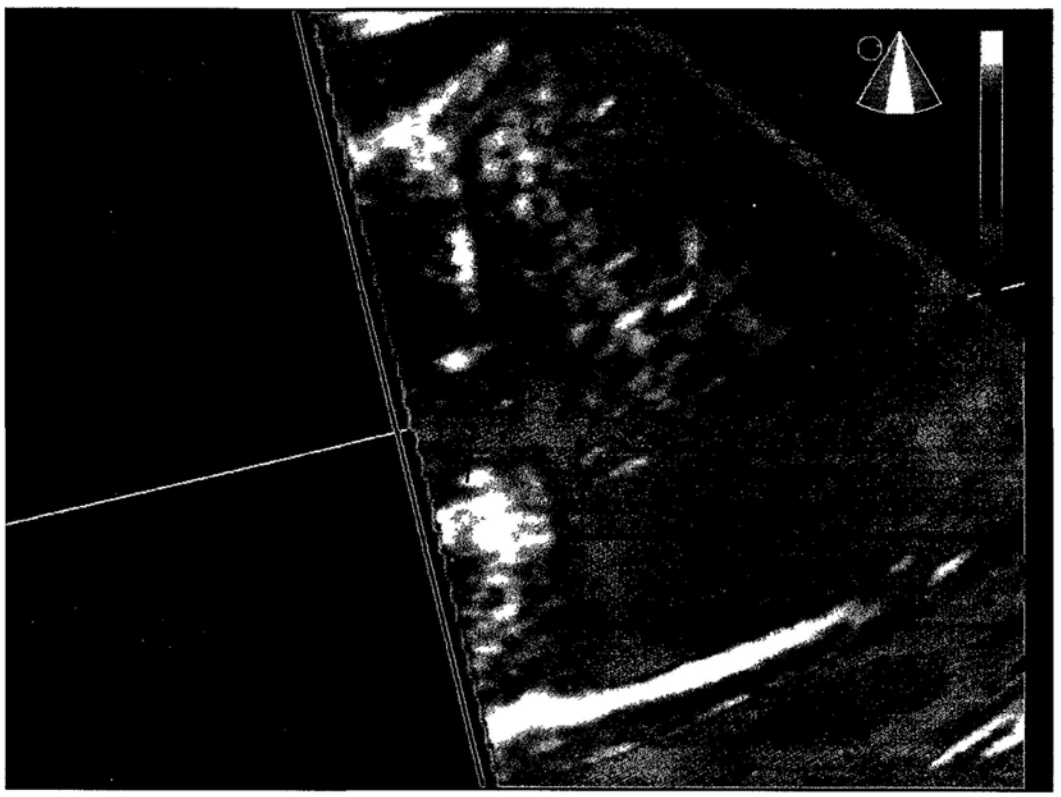

Figure 6.1d The resultant volume was then turned 90? along the y-axis to make the right side of IVS facing the operator.

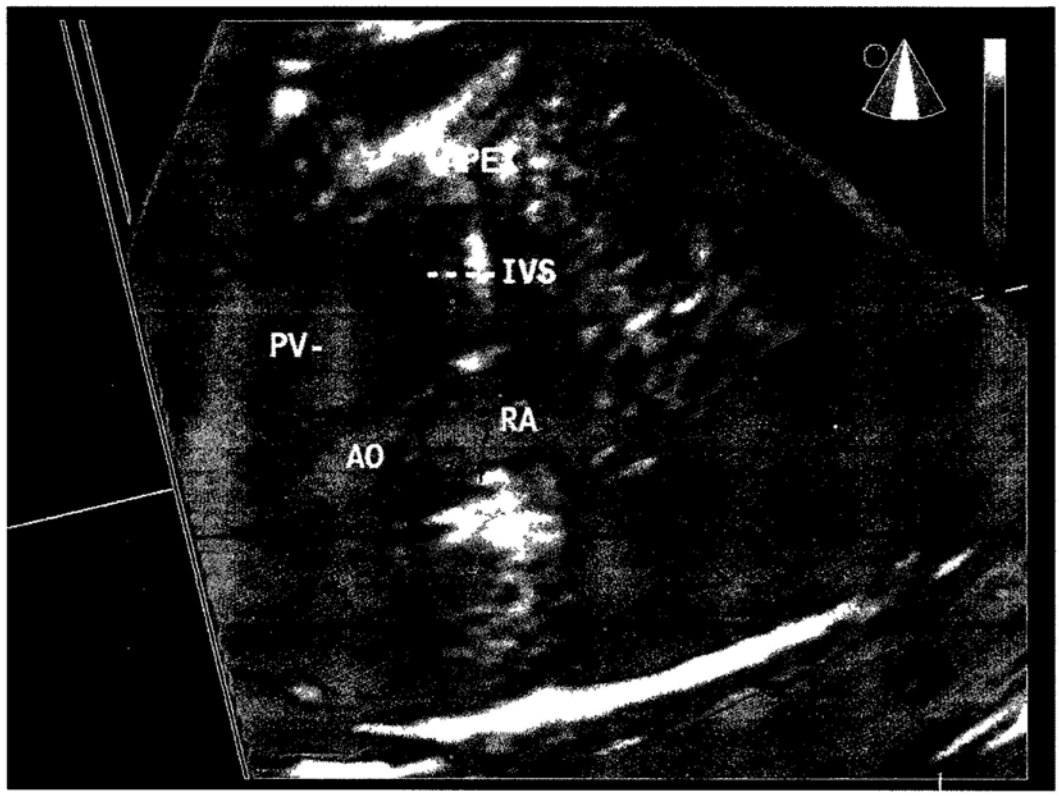

Figure 6.1e Last step was to perform additional cropping of the volume dataset along the original z-axis which was accomplished by scrolling back the green box. AO, aorta; RA, right atrium; PV, pulmonary valve; VSD, ventricular septal defect

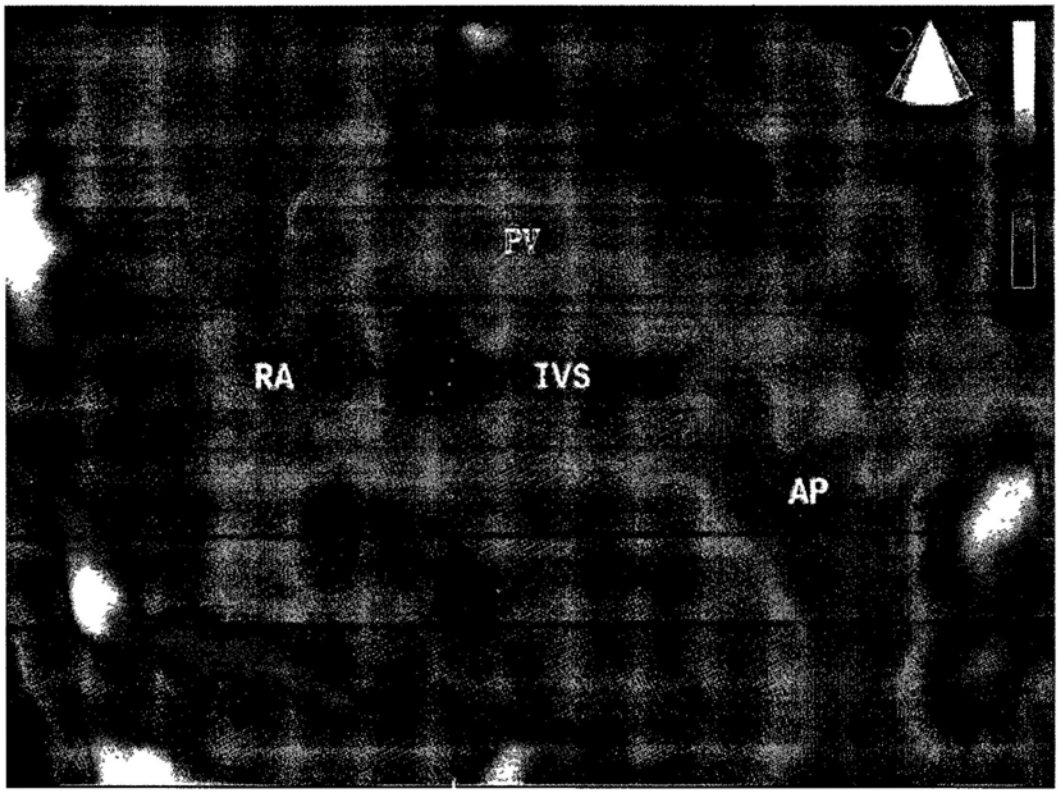

Figure 6.2 Image quality of the en face view obtained using live 3D imaging would be inferior if the axis of IVS was not parallel to the ultrasound beam, which would be seriously affected by the acoustic shadowing caused by the overlying rib cage, and the structures on the en face view were not easily interpreted. AP, apex; IVS, interventricular septum; RA, right atrium; PV, pulmonary valve

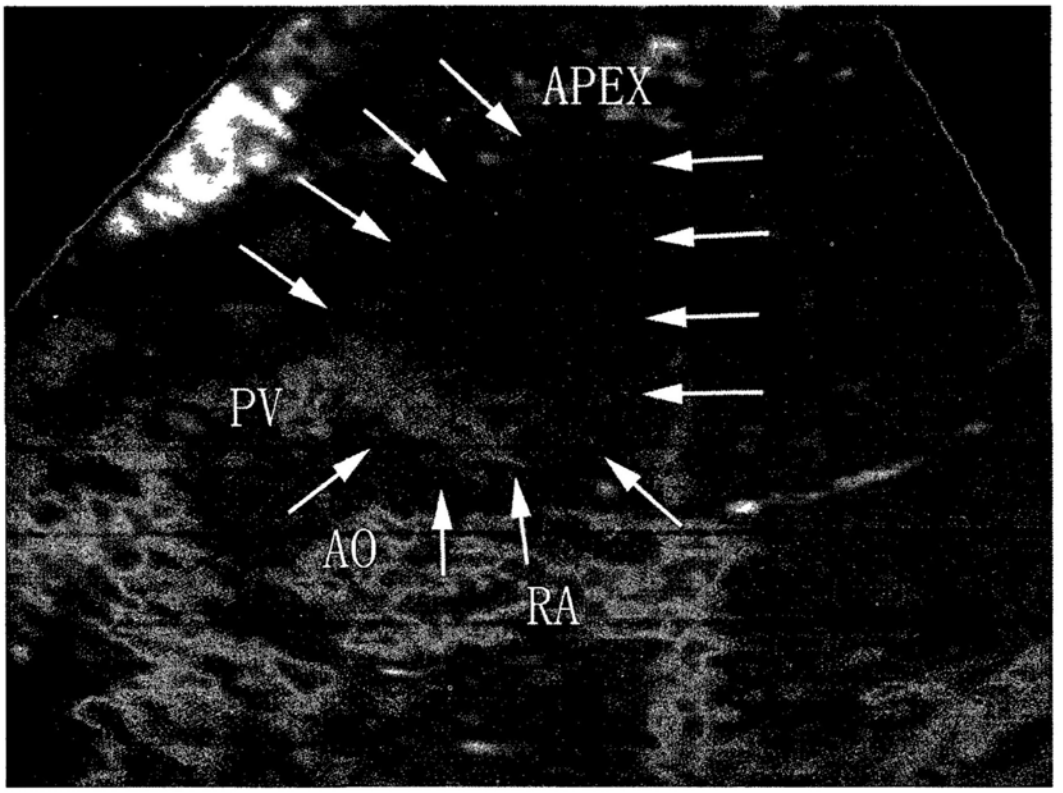

Figure 6.3 The en face view of IVS with the fetal spine posterior displayed by the live 3D imaging. A normal case is shown, with the outline of the septum indicated by the arrow. AO, aorta; RA, right atrium; PV, pulmonary valve

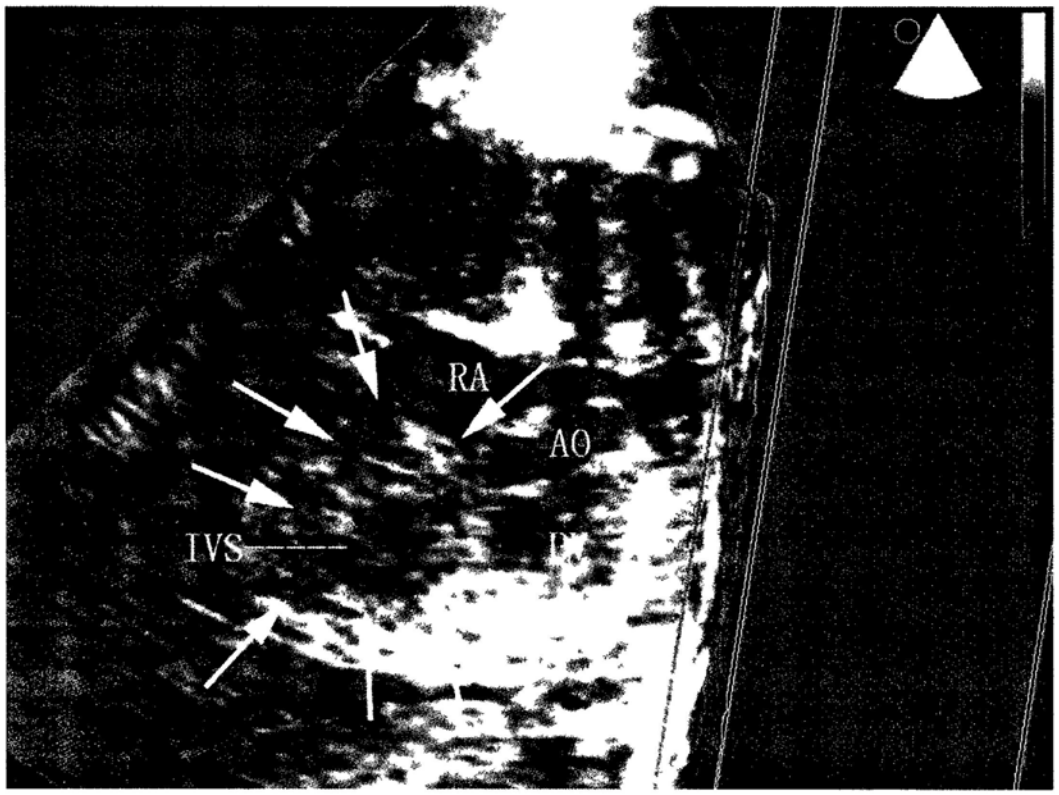

Figure 6.4 The en face view of IVS with the fetal spine anterior displayed by the live 3D imaging. A normal case is shown, with the outline of the septum indicated by the arrow. AO, aorta; RA, right atrium; PV, pulmonary valve

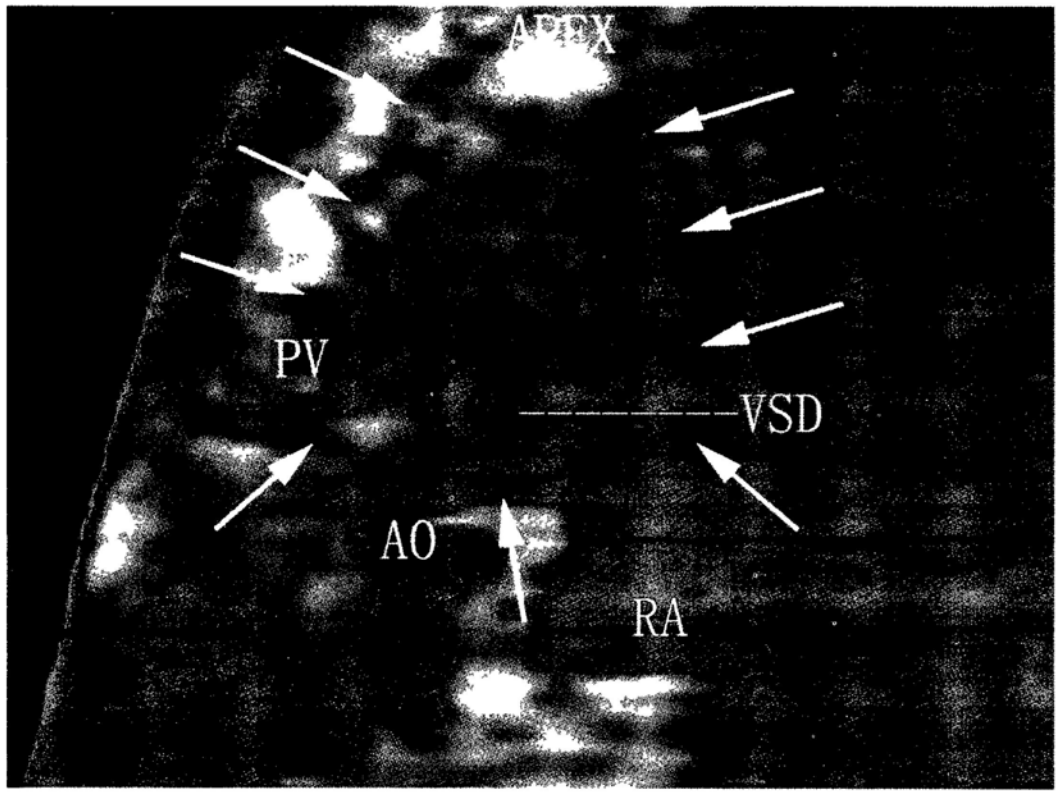

Figure 6.5 Live 3D imaging showed VSD on en face view of IVS in isolated VSD case with the fetal spine posterior. The outline of the septum is indicated by the arrow. AO, aorta; RA; right atrium; PV, pulmonary valve; VSD, ventricular septal defect

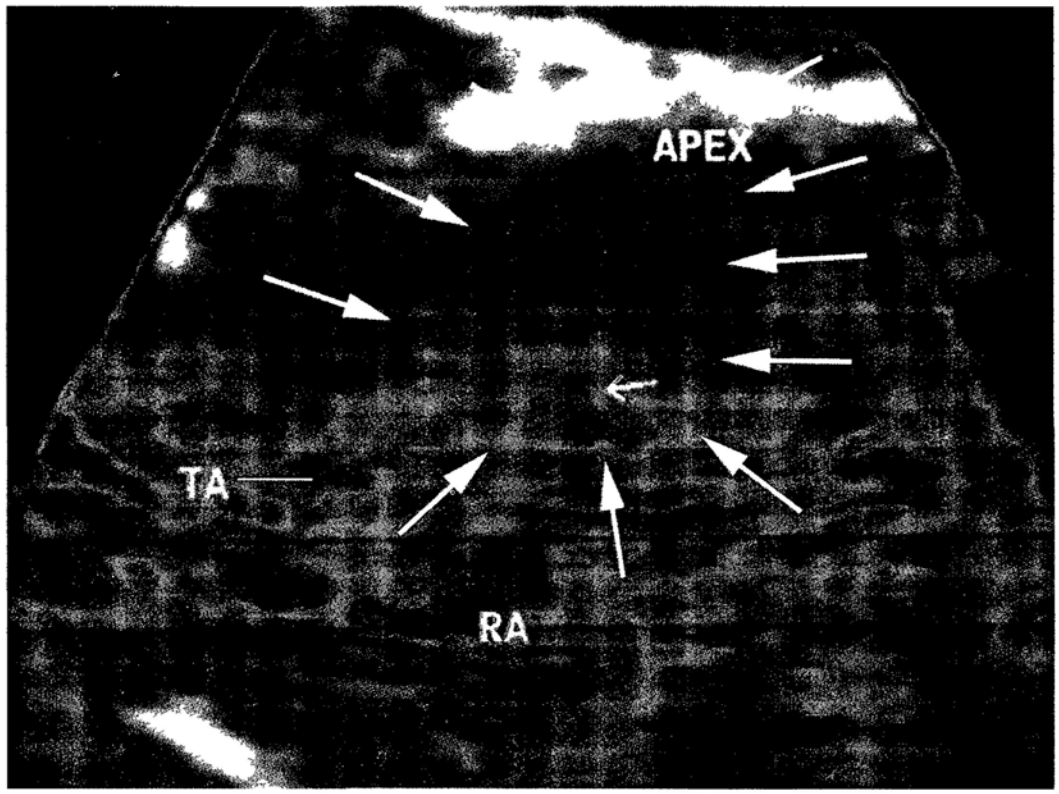

Figure 6.6 Live 3D imaging showed VSD on the en face view of IVS in truncus arteriosus with VSD case. The VSD is indicated by the small arrow and the outline of the septum is indicated by the large arrow. RA; right atrium; TA, truncus arteriosus

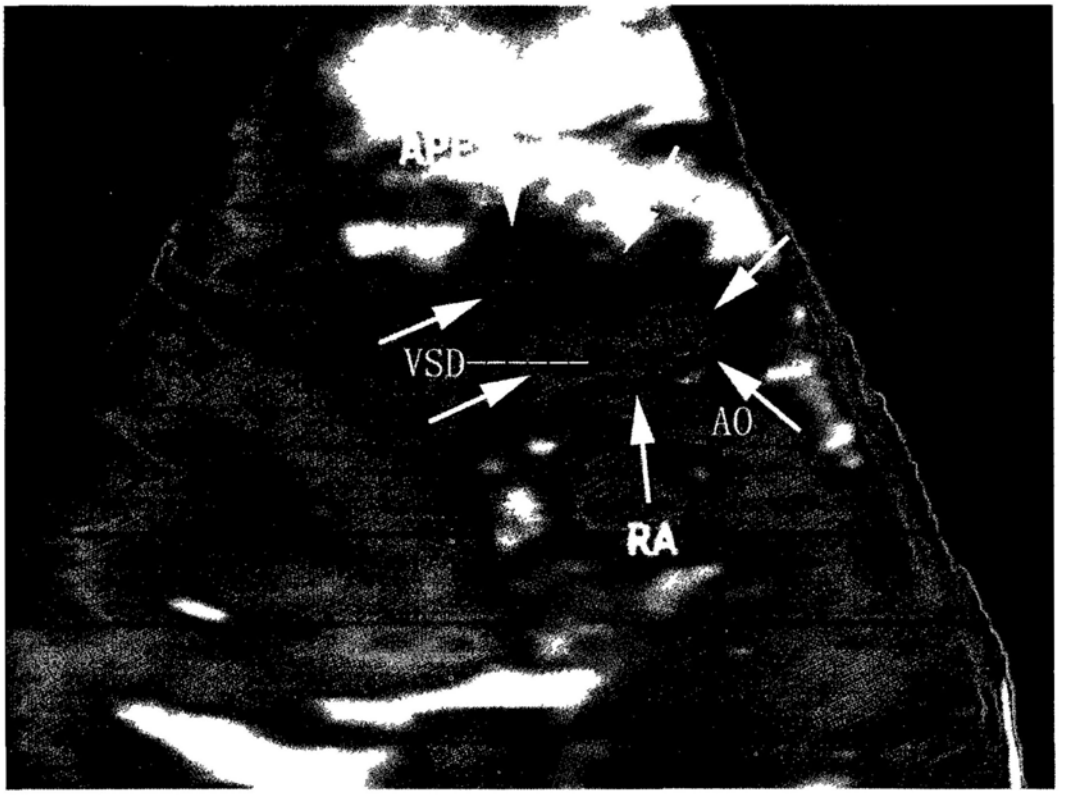

Figure 6.7 Live 3D imaging showed VSD on the en face view of IVS in AVSD case. The outline of the septum is indicated by the arrow. AO, aorta; RA; right atrium; VSD, ventricular septal defect

Figure 7.1 Visualization of the in-plane view of IVS with the STIC volumes acquired from apical four-chamber view. Firstly rotated the volumes to make the IVS parallel to y-axis and then put the reference dot at the right side of the fetal IVS in the A-plane. The lateral view of the fetal IVS (so-called 慨-plane? view of IVS) was displayed in the B-plane.

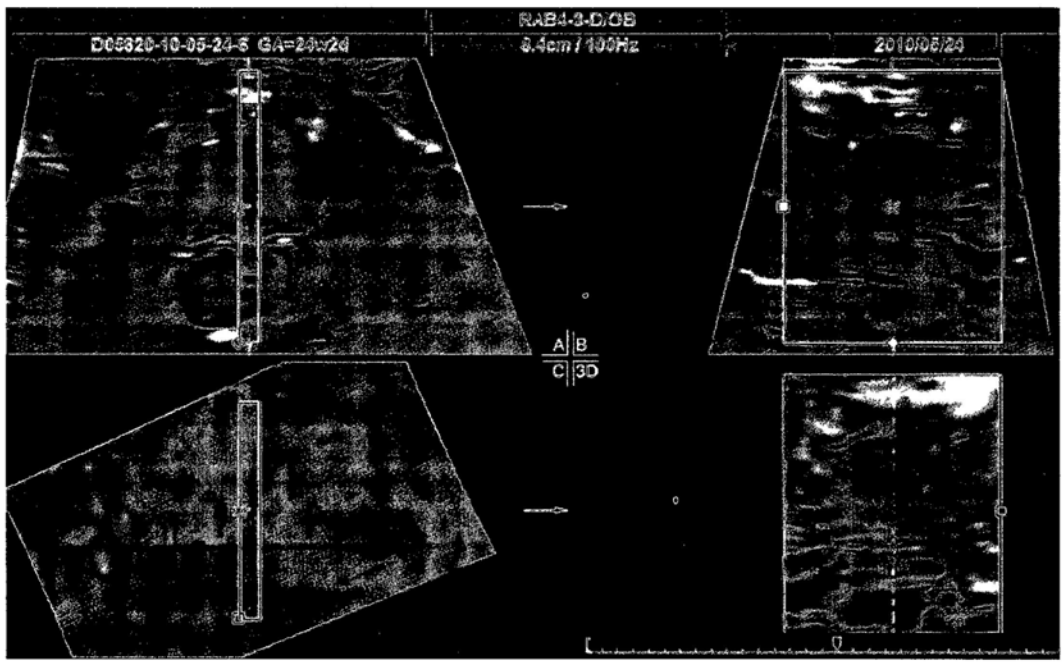

Figure 7.2 Visualization of the en face view of IVS with the STIC volumes acquired from apical four-chamber view. Firstly activated the rendered mode and adjusted the rendered box to observe the volumes from the right side of the fetal IVS in A-plane. The rendered view from the lateral side of IVS (the 慦n face?view of IVS) can be visualized by moving the green line of ROI to the right side of the IVS in the A-plane.

Figure 7.3 Visualization of the in-plane view of IVS with STIC volumes acquired from the sagittal view.

Figure 7.3b Firstly moved the reference dot to the aortic valve and the four-chamber view was displayed in the B-plane and rotated the volume to make the axis of the fetal heart parallel to the y杷xis in the B-plane.

Figure 7.3b The in-plane view of IVS was displayed in the A-plane by putting the reference dot at the right side of IVS in the B-plane.

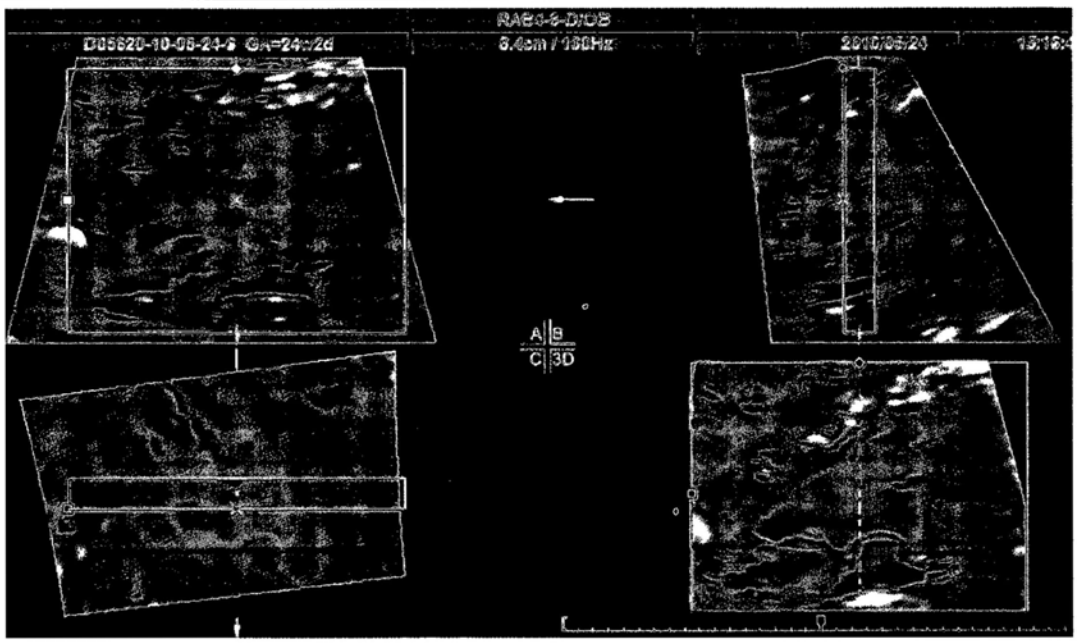

Figure 7.4 Visualization of the en face view of IVS with STIC volumes acquired from the sagittal view. Activated the rendered view and adjusted the rendered box to observe the volumes from the right side of fetal IVS in the four-chamber displayed in the B-plane. The en face view of IVS could be displayed by putting the green line of rendered box to the right side of the IVS.

Figure 8.1 Ductal arch view displayed with live xPlane imaging. When we get an apical four-chamber view and then activate the live xPlane function, the ductal arch view will be immediately displayed on the right window when we put the reference line through the sternum and descending aorta, i.e. through the right ventricle, criss-cross, left atrium and descending aorta.

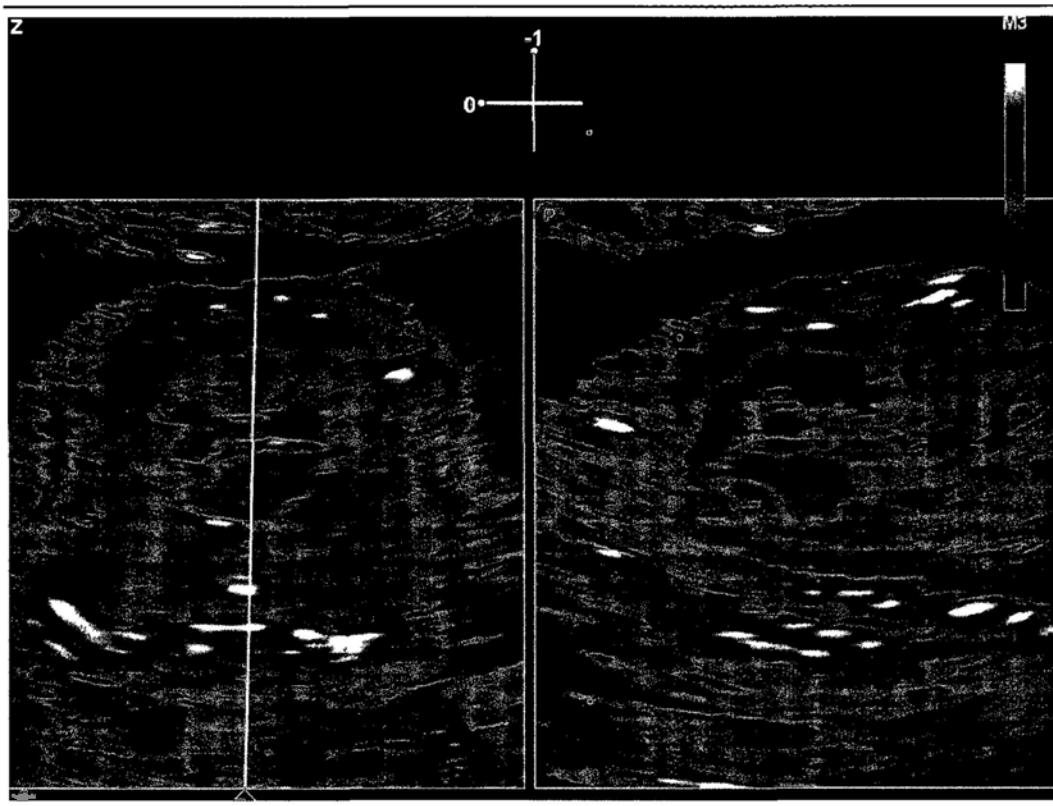

Figure 8.2 Measurement of PA and aorta on the ductal arch view.

Figure 8.2a shows a ductal arch view visualized by the live xPlane imaging.

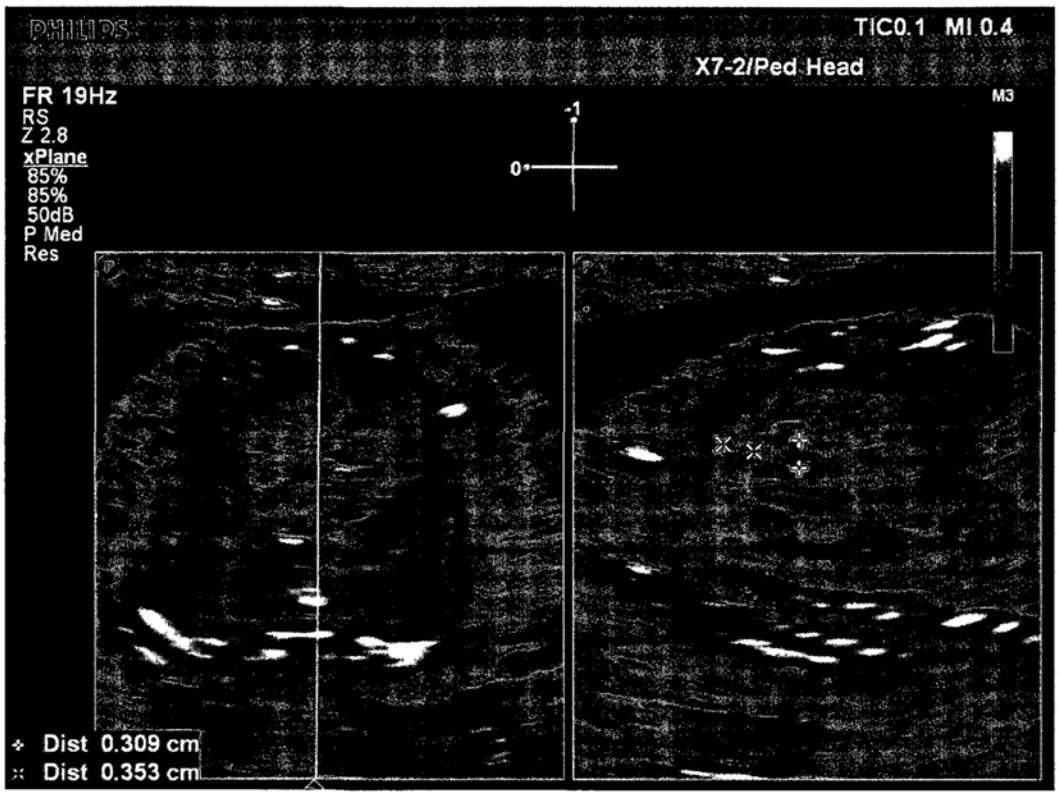

Figure 8.2b shows how to measure the diameter of PA and AO on the same ductal arch view. PA was measured just above the pulmonary valve and AAO was measured between the anterior and posterior wall on the same plane.

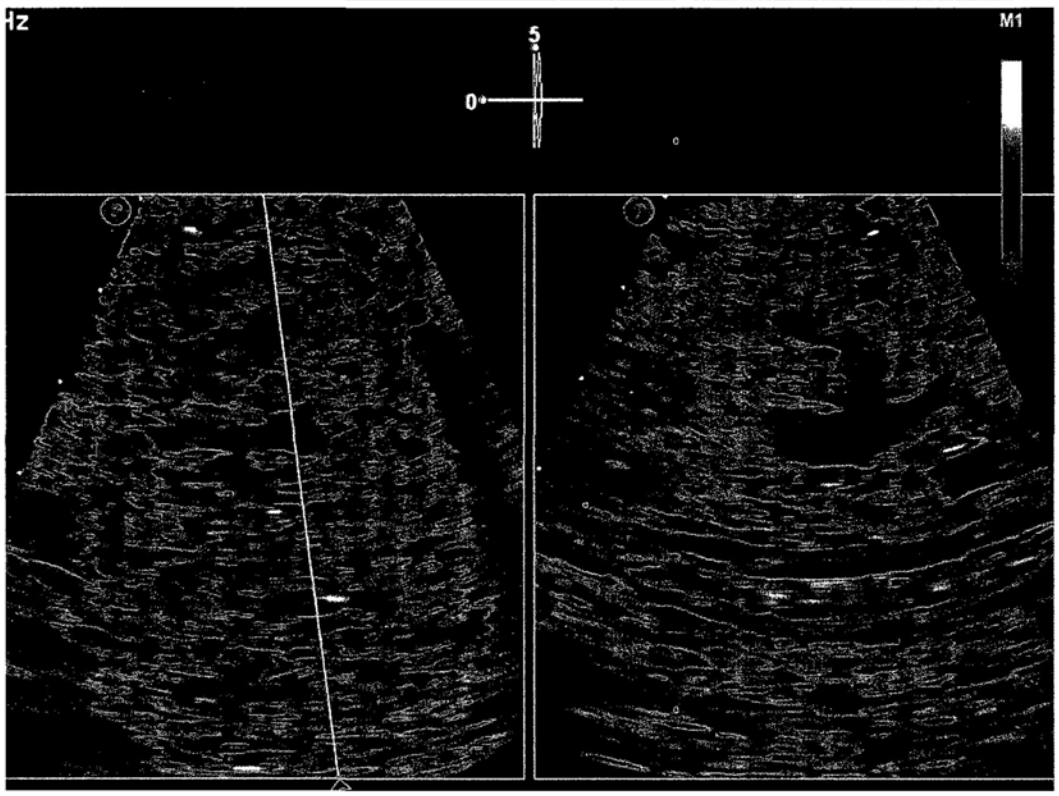

Figure 8.3 A truncus case showed by live xPlane imaging. The ductal arch view disappeared when the reference line was put through the sternum and descending aorta.

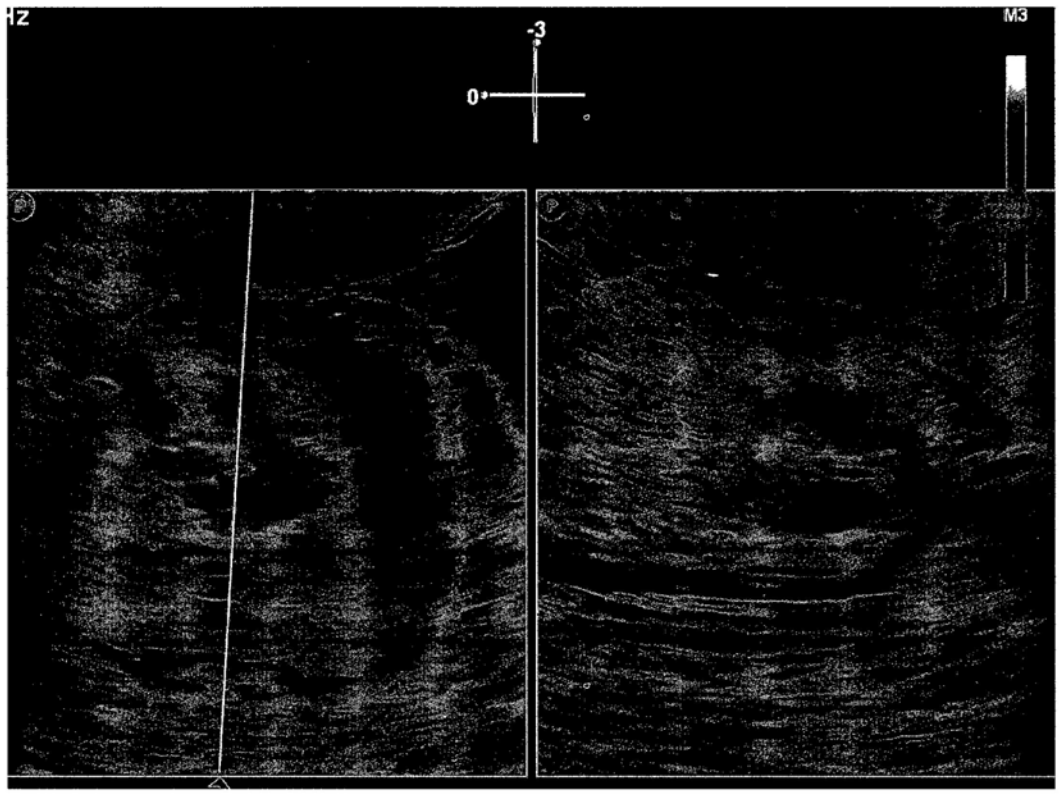

Figure 8.4 A DORV case detected by ductal arch view with live xPlane imaging. The ductal arch view lost the normal patterns栎 A surrounding the transverse view of ascending aorta.

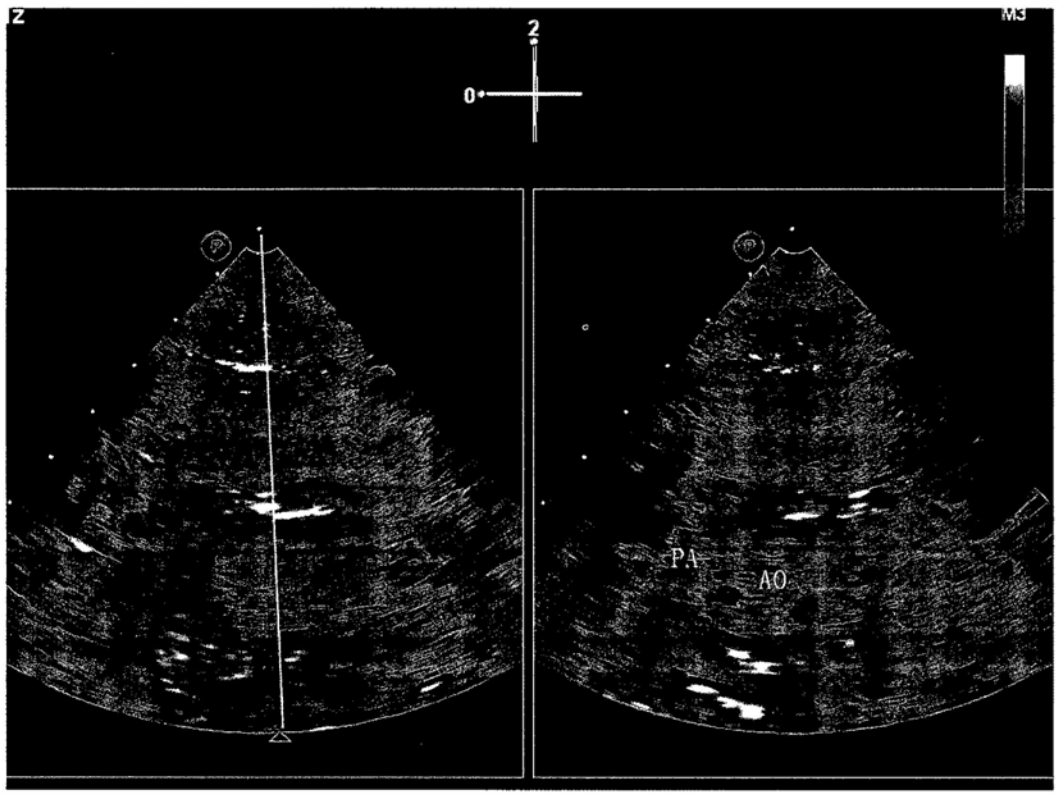

Figure 8.5 A tetralogy of Fallot cases detected by the ductal arch view with live xPlane imaging. It looks like the ductal arch view has the normal pattern. Pulmonary artery, however, is much thinner than aorta, which originally should be larger than aorta.

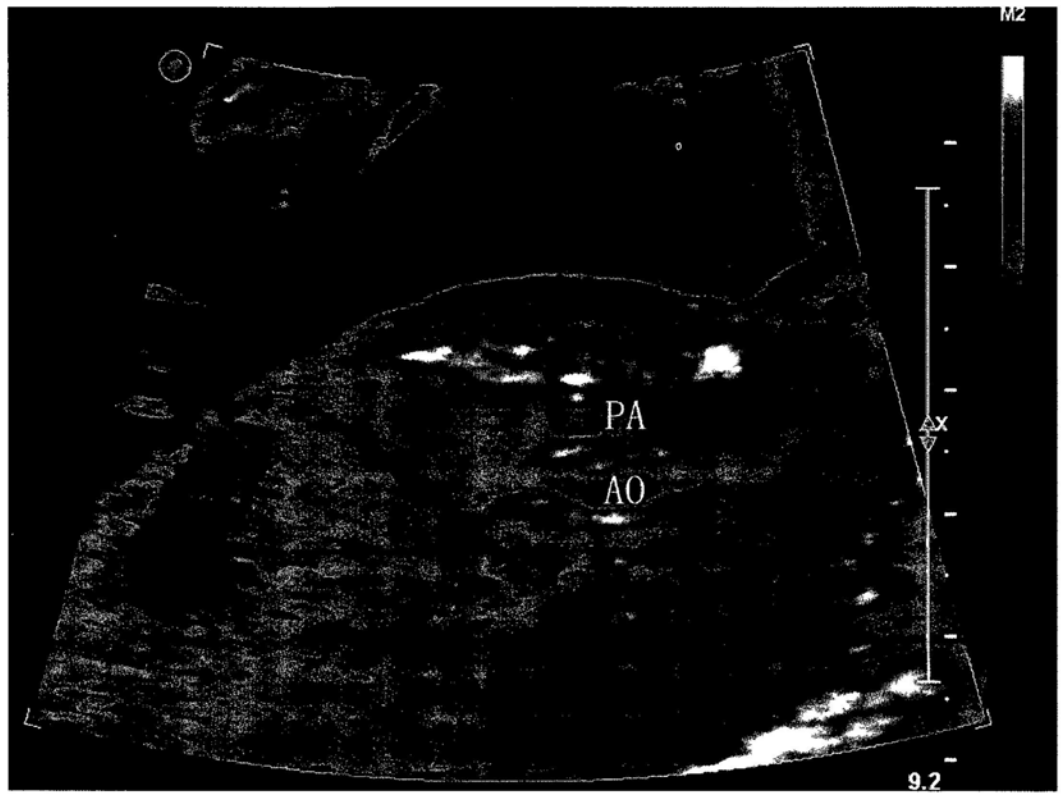

Figure 9.1 Normal in-plane view of fetal IVS. It reveals the relationship of fetal aorta and pulmonary artery. When aorta is in its longitudinal view, pulmonary artery is in its short axis. AO, aorta; PA, pulmonary artery

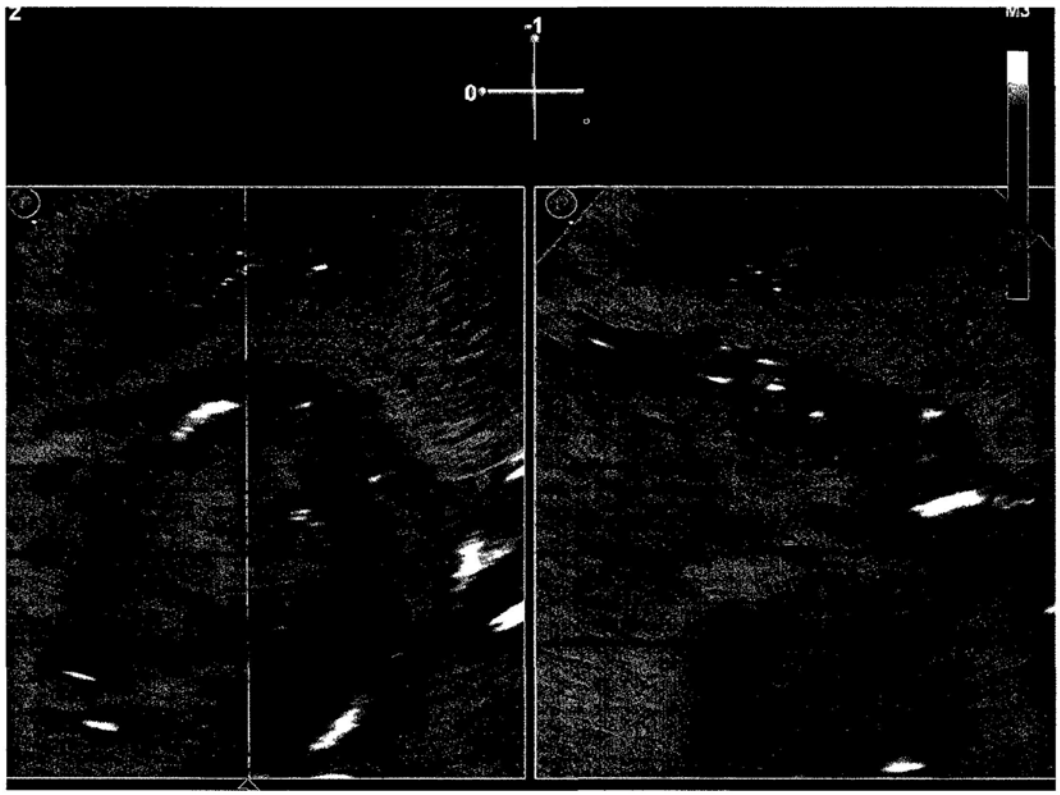

Figure 9.2 Live xPlane imaging of the in-plane view of IVS.

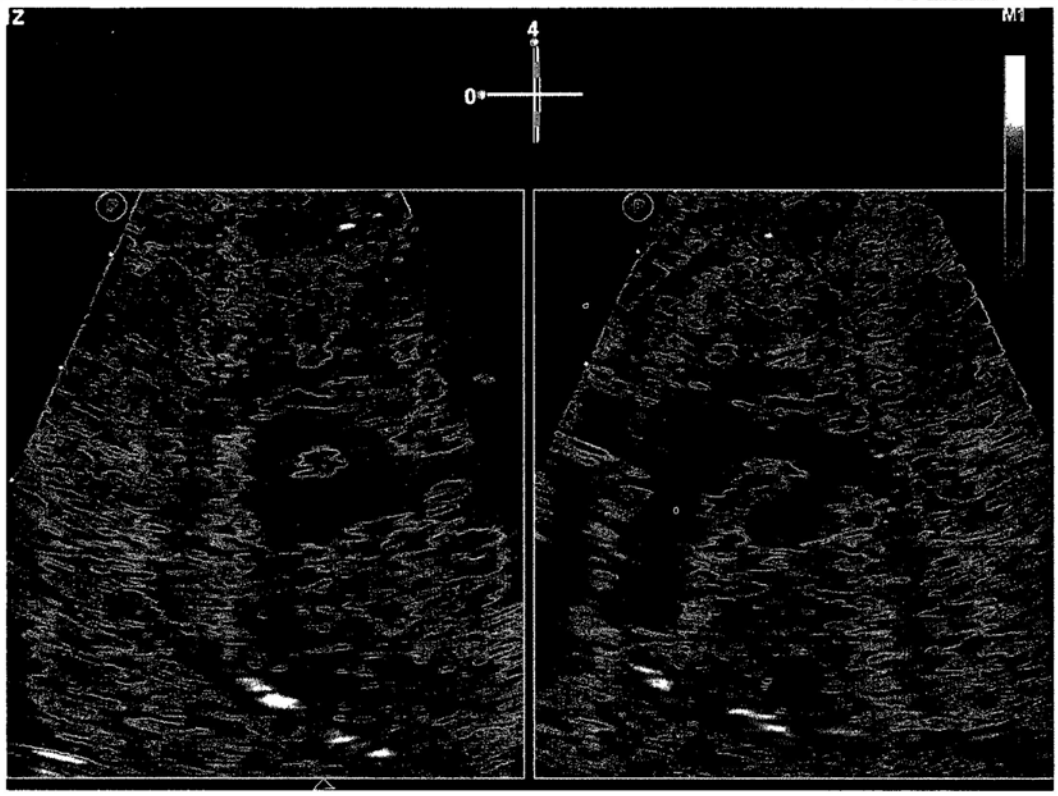

Figure 9.3 The in-plane view of IVS in a case of truncus and AVSD. It only displayed one artery.

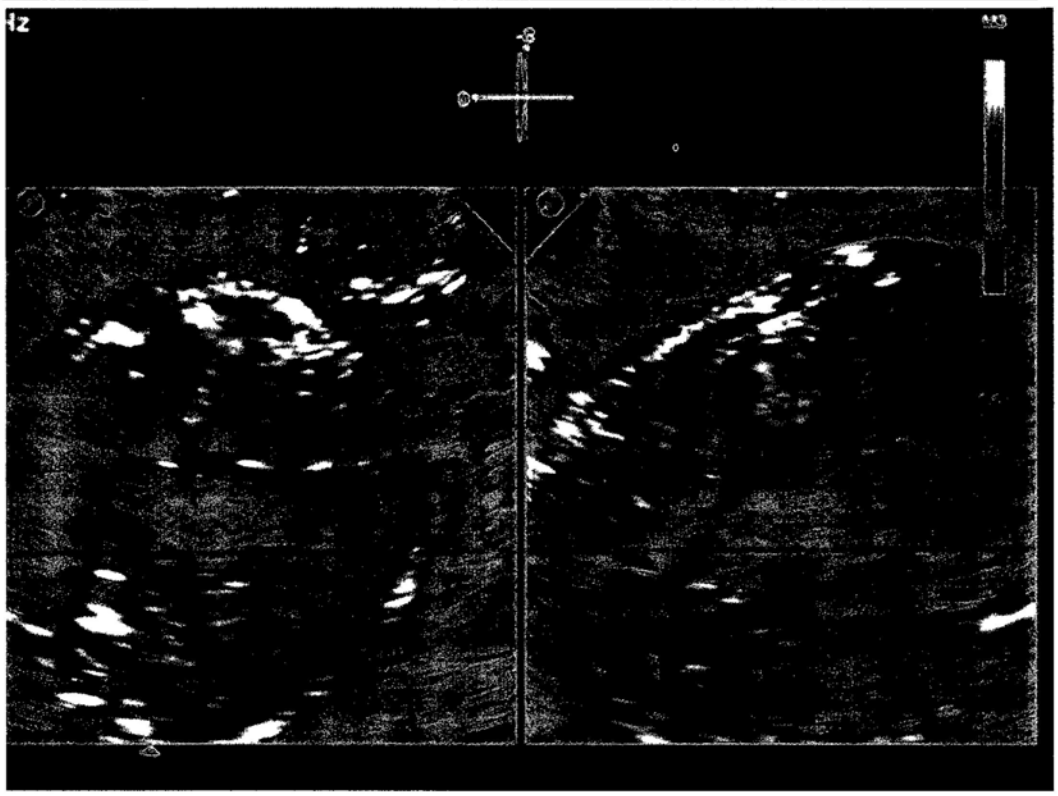

Figure 9.4 The in-plane view of IVS in a case with TGA. It also showed only one artery in the in-plane view of IVS.

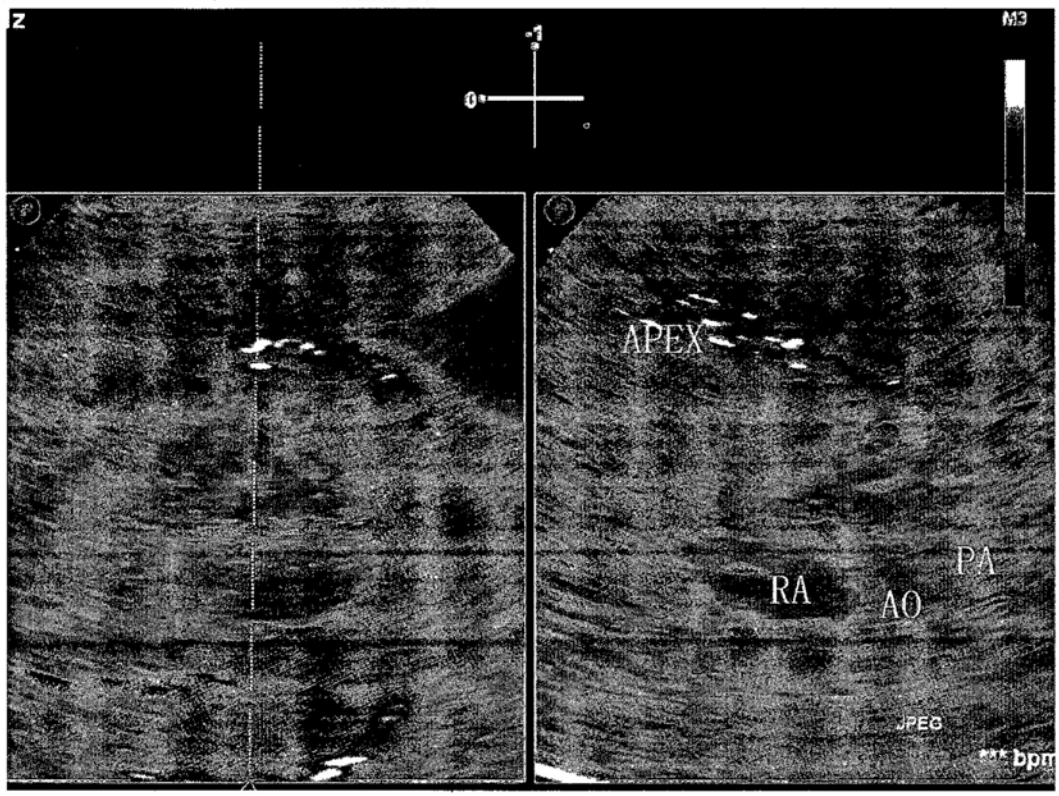

Figure 9.5 The in-plane view of IVS in a case of DORV. It showed two parallel arteries in the in-plane view of IVS. AO, aorta; PA, pulmonary artery; RA, right atrium

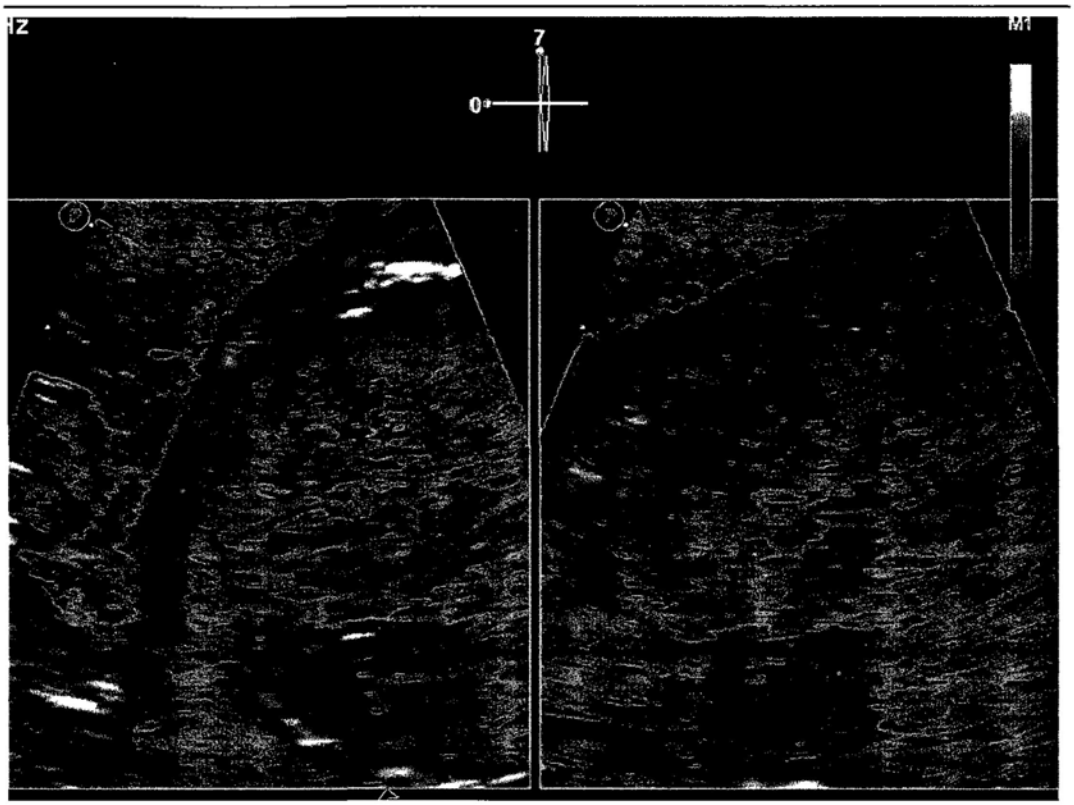

Figure 9.6 The in-plane view of IVS in a case of tetralogy of Fallot. It looks like a normal in-plane view of IVS except suspectious of a VSD.

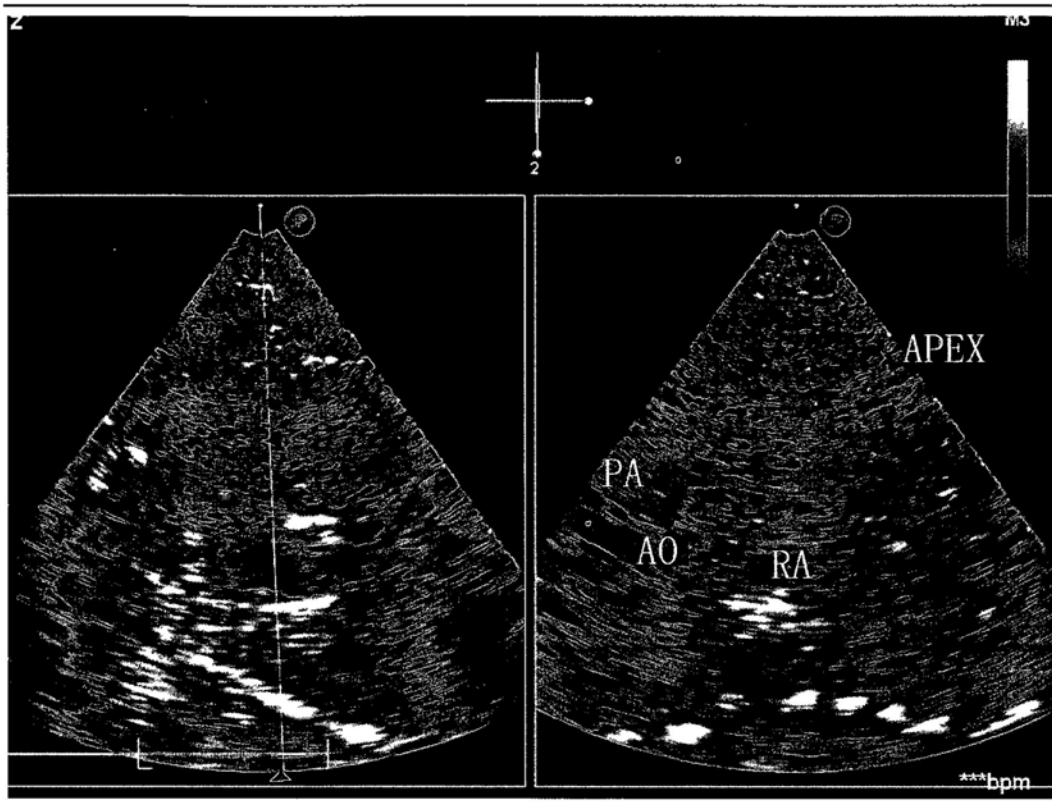

Figure 9.7 The in-plane view of IVS in a case of severe pulmonary stenosis. It showed an abnormal in-plane view of IVS. It showed two parallel arteries. This was due to the dilated pulmonary artery.

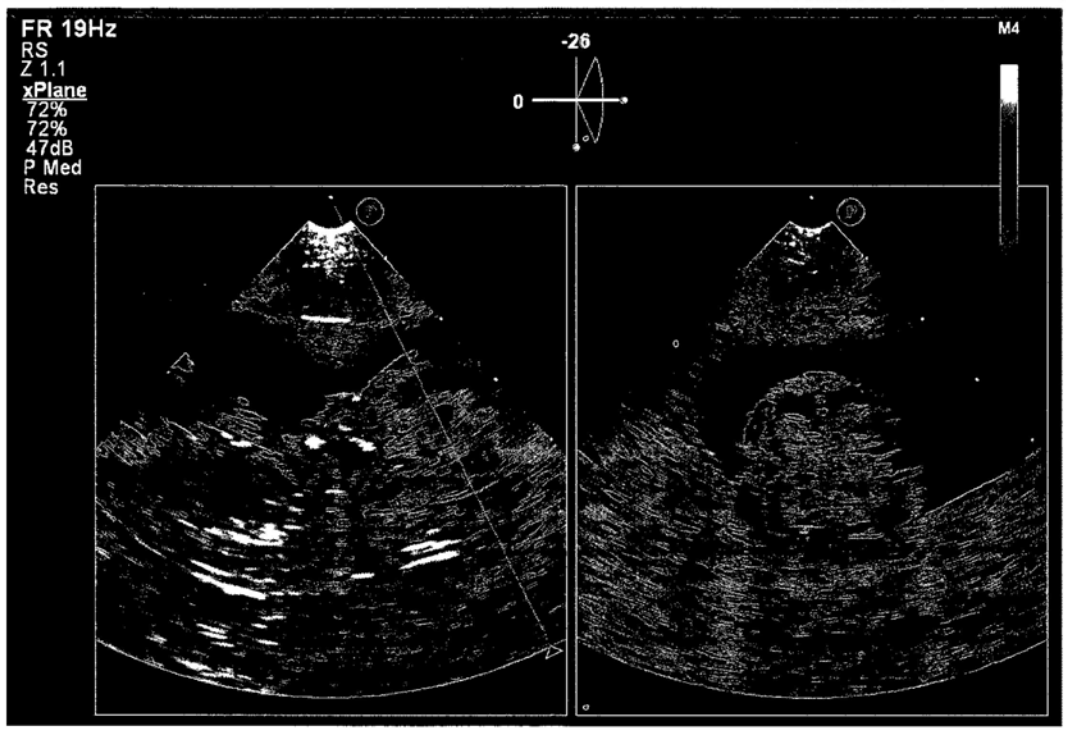

Figure 10.1 Acquisition of a midsagittal plane using live xPlane imaging. There were 2 images on the screening. The left window showed a longitudinal section of a fetus. There was a reference line in this window, representing where the image in the right window was obtained. The image in the right side was at 90? to that in the left window.

Figure 10.1a The image in left side might resemble a midsagittal section, but the orientation of the falx cerebri in the right window clearly showed that the image on the left side was not a midsagittal section.

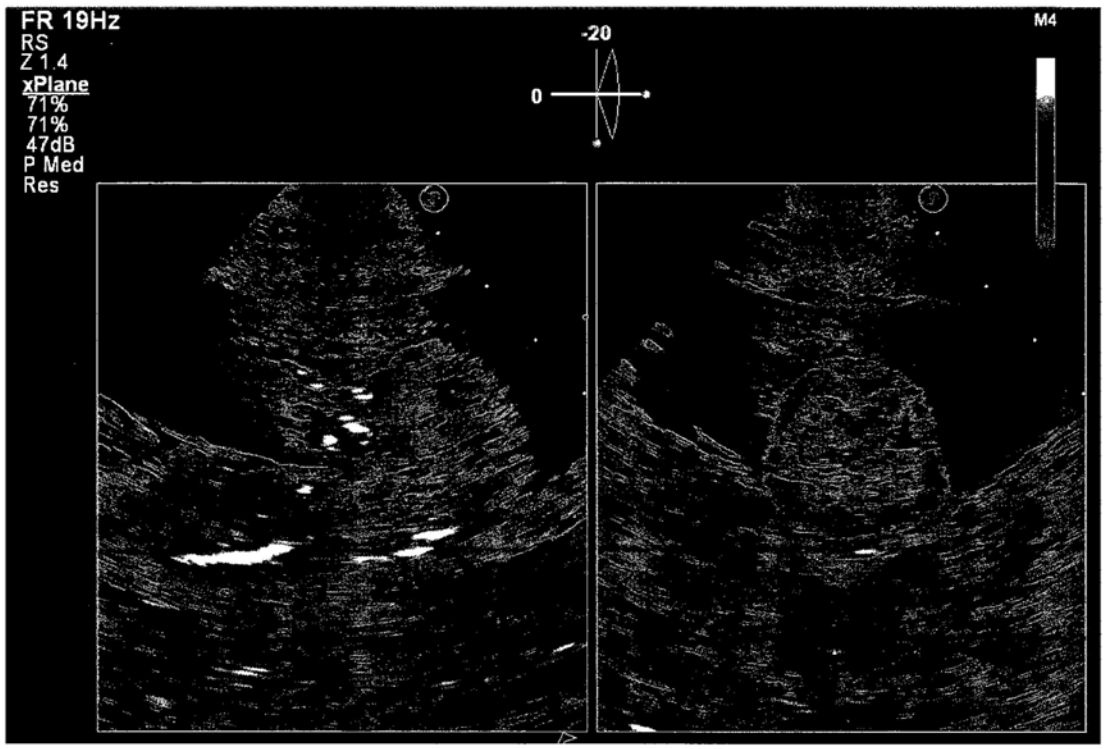

Figure 10.1b. The image was definitely a midsagittal section. The reference line was no longer visible in the left window because this reference line automatically disappeared in about 1 second after being moved.

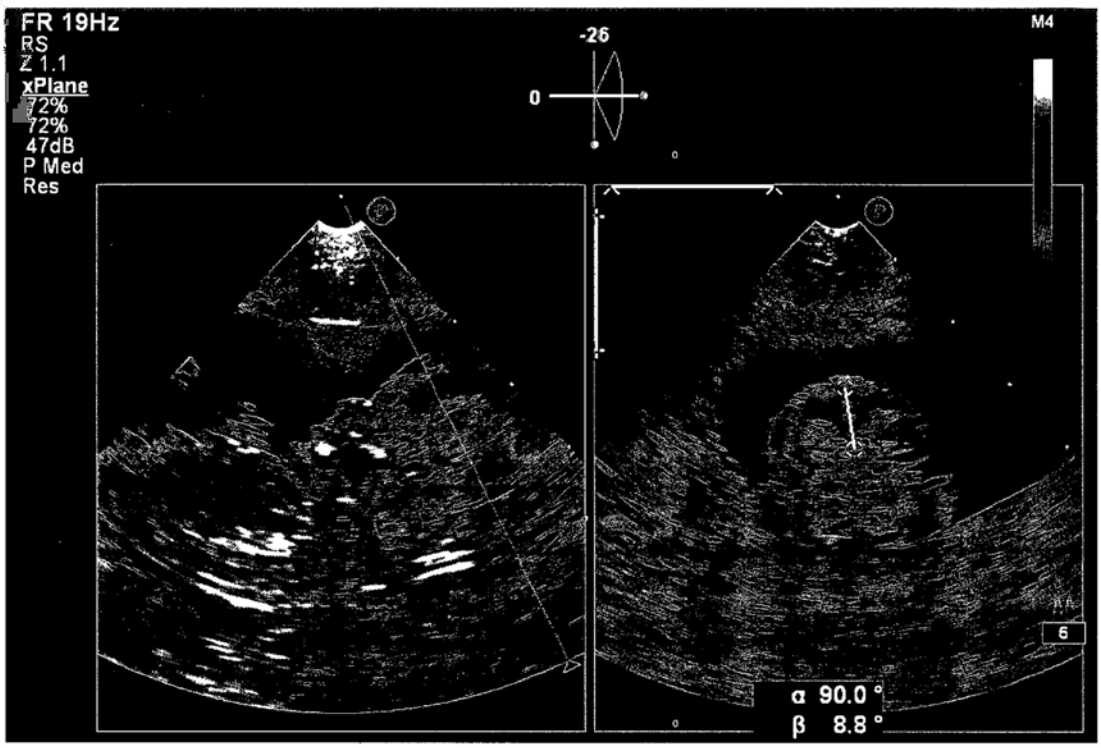

Figure 10.2 Angle of deviation was measured to test how true a presumed midsagittal section was.

Figure 10.2a It showed a 8.8? deviation between the falx cerebri and vertical axis. We first define the vertical axis and horizontal axis along the border of the frame of right window and then draw a line along the falx cerebri. The angle β means the angle between the falx cerebri and the vertical axis.

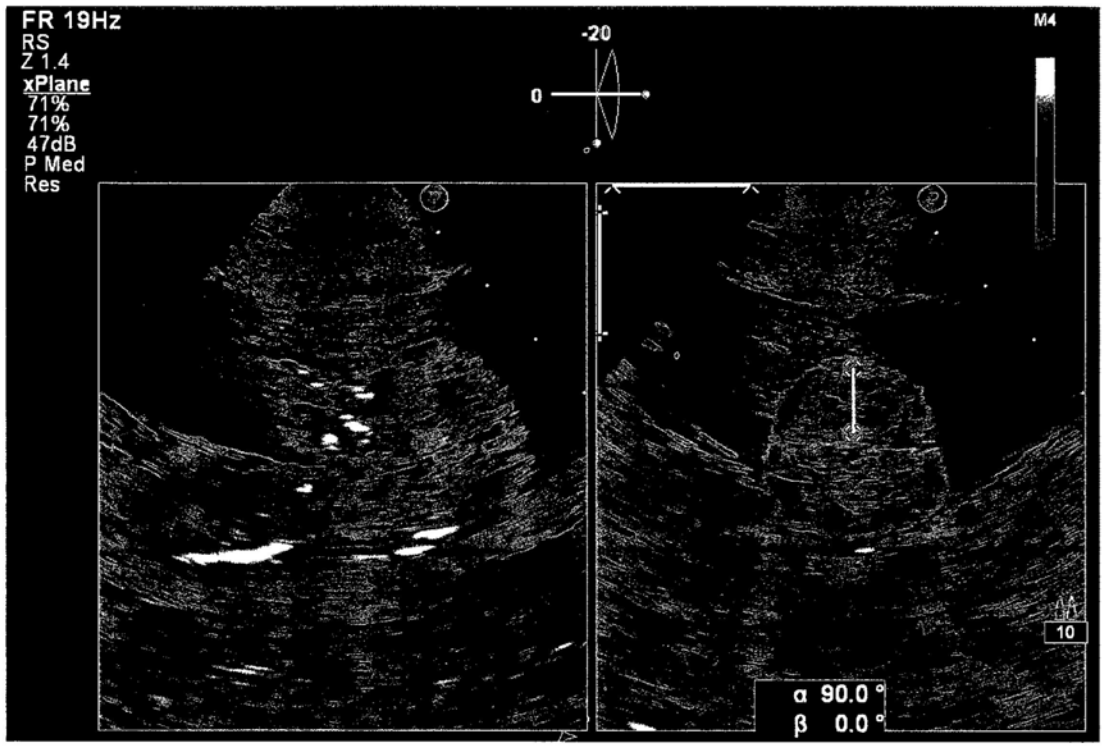

Figure 10.2b It showed an angle of 0? between the falx cerebri and vertical axis, proving the sagittal section acquired was the true midsagittal plane.

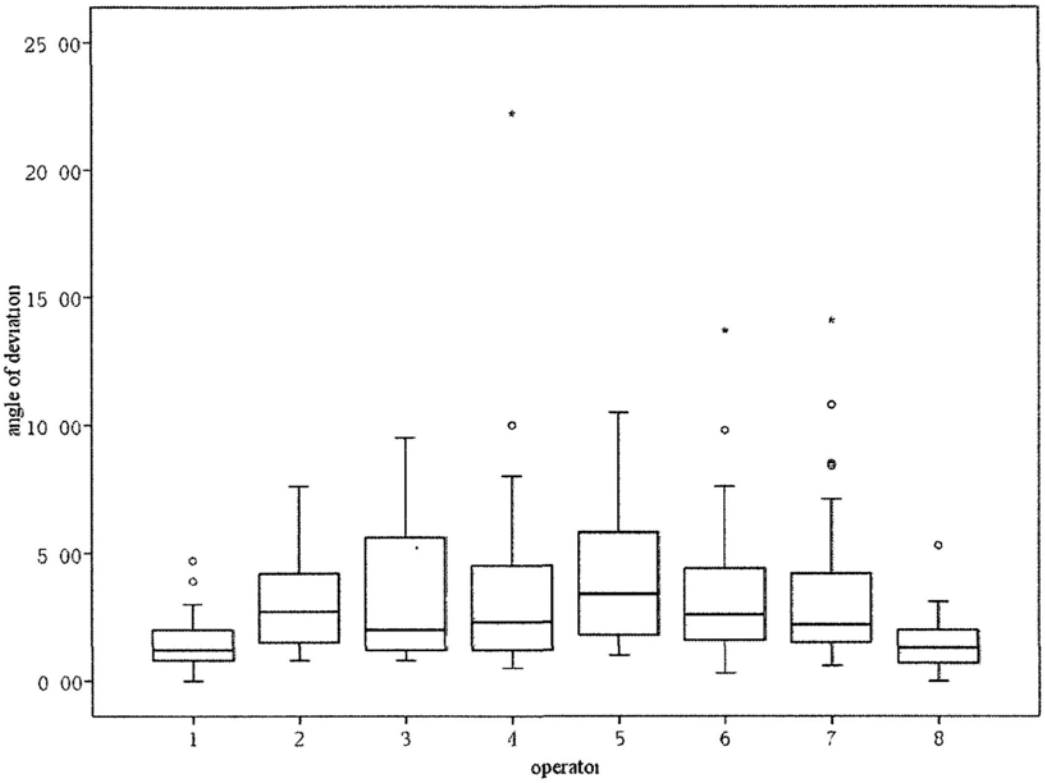

Figure 10.3 Boxplot of angle of deviation from the true midsagittal plane for FMF and non-FMF certified operators. The operator 1-4 was FMF certified operator (FMF Group) and 5-8 was non-FMF certified operator (non-FMF Group).